MECHANISTIC CONNECTIONS BETWEEN THE PROTON MOTIVE FORCE AND ATP HOMEOSTASIS IN HIGHER PLANT PHOTOSYNTHESIS UNDER DYNAMIC ENVIRONMENTAL CONDITIONS

By

Leticia Ruby Carrillo

A DISSERTATION

Submitted to
Michigan State University
in partial fulfillment of the requirements
for the degree of

Biochemistry and Molecular Biology-Doctor of Philosophy

2017

ABSTRACT

MECHANISTIC CONNECTIONS BETWEEN THE PROTON MOTIVE FORCE AND ATP HOMEOSTASIS IN HIGHER PLANT PHOTOSYNTHESIS UNDER DYNAMIC ENVIRONMENTAL CONDITIONS

By

Leticia Ruby Carrillo

Through photosynthesis, plants can capture light energy from the sun for the conversion to a more stable high-energy form, ATP and NADPH. These products are then used to fuel an array of metabolic processes including the biosynthesis of sugars and complex carbohydrates. Yet, the abundant source of solar energy used in the process is highly varied and fluctuates throughout the day, directly impacting the photosynthetic apparatus and carbon assimilation. This dissertation focuses on several mechanisms by which plants are able to respond to the dynamic environmental pressures through modulation of the proton motive force (*pmf*) and ATP homeostasis.

ATP is the primary energy currency in cells and is synthesized in plastids by the chloroplast ATP synthase. However, unlike other stromal thiol-regulated enzymes that incrementally become redox-activated in response to light, chloroplast ATP synthase acts more like an on-off switch, only requiring minimal irradiance to become fully active. Previous work suggested that the rapid sensitivity to light could be explained by the relative redox potentials of the regulatory thiols on the γ-subunit of ATP synthase. This work uncovered a new, unexpected component, NADPH thioredoxin reductase C (NTRC) that controls thiol regulation specifically under low light intensities. Mutants lacking NTRC show strong photosynthetic phenotypes, e.g., increased nonphotochemical quenching and inhibition of linear electron flow, at low irradiances, consistent with an inability to activate

ATP synthase resulting in a buildup of the thylakoid *pmf*. We predict both NTRC and the canonical ferredoxin-thioredoxin reductase system co-regulate the thiol state of ATP synthase at specific light intensities using different reducing potentials (NADPH versus ferredoxin) that allow for added flexibility.

Photosynthesis copes with, and adapts to, fluctuating environments using a wide range of mechanisms. While most of the research has been devoted to the processes occurring inside the plastid, work described here on the nucleotide triphosphate transporter (NTT) illuminates an additional mechanism of augmenting and balancing ATP. Previous work suggested that the chloroplast transporter, NTT, acted primarily as an importer of ATP during the night cycle, presumably under non-photosynthesizing conditions. However, isolated intact chloroplasts from both spinach and *Arabidopsis thaliana* export ATP at rapid rates that can constitute a large fraction of that generated by the light reactions. Furthermore, these findings suggest that earlier results of minimal rates of ATP transport were based on suboptimal assay conditions and incorrect characterization of T-DNA knockout lines, rendering NTT essential for seed germination. Work on double NTT knock-down lines (NTTdKD) have decreased gene expression levels of *ntt1* and *ntt2* and show strong photosynthetic responses, particularly in the pH and energy-dependent quenching response (qE) with related accumulation of the *pmf* under fluctuating light and/or decreased CO_2 levels. These results indicate a greater role for NTT in balancing ATP levels between the stromal and cytosolic pools than previously thought.

This dissertation is dedicated to my mother, who's strong will taught be about determination.
And all the scholars that persevere and challenge societal norms.
Si se puede.

ACKNOWLEDGEMENTS

Graduate school has been a rollercoaster of experiences, challenges and growth; not only regarding the science but also personal development. THANK YOU!

I would like to thank all my colleagues, undergraduate researchers, faculty members and friends that have made this journey possible here at Michigan State University (MSU). Particularly the KRAMER lab and all its messiness. My advisor, Dave Kramer, taught me about work ethic and how any question worth investigating is solvable. The lab, my second family, and the most loving, knowledgeable, curious, eccentric group I could have asked for. Deserah Strand and Nick "Edward" Fisher were essential throughout my graduate career, not only for the inspiration and insightful discussions but also hobbies and love for cats (Stan and Chiquis). Thank you for being there from the beginning and supporting me throughout, couldn't have done it without you two.

The Cruz's, Jeff, Mio, Hikaru and Akira, were the best to be around. Jeff didn't only have the silliest jokes but also the technical knowledge and experience to always assist. Mio was a great officemate and friend to be around, Arigato! I cannot mention technical and not include Robert Zegarac, who always had the magic touch with the specs and electronics. Thank you, Robert, for always assisting with my troubleshooting and generously providing advice (in and out of lab). John Froehlich for great collaboration and for always answering my technical questions. The Luckers (Ben, Amy and their lovely family), it was a pleasure to work with you both and of course babysit your girls. Nina and Doran were always a delight to watch and often filled the void of missing my family back home. The list can go on forever but instead I'll mention a few more that were above and beyond: Chris Hall, Kaori

Kohzuma, Sebastian Kuhlgert, Elisabeth Ostendorf, Stefanie Teitz (now Rhodes), Geoff Davis, Linda Savage, David Hall, thank you all.

The undergraduate researchers, I couldn't have done it without you guys. Especially Lola Alvarez, my sister, who even though she had zero experience or desire to pursue a career in science, took her job seriously and assisted me for years with (sometimes tedious) laboratory work. Thank you so much! Also, TJ, the first undergraduate who I took under my belt, he was always a pleasure to be around. Other undergraduates I was fortunate to work with and observe their growth include Ben Wolf, Brendan Johnson, Sarah Watkins and Vanessa Quevedo. Thank you all for always being willing to assist me and my experiments.

I was fortunate to have started my graduate career in the Biochemistry and Molecular Biology (BMB) department with an inspiring cohort. I would like to especially thank Mark Farrugia, Derrick Feenstra (even though he was in the physiology department), Neil White, Hang Nguyen and Bethany Huot. You guys were instrumental in my work ethic early on and your friendship is truly appreciated. Dionisia Quiroga, my DO-PhD, and Liz Camacho, I couldn't have asked for better friends/traveling buddies/roommates to have experienced this with, thank you so much for keeping me sane! Jose Suarez, your friendship and support is like no other, thank you! Also, Elijah Lowe, Terry Flennaugh, Gaëlle Cassin-Ross, Marcus Coleman, Julie Plasencia, Gabby Lopez and many more that helped me get through Michigan winters.

In addition to BMB, I was also fortunate to have been part of the Plant Research Laboratory with all their great faculty and staff. I would like to thank my committee members for advising and aiding me throughout this process. Particularly Beronda

Montgomery, for not only playing a major role in my decision to apply to MSU but for always making time and supporting me throughout. You exposed me the Alliance for Graduate Education and the Professoriate (AGEP) here at MSU, which played a crucial role in my development and growth. Steven Thomas, director of AGEP, also allowed me to be part of the Summer Research Opportunity Program (SROP) for the past 5 years and was such a wonderful experience. Also, the members of the Society for the Advancement of Chicanos and Native Americans in Science (SACNAS) for making a difference and starting something new!

Finally, I would like to thank my family and friends. Those back home (Los Angeles, CA) and those I've made in Michigan, you were my rock and strength throughout this journey. My mother, Leticia Tejeda, and siblings, Daisy (and son Victor), Junior, Lola, Bubba and Marky, and their significant others; thank you for motivating me to follow my dreams, even though it entailed being miles and miles apart! My closest gals back home, Liz Rangel, Lily Silva, Nancy Nguyen, Karen Rodriguez and Jenny Alvarez thank you for visiting me, always motivating and maintaining this meaningful relationship throughout the years. I couldn't have done it without your support and friendship. All my friends back home who continuously encouraged my scholarly pursuits throughout the years. My partner, Emery Max, for all the late nights in front of our computer screens and deep reflective conversations. Thank you for pushing me out of my comfort zone and always inspiring me. Your family, Jenine Grainer, Max Lawrence and Jane Hildebrand, for being my family away from home. Thank you for all your support, motivation and love. I'm truly grateful and blessed to have such a supportive group throughout the years.

TABLE OF CONTENTS

LIST OF TABLES

LIST OF FIGURES

KEY TO ABBREVIATIONS AND SYMBOLS

^{1}Chl*	Excited chlorophyll state
$^1O_2$	Singlet oxygen
^{3}Chl*	Triplet chlorophyll state
3-PGA	3-phosphoglycerate
ATP	Adenosine triphosphate
CBB	Calvin-Benson-Bassham
CEF	Cyclic electron flow
CF_1F_o	Coupling factor 1 and O, referring to the structure of ATP synthase
CO_2	Carbon dioxide
Cys	Cysteines
DEPI	Dynamic environment photosynthesis imager
DHAP	Dihydroxyacetone phosphate
DIRK	Dark interval relaxation kinetics
DNA	Deoxyribonucleic acid
DTT	Dithiothreitol
ECS	Electrochromic shift
FAD	Flavin adenine dinucleotide
Fd	Ferredoxin
FNR	Ferredoxin-NADP$^+$ reductase
FTR	Ferredoxin thioredoxin reductase
GAP	Glyceraldehyde phosphate

g_{H^+}	Conductivity of H^+ across the thylakoid membrane linked to ATP synthase
H^+	Protons
H_2O_2	Hydrogen peroxide
KEA3	*Arabidopsis thaliana* K^+ efflux antiporter mutant
LEF	Linear electron flow
LHC	Light harvesting complex
MDH	NADP- malate dehydrogenase
Mg^{2+}	Magnesium ion
NADPH	Nicotinamide adenine dinucleotide phosphate
NPQ	Nonphotochemical quenching
NTRC	NADPH thioredoxin reductase C
NTT	Nucleotide triphosphate transporter
O_2	Oxygen
P_i	Inorganic phosphate
Pmf	Proton motive force
Pmf_T	threshold of *pmf*
PQ	Plastoquinone
PQH_2	Plastoquinol
Prx	Peroxiredoxin
PsbS	PSII subunit S protein
PSI/II	Photosystem I/II
PTOX	Plastid terminal oxidase
qE	pH and energy dependent quenching component of NPQ

Q_i	Quinone reductase
qI	Irreversible long-lived component of NPQ
Q_o	Quinol oxidase
RC	Reaction centers
ROS	Reactive oxygen species
RuBP	Ribulose 1,5-bisphosphate
Trx	Thioredoxin
vH^+	Rate of H^+ flux across the thylakoid membrane
$\Delta\tilde{\mu}H+$	Electrochemical potential of protons
ΔG_{ATP}	Gibbs free energy of ATP synthesis
ΔpH	Difference in pH
ΔΨ	Difference in electric field across a membrane (i.e., thylakoid membrane)
φII	Quantum yield of photosystem II

CHAPTER 1

Literature Review: The dynamics of photosynthesis through modulation of the thylakoid proton motive force

Introduction to the dynamics of photosynthesis

Dynamics, as defined by the Oxford English Dictionary, are "the forces or properties that stimulate growth, development, or change within a system or process" and in this case the process is photosynthesis. In nature, environmental fluctuations are constantly occurring, particularly in the amount of light plants receive. Studies have confirmed that rapid changes in irradiance occur over 100-fold within seconds, are influenced by temporal and spatial factors, and impose great demands on the responsiveness of photosynthesis (Pearcy, 1990; Way and Pearcy, 2012). In spite of this, many of those mechanisms have yet to be explored.

Oxygenic phototrophs, including higher plants, perform photosynthesis by capturing solar energy and use it to drive the two tightly coupled, energy-converting circuits. The electron transfer circuit of photosynthesis uses light energy to transfer electrons from H_2O through a series of high energy intermediates and associated redox centers. Ultimately, the electron circuit reduces ferredoxin (Fd), which functions as the electron donor for $NADP^+$, the major reductant in the linear electron flow (LEF) pathway. In the protonic circuit, the proton motive force (*pmf*) is generated across the thylakoid membranes from protons (H^+) derived from the splitting of H_2O at photosystem II (PSII) and translocation at the cytochrome b_6f complex of LEF. Formation of the *pmf* functions to drive the synthesis of ATP from ADP and inorganic phosphate (P_i) by ATP synthase (Mitchell, 1961). The electron and proton transfer reactions of LEF yield NADPH and ATP, at fixed ratios, and these substrates are used to drive an array of downstream metabolic reactions including CO_2 assimilation.

During the coupled electron and proton transfer reactions, photosynthesis produces high energy intermediates that can interact with oxygen to generate harmful reactive oxygen species (ROS). Photo-oxidative stress, such as ROS formation, can occur under excess light, which leads to over-reduced photosynthetic reaction centers (Foyer and Harbinson, 1994). Therefore, apart from the intricacies in the energy conversion processes, photosynthesis must also stabilize high energy intermediates by modulating the rate of energy capture at PSII. Two main forms of regulation that have evolved in oxygenic phototrophs are modulation of the *pmf* and adenylate homeostasis. Both of these allow fine tuning of light capture and the efficient conversion to chemical energy. Work described in this dissertation aims at elucidating some of the dynamic photosynthetic processes that allow higher plants to rapidly respond to environmental fluctuations by provision of ATP and modulation of the *pmf*.

Photophosphorylation and the electron transfer reactions of photosynthesis

In order to understand the dynamics of photosynthesis, the components that make up the system must first be covered. This section describes the intricate molecular complexes (Figure 1): photosystem II (PSII), cytochrome *b6f*, photosystem I (PSI), and ATP synthase and how these components are regulated to allow for rapid modulation of energy capture. Moreover, the varying roles of the photosynthetic apparatus will be reviewed, in relation to the collective role in efficiently coping with fluctuating light and photo-protection, through modulation of the *pmf*.

Photosystem II

In photosynthetic electron transport, absorption of light energy occurs at the two multiprotein complexes found in the thylakoid membrane, known as PSI and PSII (as illustrated with lightning bolts in Figure 1). Within each PS, photons are captured by a chlorophyll- containing antenna system that forms the light harvesting complex (LHC). Light absorbing pigments are located within the antenna proteins of the LHC and comprise chlorophyll a and b molecules, as well as carotenoids (e.g., β-carotene, lutein, and violaxanthin). Together, the LHC pigments allow for a broad spectrum of the visible light to be absorbed, particularly in the red and blue regions, with absorption maxima around 660 and 428 nm (Figure 1, inset) (Lichtenthaler, 1987). In addition to capturing and

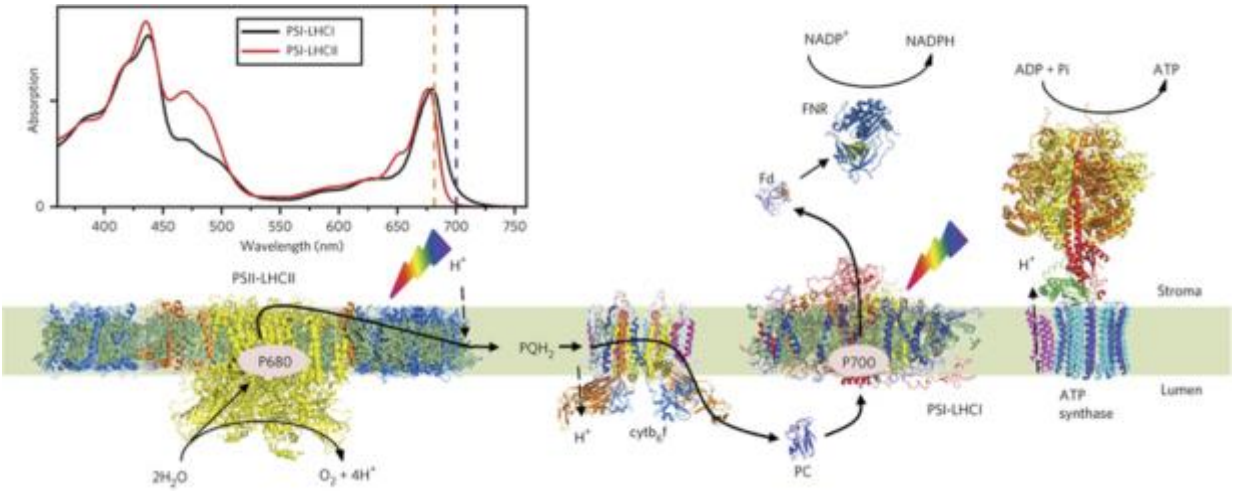

Figure 1. Photochemical reactions of linear electron flow. The major components of the light reactions found on the thylakoid membrane involved in oxygenic photosynthesis; beginning with PSII being light activated and splitting H_2O at the oxygen evolving complex. Electrons from PSII are then transferred through the membrane to cytochrome *b_6f* by plastoquinone pool (depicted as PQH_2). Following the electron chain to PSI via plastocyanin (PC) to reduce Fd and NADPH. The fourth major complex is ATP synthase using the protons (H^+) generated through electron transport to synthesize ATP from ADP and P_i. The inset spectra indicate the absorption wavelengths for both PSII (680 nm, orange) and PSI (700 nm, blue). Image reproduced from Croce, R. and Amerongen, H. Van. (2014) with permission of the rights holder (RightsLink license #4123691481624).

distributing the light energy, the LHCs are also involved in the photo-protective mechanisms induced under excess light (see non-photochemical quenching) (Nevo et al., 2012).

Following light capture by LHCs, energy is transferred excitonically to the reaction centers (RC) where it can be converted, through a series of electron transfer reactions, into chemical energy. The two RCs contain a special pair of chlorophyll a molecules, identified by their visible absorption maxima: P680 in PSII and P700 in PSI (Figure 1) (Ort and Yocum, 1996). The RC of PSII is composed of D1 and D2 heterodimer proteins with a P680 center and an array of electron transferring molecules, i.e., pheophytin and plastoquinone (PQ) molecules, Q_A and Q_B (Ort and Yocum, 1996).

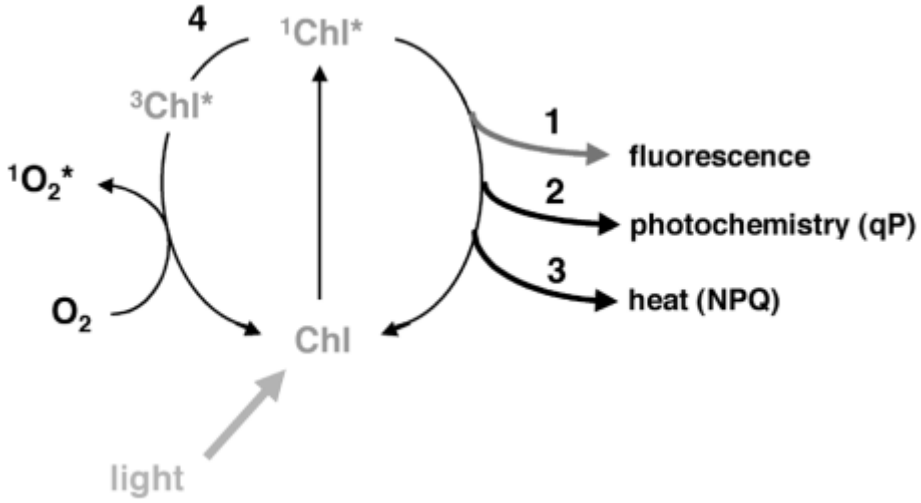

Figure 2. Simplified model of the different excited chlorophyll fates. Model illustrates the excited chlorophyll state at PSII, P680 with four fates of electron transfer. Electrons can shuttle through the reaction centers (2) via LEF or can be lost as fluorescence (1) and as a photoprotective mechanism through NPQ (3). The relationship of these three possibilities are directly related and in competition. Lastly, (4) can occur when there is an excess amount of light causing a backup in the light reactions and an accumulation of high-energy excited chlorophylls that can lead to formation of ^{3}Chl* and ultimately $^1O_2$. Reviewed in (Baker, 2008).

The photochemically excited singlet form of P680 (P680*, or ^{1}Chl*) is capable of relaxing down to ground state by one of four competing pathways, illustrated in Figure 2 (Müller et al., 2001). Relaxation can occur through (1) fluorescence, (2) photochemical reactions, i.e., LEF, (3) dissipation as heat via non-photochemical quenching (NPQ), or (4) the formation of a triplet chlorophyll (^{3}Chl*). The ^{3}Chl* can be dangerous in the presence of O_2 because it can easily form ROS (e.g., $^1O_2$) which can oxidize and damage photosynthetic membranes (Aro et al., 1993; Krieger-Liszkay, 2005; Triantaphylidès et al., 2008).

Cytochrome b_6f

When the excitation energy is used for LEF, a series of electron transfer reactions occur succeeding PSII. Protonation of the dissociable PQ molecule, Q_B, is converted to a mobile electron carrier plastoquinol (PQH_2), which allows for the transfer of protons and electrons to the second main complex in the chain, cytochrome b_6f (Ort and Yocum, 1996; Kramer et al., 2004a). Cytochrome b_6f (Figure 3) is an integral membrane protein complex that mediates the transfer of electrons between the two PSs while also contributing to the *pmf* as a proton pump. The core structure of cytochrome bc complexes are highly conserved across species and composed of three main parts: cytochrome b, the Rieske iron sulfur protein, and cytochrome f in higher plants (Cape et al., 2006). Electrons are transported through the complex by a mechanism known as the Q-cycle (illustrated in Figure 3) consisting of two redox pathways that are differentiated by their redox potentials (Cape et al., 2006). As a result, the Q-cycle has a role in energy conservation by contributing to the buildup of the *pmf* as well as electron transfer (Mitchell, 1976; Crofts et al., 1983). Through the Q-cycle electrons are both recycled through the thylakoid membrane and onto the next electron carrier plastocyanin.

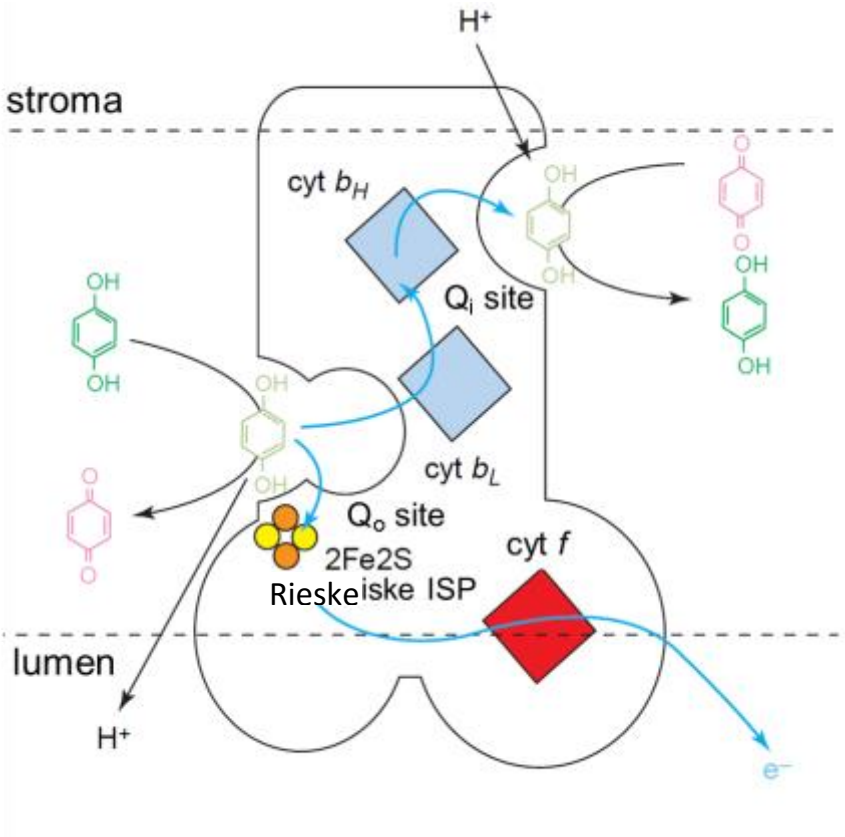

Figure 3. Simplified diagram of cytochrome *b6f* complex and the Q-cycle pathway. In the Q-cycle one electron travels through the high-potential chain, while the second electron retains its energy at the b_L site. Equilibration of the b_L electron through b_H and Q_i site allows for the displacement of the now oxidized PQ at the Q_o site to be replaced with a new PQH_2. A second turnover of PQH_2 through the low-potential chain, results in the reduction and protonation of the intermediate at the Q_i site by acquiring stromal protons. The resulting PQH_2 at the Q_i site is then recycled back into the membrane becoming a source of electrons in addition to aiding in H^+ translocation, because the initial Q-cycle oxidation step at the Q_o site releases H^+ into the lumen space. Image modified from (Cape et al., 2006). Permission to use this figure was granted by the present copyright holder (RightsLink license #4123700803360).

Photosystem I

The last complex of the electron transfer pathway involves the second RC, PSI. Much like in PSII, the RC of PSI is surrounded by LHC chlorophyll-bound proteins that funnel the photon energy to the primary electron donor P700 (Figure 1). The chlorophyll a dimer,

P700, also undergoes a charge separation ($P700^+$) followed by an electron transfer through a chain of electron acceptors: A_o-chlorophyll a monomer, A_1-phylloquinone and a chain of [4Fe4S] clusters (F_x, F_A, F_B) (depicted in Figure 4) (Ort and Yocum, 1996). Accumulation of two reduced Fd molecules leads to the final reduction step of $NADP^+$, catalyzed by ferredoxin-$NADP^+$ reductase (FNR).

The electron transfer reactions of photosynthesis have been historically referred to as the "z-scheme" (as illustrated in Figure 4)(Hill and Bendall, 1960), based on the redox behaviors involving the electron transfer from the two excited chlorophyll states (P680 and P700) through cytochrome b_6f (Govindjee et al., 2017). In addition to the cytochrome b_6f

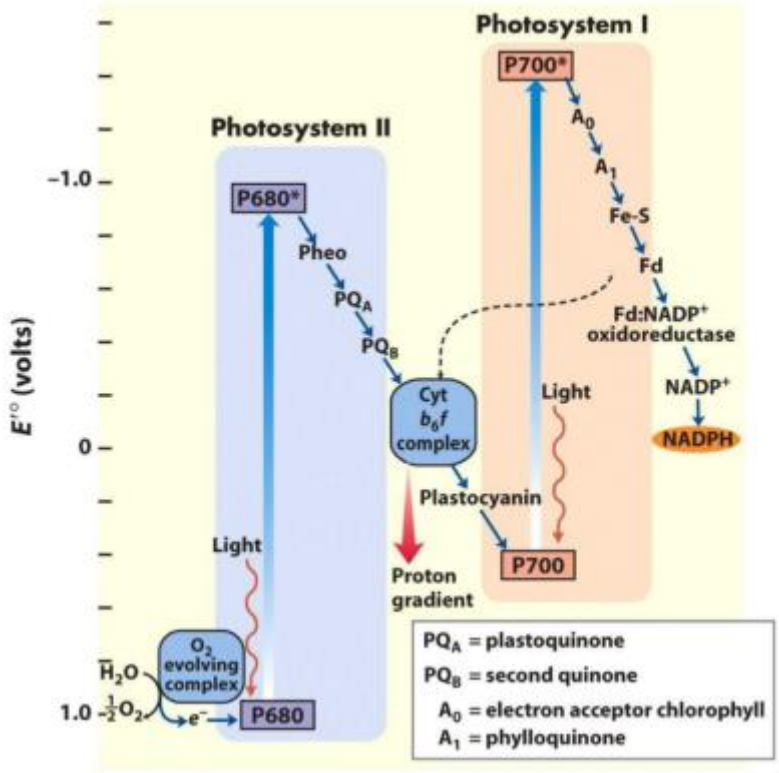

Figure 4. The Z-scheme of oxygenic photosynthesis. The change in reducing potentials following photoexcitation of PSII and PSI (Nelson et al., 2008).

complex, protons are accumulated in the thylakoid lumen through the activity of the oxygen evolving complex at PSII (Figure 4). Therefore, the electron and proton transfer reactions of LEF work in concert to yield a fixed ratio of both reducing potential, NADPH, and chemical energy in the form of ATP.

ATP synthase

The *pmf* buildup from LEF is used to drive the energy-transducing enzyme, ATP synthase. It is a multi-subunit membrane-associated enzyme, which harnesses the proton (H^+) gradient to reversibly synthesize ATP from ADP and P_i. ATP synthase (Figure 5) is composed of two, functionally linked sub-complexes termed coupling factor 1 (CF_1) and CF_o. The CF_o consists of four subunits (a, b, b', and c-ring rotor, also referred to as VI, I, II, III, respectively) and is the integral membrane-spanning portion involved in H^+

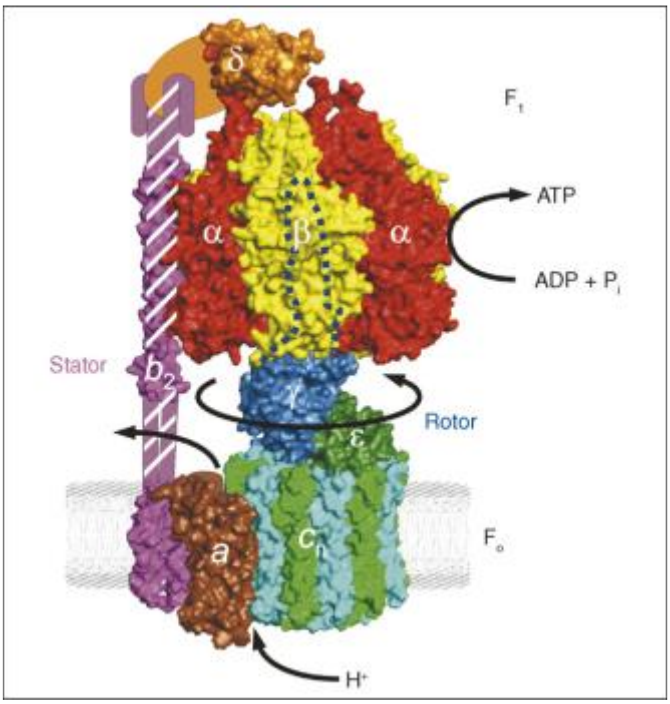

Figure 5. Structure of *E. coli* ATP synthase. Image depicts the major components of ATP synthase rotary mechanism and described in text. Image reproduced from Weber (2007) with permission of the rights holder (RightsLink license #4123711273872).

translocation (Seelert et al., 2000; Varco-Merth et al., 2008). While the other-half, CF_1, is composed of five subunits (α_3, β_3, γ, δ and ε) and is located on the peripheral membrane side containing the catalytic sites for synthesis of ATP (Boekema et al., 1988).

The amount of H^+ required for rotational catalysis and thus the synthesis/hydrolysis of ATP is of major interest because of its involvement in energy metabolism (Strelow and Rumberg, 1993; Van Walraven et al., 1996; Watt et al., 2010). In higher plants, including *Arabidopsis thaliana*, there are 14 c-subunits in CF_0, which lead to the requirement of 14 H^+ to synthesize 3 molecules of ATP, given that the catalytic portion of CF_1 contains 3 $\alpha\beta$ subunits (Seelert et al., 2000). When compared to the H+/2e- stoichiometry produced through LEF (i.e. 6 H^+ per 2 electrons), the net ratio of ATP per NADPH is 1.28 (reviewed in Kramer and Evans, 2011). However, downstream metabolic reactions, e.g., the Calvin-Benson-Bassham (CBB) cycle requires a fixed ratio of 1.5 ATP per NADPH for carbon assimilation (see Appendix A) (Bassham et al., 1954; Allen, 2002). This implies the ratio of ATP per NADPH produced under LEF steady-state conditions is not sufficient for ribulose-1, 5-bisphosphate (RuBP) regeneration by the CBB cycle (Allen, 2002; Kramer et al., 2003). Other thylakoid metabolic reactions, e.g., photorespiration and nitrogen assimilation, also require a fixed stoichiometry of ATP and reductant but at different (often higher) ratios compared to carbon assimilation (Noctor and Foyer, 2000). Therefore, under optimal growth (not including fluctuating light conditions) the amount of ATP being produced from LEF alone is insufficient to drive downstream coupled ATP/NADPH-consuming metabolic reactions.

The chloroplast redox regulation

An added factor to the uniqueness of chloroplast ATP synthase compared to respiratory homologs is a regulatory dithiol domain located on the γ-subunit of CF_1 (Hisabori et al., 2003). The characteristic 40 amino acid residues (196-242 in *Arabidopsis thaliana*), containing the regulatory cysteines (Cys199 and Cys205), are only found in chloroplast ATP synthase complexes (Hisabori et al., 2003; Richter, 2004). It is thought that the regulatory region evolved as a mechanism allowing optimal production and conservation of ATP in response to light (i.e. to minimize wasteful hydrolysis of ATP at night).

Junesch and Gräber (1987) first proposed a model for the different activation energy states ($\Delta\tilde{\mu}_{H+}$), also termed pmf_T (threshold of *pmf*), needed to drive the chloroplast

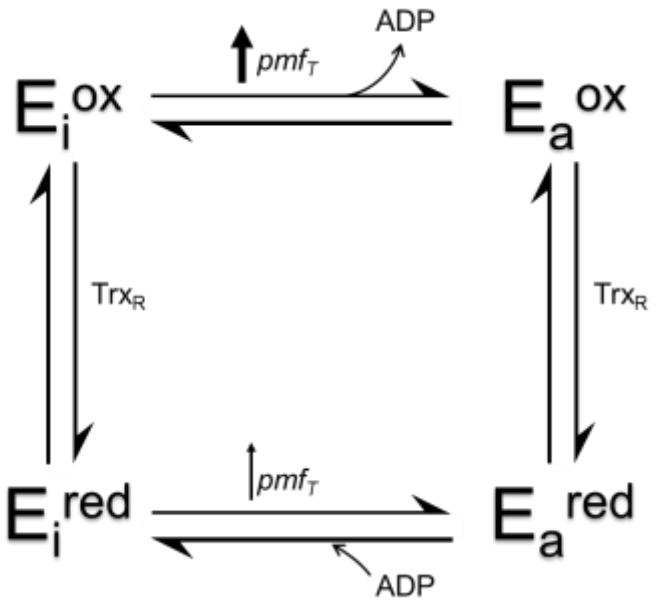

Figure 6. Schematic of the four different energy states of ATP synthase. Based on the influence of the redox state in the γ-subunit thiols, ATP synthase requires different membrane energization potentials (also termed pmf_T) as depicted with the intensity of the arrows, for the synthesis of ATP. (E) energy state, (i) inactive, (a) active, (ox) oxidized, and (red) reduced. The mechanism of the different states is described in the text.

ATP synthase. The different energy states are regulated by electron transport reactions and their immediate (ΔpH) and secondary (redox state of the enzyme) effects. In the model (Figure 6), the pmf_T requirement is higher when ATP synthase is in an oxidized disulfide state, e.g., in the dark, while a lower energization is required under reducing conditions, such as under high light exposure (due to the presence of reduced Fd) or in the presence of exogenous reducing agents, e.g., dithiothreitol (DTT) (Junesch and Gräber, 1987; Kramer and Crofts, 1989). This implies that when the CF_1 γ-subunit thiols are reduced, the pmf_T needed to synthesize ATP is much smaller, i.e., ~1 pH unit lower (i.e. 60 mV), compared to the oxidized thiol-state, leading to increased photophosphorylation at limiting *pmf* (Vallejos et al., 1983; Ketcham et al., 1984; Junesch and Gräber, 1987; Kramer and Crofts, 1989; Junesch and Gräber, 1991). The outcome of a higher pmf_T under unfavorable or oxidizing conditions for CF_oF_1 is the hindrance of wasteful ATP hydrolysis in the dark and hence conservation of energy.

The proton motive force (*pmf*)

The energetic link between the electron transport reactions of photosynthesis and the metabolic energy currency in cells, ATP, is the *pmf*. Therefore, to get a better understanding of the key player in the dynamics of photosynthesis we will further discuss the properties that constitute the *pmf*. The *pmf* is differentiated into two components: an electric potential (ΔΨ) between the aqueous phases and the pH gradient (ΔpH) established across the thylakoid membrane (Mitchell, 1966; Hangarter and Good, 1982; Cruz et al., 2001). The thermodynamic contributions of these two components to *pmf* is given by

$$pmf = \Delta\Psi(\mathrm{i} - \mathrm{o}) + \left(\frac{2.3\mathrm{RT}}{\mathrm{F}}\right)\Delta\mathrm{pH}(\mathrm{o} - \mathrm{i})$$

The sum of the two components (expressed in volts) make up the driving force for the synthesis of ATP (Mitchell, 1966; Cruz et al., 2001). The constants R and F are the universal gas and the Faraday constant, respectively.

Although the two components of *pmf* are thermodynamically equivalent, meaning that a change in one ΔpH unit will equally affect the ATP/ADP equilibrium as a shift in ΔΨ by ~60 mV (Nicholls and Ferguson, 2002; Junge and Nelson, 2015), the distribution of ΔΨ and ΔpH differ between species (Kramer et al., 1999). Moreover, the distribution of the two *pmf* components influence cellular processes differently. For example, acidification of the thylakoid lumen, attributed to the ΔpH component, is associated with photo-protection.

In yeast mitochondria and aerobic bacteria the major contribution of *pmf* is ΔΨ rather than ΔpH, presumably as an evolutionary mechanism to function in a broad pH range (Fischer and Gräber, 1999; Petersen et al., 2012). However, in chloroplasts, ΔΨ and ΔpH are kinetically equivalent, i.e., they equally influence the rate of ATP synthesis, and the magnitude of each component can be influenced by a variety of parameters, e.g., ADP, P_i, Mg^{2+}, and the redox state of CF_oF_1 (Gräber et al., 1984; Turina et al., 1991; Kramer et al., 1999; Fischer et al., 2000; Turina et al., 2016).

The *pmf*, therefore, functions as more than a driving force for ATP synthase, but also a regulatory sensor involved in photo-protection, redox signaling, and feedback regulation for photosynthesis (Kramer et al., 2003; Cruz et al., 2005a). Recent studies have supported the importance of *pmf* partitioning and its role in modulating ATP synthase, while also protecting against over-acidification of lumenal components, modulating the activity of the cytochrome *b6f* complex, and activation of the photo-protective mechanisms (Cruz et al.,

2005b; Takizawa et al., 2007; Rott et al., 2011; Armbruster et al., 2014; Strand and Kramer, 2014; Carrillo et al., 2016).

A high-degree of regulation is required for the light-reactions

Unlike a majority of the photosynthetic research currently being conducted under steady-state conditions our work focuses on stochastic (i.e. more naturalistic) environmental settings. Most higher plants experience quickly alternating periods of light and shade (Figure 7), known as sunflecks, which can adversely affect photosynthesis (Pearcy, 1990). For this reason, this research aims at understanding those dynamic

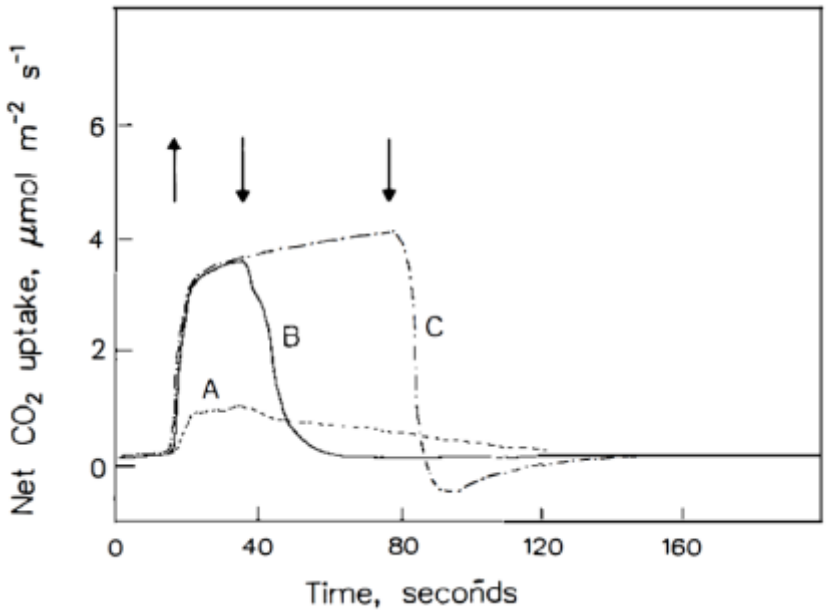

Figure 7. Dynamic photosynthetic responses dependent on light. Illustrating the relationship between net photosynthetic CO_2 uptake in response to different light conditions and plant induction state. When plants are kept in the dark for long periods of time (+2 hr), take longer to acclimate and respond to light exposure (A). When plants have been exposed to light, they can more quickly react to light exposure and CO_2 assimilation (B). The duration of high-light exposure also effects photosynthetic processes and can result in post-light CO_2 burst (C). The arrows indicate the point of light exposure activation/deactivation. Image from (Pearcy, P.W. 1990).

environmental conditions occurring in nature and the role by which the *pmf* aids in regulation. This section will emphasize the different forms by which *pmf* alleviates and augments photosynthesis under varying dynamic conditions. Beginning with the ΔpH component of *pmf* and its role in photo-protection and NPQ.

Non-photochemical quenching

The thermal dissipation pathway of NPQ (third route of Figure 2) can be further differentiated into several different quenching forms: qE, energy dependent (i.e. ΔpH) quenching; qT, state transition component; and qI, photoinhibition component, according to the dark relaxation kinetics of each (Horton and Hague, 1988). While qI and qT play a role on a longer (i.e. minutes) time-scale, the most relevant and influential component in the immediate photo-protective mechanism is qE. This mechanism is rapidly induced (seconds time-scale) by a decrease in pH of the thylakoid lumen. Moreover, the reversibility of the mechanism allows for optimal sensing of fluctuating light and the direct effects of ΔpH.

Sensing a decrease in pH occurs through two mechanisms, protonation of PSII subunit S protein (PsbS) (Li et al., 2004) and activation of the violaxanthin de-epoxidase enzyme of the xanthophyll cycle (Demmig-Adams and Adams III, 1996). The PsbS protein, also known as CP22, is part of the LHC antenna system of PSII and functions as a pH sensor through two lumen-exposed glutamates (Li et al., 2004). Protonation of the glutamates leads to a conformational change of PSII and its associated LHCs to aid in the zeaxanthin dissipative state (Johnson and Ruban, 2011). Activation of the violaxanthin de-epoxidase, which is strictly controlled by the lumen pH, catalyzes the conversion of violaxanthin to the intermediate antheraxanthin and finally to the quenching pigment zeaxanthin (Demmig-

Adams and Adams III, 1996). Both mechanisms work together in altering the PSII antenna system and quenches the ^{1}Chl* state (Gilmore, 1997; Ruban et al., 2012). While qE prevents photo-damage by dissipating the energy of ^{1}Chl* as heat, it also affects the alternative routes, including photochemistry.

Photoinhibition

Contrary to the qE mechanism, the irreversible photoinhibitory component, qI down-regulates PSII at a longer time-scale (min to hr). This can occur under extended exposure to elevated light intensities causing the rate of energy absorption to outcompete the transfer of chemical energy (fourth route in Figure 2). This can result in the accumulation of ^{1}Chl* molecules, (through forward- or reverse electron transfer reactions), which are capable of generating damaging $^1O_2$ via electron spin exchange (Krieger-Liszkay, 2005; Ruban et al., 2012).

Metabolic flexibility

In addition to the sensitivity of light intensities, photosynthesis also requires metabolic flexibility. The tightly coupled H^+ and electron transfer reactions of LEF generate ATP and NADPH at fixed stoichiometric ratios required to fuel downstream metabolic reactions (Arnon et al., 1958; Sivak and Walker, 1986; Furbank and Horton, 1987; Allen, 2002). However, as mentioned above, under steady-state conditions the metabolic (ATP/NADPH) ratio from LEF alone is insufficient to drive the metabolic reactions. Moreover, the turnover rate of ATP and NADPH pools in the chloroplasts are very fast, on the order of tens to hundreds of milliseconds (Lilley et al., 1982; Noctor and Foyer, 2000; Kramer and Evans, 2011). Therefore, the production and consumption of these molecules must be tightly coordinated to prevent thermodynamic constraints on photosynthesis.

Previous work has demonstrated that mismatches in the ATP/NADPH pools, induced by rapid fluctuations of light and/or introduction of biotic and abiotic stresses, can quickly inhibit photosynthesis (Avenson et al., 2005; Cruz et al., 2005a; Amthor, 2010). Therefore, adequate regulatory mechanisms are required to keep plastidial reactions in balance in the face of a stochastic environments.

Mechanisms that modulate the *pmf* and ATP homeostasis

To decipher the way in which photosynthesis copes with dynamic conditions, a better understanding of how the *pmf* and ATP is modulated is imperative. Modulation of

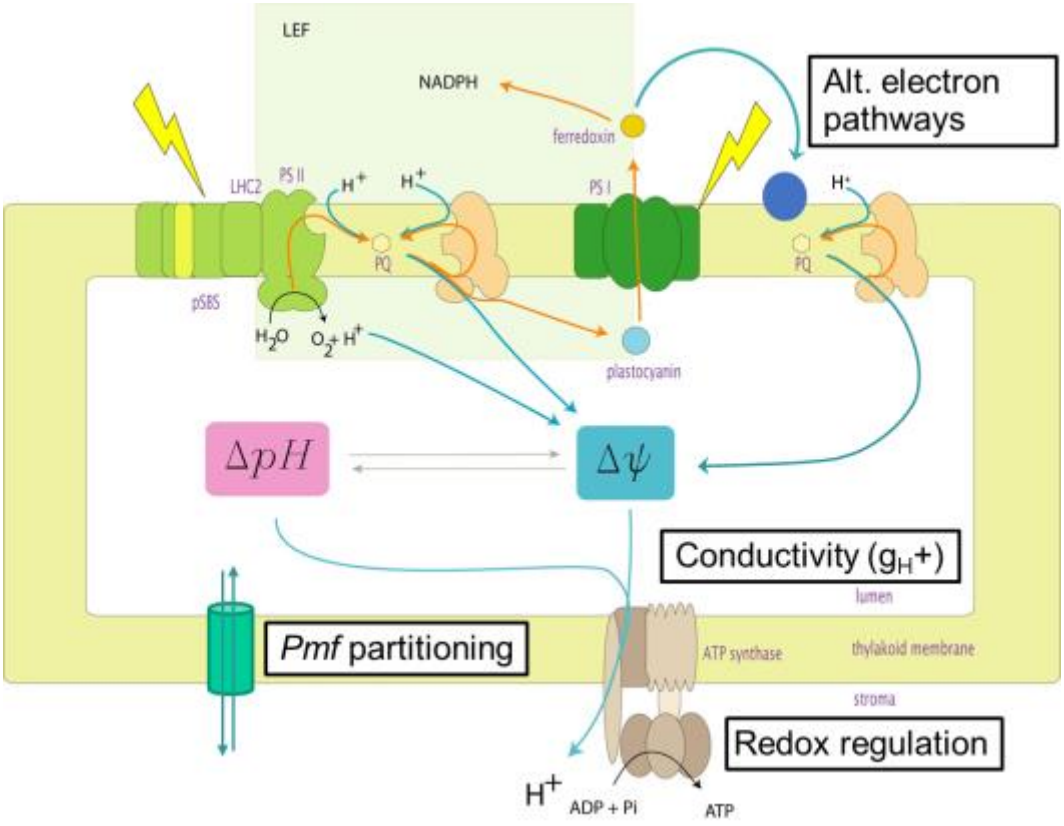

Figure 8. Mechanisms that modulate the *pmf*. The image depicts the thylakoid membrane with the major photosynthetic components embedded. The four mechanisms (boxed) are involved in *pmf* modulation in response to the light reactions of photosynthesis. Image modified from (Kramer et al., 2004).

the *pmf* is linked directly and indirectly to ATP synthase (Kramer et al., 2004a; Armbruster et al., 2014; Carrillo et al., 2016). This relationship is illustrated with four mechanisms (Figure 8): 1) alternative electron pathways, 2) *pmf* partitioning, 3) ATP synthase proton conductivity (g_H+), and 4) redox regulation. These reveal critical connections between the light induced *pmf* and downstream metabolism of the chloroplast.

Alternative electron pathways within the chloroplast

Currently, there are four predicted electron flow pathways (Figure 9): 1) cyclic electron flow (CEF), 2) water-water cycle, 3) malate valve, and 4) plastid terminal oxidase, that can augment ATP and/or displace electrons and thus reductant (Cruz et al., 2005a; Eberhard et al., 2008; Kramer and Evans, 2011). The CEF pathway functions to supplement the ATP produced through LEF, by also contributing to the *pmf*, but without concomitant NADPH production. The electron transfer pathways of CEF are under intensive investigation, although all require the transfer of stromal reducing equivalents back to PSI through the PQ pool without the involvement of PSII (Joliot and Johnson, 2011; Kramer and Evans, 2011).

The water-water cycle (Figure 9), also known as the Mehler peroxidase reaction, is like CEF in that electrons are prevented from reducing $NADP^+$ but serve to reduce oxygen to superoxide radical ($O_2^{-\cdot}$) (Asada, 1999). Superoxide is then dismutated to hydrogen peroxide (H_2O_2), which is reduced by ascorbate peroxidase to form oxygen and water. The overall process uses electrons derived from the splitting of water at the PSII OEC as well as the electrons from PSI to regenerate water from oxygen, hence the name water-water cycle (Asada, 1999; Asada, 2006).

The malate valve pathway uses NADPH to reduce oxaloacetate to malate by NADP-dependent malate dehydrogenase (MDH), which is shunted from the chloroplasts to mitochondria (Scheibe, 2004). In the mitochondria, this reducing power can be dissipated by alternative oxidase respiration. Lastly, the plastid terminal oxidase (PTOX) augments the ATP deficit in a related manner by shunting electrons from the PQ pool to oxygen (Scheibe, 2004). These alternative pathways (Figure 9) aid in augmenting the ratio of ATP/NADPH by either contributing to the generation of the *pmf* without supplying reducing potential or by selectively consuming the NADPH.

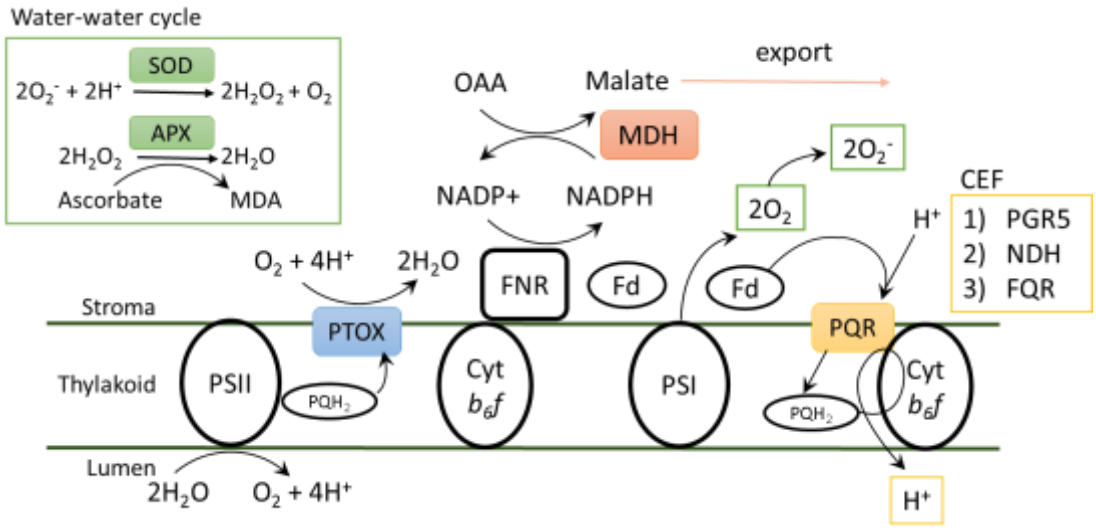

Figure 9. Schematic representation of the alternative chloroplast electron transport pathways. These alternative chloroplast pathways augment ATP by either pumping additional protons into the thylakoid lumen (CEF-yellow) or by consuming forms of reducing potential. The plastid terminal oxidase (PTOX-blue) reduces O_2 by using the reducing potential from PSII, while the water-water cycle (green) takes electrons directly from PSI and NADP-malate dehydrogenase (MDH-orange) derives its reducing potential also from PSI. Detailed mechanisms described in text.

Pmf partitioning

The mechanisms described above are particularly useful in the presence of environmental stresses, e.g., when ATP demand is high. For instance, CEF is induced under low temperature and drought (Clarke and Johnson, 2001; Kohzuma et al., 2009); however, under non-stressed steady-state conditions CEF is minimally engaged (Bendall and Manasse, 1995; Cruz et al., 2005a; Livingston et al., 2010). The same applies for water-water cycle, malate valve and PTOX with less than 5% contribution to the ATP/NADPH budget compared to LEF, even in the presence of severe stress (Clarke and Johnson, 2001; Joët et al., 2002; Scheibe, 2004; Streb et al., 2005).

Modeling and kinetic studies of the production and consumption products from the photochemical reactions with these alternative ATP augmenting mechanisms (Figure 9) have only confirmed minimal contributions to the quantum yield of CO_2 fixation (Genty et al., 1989; Foyer et al., 1992; Cruz et al., 2005a; Eberhard et al., 2008). These studies were led by earlier work using isolated chloroplasts that assumed an enclosed plastid system, where the metabolic pools are self-contained. Nonetheless, a great deal of evidence is arising focused on 'crosstalk' and the interaction of metabolites between the plastid and other cellular compartments (Noctor and Foyer, 2000; Weber, 2004; Weber and Fischer, 2007; Weber and Facchinelli, 2011).

These observations lead to a different type of mechanism, often excluded from the list, the role of transporters in supplying adenylate balance across the chloroplasts membrane. Chloroplasts are enclosed by two membranes: a permeable outer membrane layer for proteins <10 kDa and an inner, more selective, membrane embedded with transporters for specific metabolic transport. It seems imperative that interaction between

the chloroplasts and mitochondria, the two major ATP producing organelles via photophosphorylation and oxidative phosphorylation, respectively, would allow for metabolic exchange.

In chloroplasts, an specific ATP transporter, termed nucleoside triphosphate transporter (NTT), allows for direct reversible-exchange of ATP with ADP and P_i (Kampfenkel et al., 1995; Neuhaus et al., 1997). Based on the early studies of adenylate transport (Heldt, 1969; Strotmann and Berger, 1969), showing minimal rates of adenylate exchange (~4.5 μmoles ATP mg^{-1} Chl hr^{-1}), ATP transport is not considered a major contributor to energy balance. It has been proposed that energy provision by NTT occurs under more severe ATP limited conditions, e.g., in the dark when the light reactions of photosynthesis are not driving ATP production (Reiser et al., 2004; Reinhold et al., 2007).

Recent studies on ATP transporters of pathogenic obligate intracellular bacteria, such as *Rickettsia prowazekii* and *Chlamydia trachomatis*, revealed high homology to plastid NTTs and require P_i as a co-substrate with ADP for effective hetero-exchange of adenylates (Trentmann et al., 2007; Trentmann et al., 2008). These observations suggest issues with some of the experimental setup for the early ATP kinetic measurements and warrants reinvestigation. Chapter 3 "Evidence for Rapid ATP Exchange across the Chloroplast Envelope," focuses on our new measurements of ATP exchange via NTT and reasons why this mechanism is important for chloroplast ATP balance.

ATP synthase proton conductivity

Under specific conditions, environmental stresses can modulate ATP synthase activity, generating an acidified thylakoid lumen that upregulates the qE response (Kramer et al., 2004a; Avenson et al., 2005). Modulation of the activity occurs by either decreasing

the conductivity of ATP synthase (g_H+) with a constant LEF, thus creating a back pressure of H^+, or by altering the fraction of the *pmf* components, e.g., to increase the ratio of ΔpH to ΔΨ (Kanazawa and Kramer, 2002; Kramer et al., 2004a; Kramer et al., 2004b). The activity of stromal assimilatory enzymes are controlled by the levels of ATP, ADP and P_i (Sharkey, 1990), altering those levels by modulating the g_H+, which has been demonstrated under low CO_2 conditions adds another form of flexibility to photosynthesis.

One example of this form of regulation is demonstrated in *Arabidopsis thaliana* K^+ efflux antiporter (KEA3) mutant, described further in the Appendix B. The KEA3 antiporter is located on the thylakoid membrane and functions by transporting lumenal protons in exchange for potassium ions across the membrane (Armbruster et al., 2014). We proposed that KEA3 accelerates photosynthetic acclimation, particularly under rapid changes in light intensities, by aiding in the downregulation of qE (Armbruster et al., 2014). The *kea3* mutants display increased levels of NPQ and qE response induced by the *pmf* partitioning mechanism demonstrating a greater proportion of the ΔpH component of the *pmf* compared to wild type (see Appendix B).

Chloroplast redox regulation

As mentioned with ATP synthase and illustrated in Figure 8, redox regulation is another form of *pmf* modulation and the flexibility that plants have adapted that is light-dependent, abundant and rapidly regulated. This form of regulation is not only important in plants but in most living systems and functions as a reversible post-translational modification affecting the activation of genes (Buchanan and Balmer, 2005). Regulation occurs by the ubiquitous disulfide thioredoxin proteins and in some cases a reductase that catalyzes the reduction of regulatory cysteine (Cys) on proteins (illustrated in Figure 10).

Altering of the disulfide from a reduced form (-SH HS-) to an oxidized form (-S-S-) is a reversible mechanism and affects stability of the structure and redox state leading to a catalytic or regulatory change (Buchanan, 1980; Yano et al., 2002; Hogg, 2003).

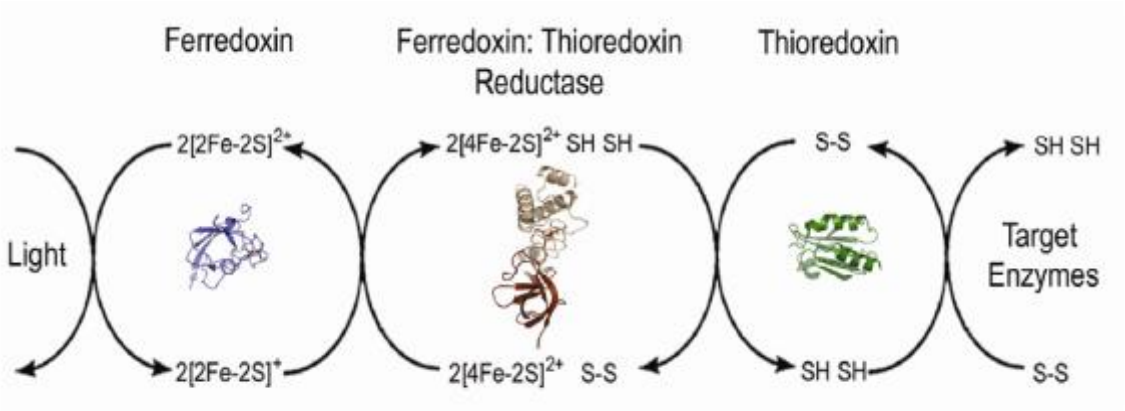

Figure 10. The FTR system in relation to the light reactions. Reducing potential, Fd, is derived from the light reactions allow for ferredoxin: thioredoxin reductase (FTR) system to reduce thioredoxin. This central redox signaling system functions in symmetry with light allowing for activation and deactivation of enzymes with respect to light. Image adapted from Dai et al. (2007) with permission of the rights holder (RightsLink license #4123730075446)

The first discovered and well-established thioredoxin system in plastids is the ferredoxin thioredoxin reductase (FTR). It is considered the primary mechanism (Figure 10) that coordinates activation of the light-dependent reactions and enzyme activity of photosynthesis, first reviewed in 1980 (Buchanan, 1980). FTR was initially proposed to target two types of thioredoxin (Trx) in chloroplasts: Trx-f and Trx-m, names derived from the selectivity in activating CBB cycle enzymes (Buchanan, 1980). Trx are widely distributed proteins of low molecular weight (~12 kDa) with a conserved redox-active motif (WCGPC), especially in plants, that efficiently reduce (or oxidize) regulatory thiols on target enzymes.

For example, one target enzyme being ATP synthase, which is considered a dormant enzyme, i.e., it remains inactive in the dark and oxidizing conditions. With only a minimal amount of light (~4 μmol photons m^2 s^{-1}) the redox-sensitive Cys on the γ-subunit of ATP synthase are readily reduced (Kramer et al., 1990). Reduction of the disulfide bonds of ATP synthase, as well as CBB cycle enzymes occur by Trx redox regulation (Figure 10), derived from reduced Fd of the PSI light reactions (Buchanan, 1980; Capitani et al., 2000). In the dark (and most likely under oxidizing conditions) the reverse sequence of events occur, leading to the deactivation of enzymes (Leegood and Walker, 1980).

Following the sequencing of the *Arabidopsis thaliana* genome, numerous additional Trx isoforms (~20) were found in the chloroplast and classified into 7 different subtypes: Trx f1-2, m1-4, x, y1-2 and z, based on the molecular characteristics and redox midpoint potential properties (Collin et al., 2003; Yoshida et al., 2014; Thormählen et al., 2017). Biochemical studies suggest that each of the different Trxs function in a distinct manner and target specific regulatory enzymes, possibly to aid in the flexibility of the photosynthetic system (Collin et al., 2003; Yoshida et al., 2014; Yoshida and Hisabori, 2016). Currently there are two known reduction systems in plants: 1) a variant of the prokaryotic system called NADPH-thioredoxin reductase C (NTRC) and the canonical 2) FTR system, described above.

The second chloroplast reductase system, NTRC, was more recently discovered during rice genome sequencing and is found exclusively in oxygenic organisms (Serrato et al., 2004; Pascual et al., 2010). As discussed further in chapter two, NTRC is different from the canonical FTR system with a distinct structure, source of reducing power and potentially regulatory target. NTRC contains both a reductase (NTR) and Trx on a single

polypeptide using NADPH as the electron source (Serrato et al., 2004; Pérez-Ruiz et al., 2006). The reducing agent being NADPH rather than Fd, complements the FTR system and provides additional flexibility in redox regulation because the production of NADPH can also occur in the dark via oxidative pentose phosphate pathway (Neuhaus and Emes, 2000).

Studies have shown high reduction affinity between the dimeric 2-Cys peroxiredoxin (Prx) and NTRC (Pérez-Ruiz et al., 2006; Cejudo et al., 2012; Bernal-Bayard et al., 2014). This implies a different form of redox regulation for NTRC, possibly involved in protection from photo-oxidative stress. Moreover, NTRC has been proposed to regulate a wide range of systems, including ADP glucose pyrophosphorylase involved in starch biosynthesis (Michalska et al., 2009; Lepistö et al., 2013), enzymes involved in chlorophyll biosynthesis (Richter et al., 2013; Pérez-Ruiz et al., 2014) and most interestingly ATP synthase and photosynthesis (Carrillo et al., 2016; Naranjo et al., 2016; Nikkanen et al., 2016). There has been a growing concern in the field of redox regulation and photosynthesis, to better understand the differences between the highly similar redox regulators: FTR and NTRC (Yoshida and Hisabori, 2016; Gütle et al., 2017; Thormählen et al., 2017), with relation to the dynamics of photosynthesis.

Aims of Dissertation

The focus of this dissertation is aimed at better understanding the dynamics of photosynthesis in coping with rapid changes in light intensity. Unlike most ATP synthase enzymes, CF_oF_1 can be rapidly activated in the light and involves a structural conformational change in the ε- and γ-subunit. The shift in conformation lowers the

activation state/kinetic barrier for the $\Delta\tilde{\mu}_{H+}$ requirement, allowing the enzyme to rapidly sense and respond to sensitive light ranges (Richter and Gao, 1996; von Ballmoos et al., 2009).

Chapter two centers on the Trx redox regulation of the γ-subunit of ATP synthase that allows for the rapid activation of the enzyme. Previous work has demonstrated the uniquely rapid reduction of the regulatory thiols of CF_oF_1 only require minimal light and the work presented here link it to NTRC. NTRC derives its reducing potential from the more reducing substrate, NADPH, which can be supplied independent of the light reactions of photosynthesis. This work proposes that NTRC complements FTR-Trx redox regulation in allowing for the reduction of the regulatory thiols of CF_oF_1 at different (lower) irradiance levels. Both Fd and NADPH contain varying redox potentials (~-300-330, $E_{m,7.5}$ versus ~-275, $E_{m,7.5}$, respectively) and enzymatic targets (CBB cycle enzymes versus 2-Cys Prx) (Yoshida and Hisabori, 2016; Yoshida and Hisabori, 2017). One could propose that having two redox pools allows for a greater flexibility in the activation and deactivation of photosynthetic enzymes.

Chapter three adds flexibility to the photosynthetic metabolic system with a focus on NTT. Our findings provide evidence for rapid exchange of ATP across the chloroplast membrane and the adverse photosynthetic effects caused by a decrease in the activity of both NTT isoforms. Direct exchange of adenylates through the plastidial and other cellular compartments is vital in ATP and metabolic homeostasis. The research supports the hypothesis of direct exchange of ATP and ADP plus P_i.

Plants have evolved diverse mechanisms to allow them to withstand the dynamics of environmental pressures, e.g., rapid alterations in light intensity. By addressing the

mechanisms involved in modulating ATP homeostasis through ATP synthase and the *pmf*, we are closer to better understanding the complexities and dynamics of the photosynthetic system.

APPENDICES

APPENDIX A:

Carbon assimilation

Carbon assimilation is the second component of photosynthesis and occurs in the stroma of chloroplasts using the end products of the photochemical reactions, ATP and NADPH. The carbon fixation process is divided in three phases: carboxylation, reduction and regeneration, to complete the CBB cycle (Supplemental Figure 1). The process of photosynthesis was once proposed to consist of light and dark reactions, implying the CBB cycle occurred in darkness; however, several enzymes of the CBB cycle are regulated by light and become inactivated in the dark making light and dark reaction titles misleading (Buchanan, 1980). The photosynthetic light reactions provide more than the ATP and NADPH required to fuel the CBB cycle. For instance, there are four redox-regulated enzymes in the CBB cycle directly activated by light-induced thioredoxin reduction (Michelet et al., 2013). Photochemical products from LEF are used in the CBB cycle to fix atmospheric CO_2 into two main carbon products, starch and sucrose synthesized in the chloroplasts and cytosol, respectively (Cséke and Buchanan, 1986; Quick and Neuhaus, 1997).

Within the CBB cycle, there are 11 different enzymes involved in catalyzing the 13 reactions, as shown in Supplemental Figure 1 (Wilson and Calvin, 1955; Raines, 2003; Michelet et al., 2013). The cycle begins with the enzyme ribulose-1, 5-bisphosphate carboxylase oxygenase, commonly referred to as Rubisco, to catalyze the carboxylation of ribulose-1, 5-bisphosphate (RuBP) with CO_2 to make 2 molecules of 3-phosphoglycerate (3-PGA). Rubisco is also capable of catalyzing the oxidation of RuBP in competition with carbon assimilation (Hartman and Harpel, 1994). A great deal of effort has been devoted to the optimization of the rate-limiting step in carbon fixation (Hartman and Harpel, 1994);

however, more recent work has proposed an evolutionary motive for the 'so-called inefficient' Rubisco in photoprotection against excess O_2 levels (Ort and Baker, 2002).

The reduction phase of the CBB cycle utilizes 3-PGA along with ATP and NADPH for two sequential events producing triose phosphates, glyceraldehyde phosphate (GAP) and dihydroxyacetone phosphate (DHAP) (Quick and Neuhaus, 1997; Raines, 2003). At this point in the cycle, the triose phosphates can be utilized to fuel the regenerative phase of the cycle via fructose-bisphosphate aldolase enzyme making fructose-1,6-bisphosphate, or alternatively exit the cycle to synthesize sucrose. The regenerative phase allows for the conversion of 3-carbon molecules into 5-carbon intermediates starting with fructose-6-phosphate (F6P) using the transketolase enzyme and an additional GAP molecule. The enzyme, fructose-1,6-bisphosphatase, that catalyzes F6P formation is one of the four light-regulated CBB cycle enzymes through reduction via Fd-Trx reductases system (highlighted in blue, Supplemental Figure 1)(Buchanan, 1980; Lemaire et al., 2007; Schürmann and Buchanan, 2008). During this point of the cycle, F6P can take an alternative path for the synthesis of starch. However, many of the triose phosphates produced in the cycle are utilized for the regeneration of RuBP. The remaining steps in the cycle involve the catalysis of six reactions and utilize an additional ATP molecule to produce RuBP and a net gain of carbon sources.

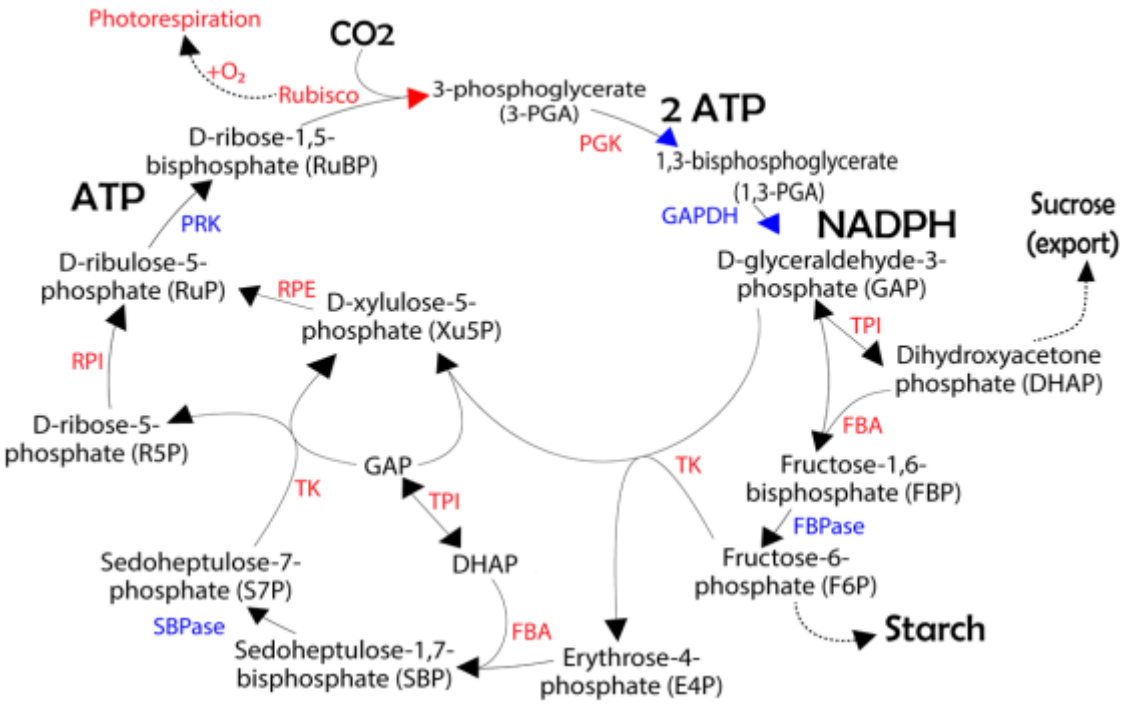

Supplemental Figure 1. The metabolites and redox regulated enzymes of the CBB cycle. The metabolites are depicted in the main ring (black) with enzymes (red and blue). The four thioredoxin activated enzymes are in blue and the blue arrows indicate carboxylation steps, black arrows for reduction and red for regeneration. The enzymes include: Rubisco (ribulose-1,5-bisphosphate carboxylase/oxygenase), PGK (phosphoglycerate kinase), GAPDH (glyceraldehyde-3-phosphatedehydrogenase), TPI (triose phosphate isomerase), FBA (fructose-1,6-bisphosphatealdolase), FBPase (fructose-1,6-bisphosphatase), TK (transketolase), SBPase (sedoheptulose-1,7-bisphosphatase), RPE (ribulose-5-phosphate 3-epimerase), RPI (ribose-5-phosphate isomerase) PRK (phosphoribulokinase). The metabolites involved are: RuBP (ribulose 1,5-bisphosphate), 3-PGA (3-phosphoglycerate), 1,3-PGA (1,3-bisphosphoglycerate), GAP (glyceraldehyde 3-phosphate), DHAP (dihydroxyacetonephosphate), F1,6P (fructose 1,6-bisphosphate), F6P (fructose 6-phosphate), Xu5P (xylulose 5-phosphate), E4P (erythrose 4-phosphate), SBP (sedoheptulose 1,7-bisphosphate), S7P (sedoheptulose 7-phosphate), R5P (ribulose 5-phosphate), and Ru5P (ribulose 5-phosphate).

APPENDIX B:

The thylakoid K^+/H^+ antiporter KEA3 facilitates lumenal H^+ efflux and photosynthetic acclimation under low lumenal pH

The thylakoid K+/H+ antiporter KEA3 facilitates lumenal H+ efflux and photosynthetic acclimation under low lumenal pH

L. Ruby Carrillo, Ute Armbruster, and David Kramer

Some of the work presented in this Appendix has been published:

Ute Armbruster, L. Ruby Carrillo, Kees Venema, Lazar Pavlovic, Elisabeth Schmidtmann, Ari Kornfeld, Peter Jahns, Joseph A. Berry, David M. Kramer & Martin C. Jonikas

(2014)

Nature communications doi:10.1038/ncomms6439

Abstract

Due to the sessile nature of plants, they have evolved a number of mechanisms to cope with fluctuating environmental conditions. One mechanism being nonphotochemical quenching (NPQ), which reversibly allows for excess irradiance to be dissipated as heat and prevents the photosynthetic apparatus from being damaged. The *Arabidopsis thaliana* K^+/H^+ antiporter (KEA3) is located on thylakoid membrane and our work led us to believe it plays a role in NPQ upon transitioning from extreme light conditions (prolonged dark or high light exposure) to low light. Kea3 displays a persistent recovery of NPQ, specifically qE, the pH and energy-dependent form of NPQ after shifting mutants to low light. Additionally, when leaves were treated with an artificial PSI electron acceptor methyl viologen, which causes very low lumenal pH, *kea3* showed a lower thylakoid membrane conductance to protons. This suggests that under stressful conditions, such as under very low lumenal pH, KEA3 functions as a proton safety valve that mediates proton efflux from the lumen. Our results imply a protective role for KEA3 in photosynthesis, activated at a low lumen pH, presumably to aid in photosynthetic efficiency under fluctuating light conditions.

Introduction

Plants can experience periods of extremely stressful environmental conditions during their lifetime. To be able to survive and reproduce in e.g., temperature, salt and/ or water stress they have evolved intricate coping strategies. Particularly, photosynthesis, the engine of plant growth and reproduction is tightly tuned to maximize light capture efficiently and avoid the potentially detrimental effects of stress that can damage the cell and even decrease the overall photosynthetic capacity (Li et al., 2009).

Most abiotic stresses massively inhibit the rate of photosystem II (PSII) repair, which has been linked to the activity of CO_2 fixation via the CBB cycle (reviewed by (Takahashi and Murata, 2008). Damaging effects on the CBB cycle cause a cascade of events including back pressure restrictions on the photosynthetic apparatus, resulting in increased exposure to excitation pressures at PSII which can be detrimental.

A number of mechanisms have been proposed to alleviate misbalances of metabolites caused by abiotic stresses or a damaged CBB system such as, enhancing cyclic electron flow around PSI and decreasing the conductivity of ATP synthase (g_{H^+}) (Clarke and Johnson, 2001; Kohzuma et al., 2009a). These mechanisms result in a lower lumenal pH that is advantageous because it triggers mechanisms that quench excess light energy (Krause, 1988; Demmig-Adams and Adams III, 1996; Li et al., 2004) and thereby relieves the photosynthetic electron transport chain of the high excitation pressure. Despite the fact that high levels of the photoprotective energy quenching, such as non-photochemical quenching (NPQ) response are beneficial in stress conditions, it is essential that the proton concentration that attributed the quenching stay below a critical threshold (Kramer et al., 1999). If rising above this threshold, it causes the denaturation and continuous inactivation

of important lumenal components of the photosynthetic electron transport chain. Specifically, the PSII oxygen evolving complex, plastocyanin, and cytochrome b_6f are susceptible to denaturation by low lumenal pH (Krieger et al., 1992; Gross et al., 1994; Kramer et al., 1999).

The overall photosynthetic capacity is susceptible to environmental pressures, especially when experienced at a longer time-scale (Li et al., 2009). As a preventative solution, photosynthesis has evolved regulatory mechanism that aid with the environmental dynamics which adjust lumenal pH to levels that maximize energy quenching and photoprotection, but maintain the intactness of the photosynthetic apparatus. Much effort has been devoted to the mechanisms that allow plants to cope with the extreme conditions (Kramer et al., 2004a; Cruz et al., 2005; Eberhard et al., 2008), yet inactivation and regulation of those methods to a lesser extent.

This research presents one form of photosynthetic acclimation via a proton safety valve called KEA3 that can stabilize the lumen pH above a certain threshold. Due to its trans-thylakoid proton transport properties, we set out to investigate whether KEA3 could have a role, as part of a thylakoid proton safety valve, in dissipating excess *pmf* under rapid fluctuations in light intensities. Here, we show that the K^+/H^+ antiport activity of KEA3 facilitates the photosynthetic efficiency of PSII by accelerating the downregulation of the pH-dependent NPQ response under fluctuating light conditions. Furthermore, if treated with the PSI electron acceptor methyl viologen (MV), which causes an acidified thylakoid lumen, *kea3* mutants display a lower membrane conductance to protons as compared to wild type (WT). Altogether, these data suggest that KEA3 may indeed be (part of) a

thylakoid proton safety valve that operates in stress conditions, to avoid long-term inactivation of photosynthetic electron transport.

Results

KEA3 displays rapid photosynthetic acclimation response under fluctuating light

The photosynthetic regulatory responses of the KEA3 K^+/H^+ antiporter was investigated by first accessing the chlorophyll a fluorescence response under an array of light conditions using the DEPI (Dynamic Environment Photosynthesis Imager) system. KEA3 is localized in the thylakoid membrane (Armbruster et al., 2014) and since it could potentially function to alleviate the proton motive force (*pmf*) we performed a 5-day experiment under three different light regimes: flat day (~100 µmol photons m^2 s^{-1}), sinusoidal (~40 to 500 µmol photons m^2 s^{-1}), and fluctuating light which is similar to sinusoidal but has superimposed peaks of a higher light intensities (~40-1,000 µmol photons m^2 s^{-1}). As predicted the photosynthetic responses most apparent were NPQ and more specifically the energy-dependent quenching (qE) of NPQ (Supplemental Figure 2).

The log_2-fold differences of the photosynthetic efficiency of PSII (φII) were minimal compared to NPQ and qE. Based on the DEPI results, both KEA3 *Arabidopsis thaliana* mutants, *kea3-1* and *kea3-2*, displayed the largest log_2-fold differences consistently at the onset of increasing light intensity for both sinusoidal and fluctuating light regimen (day 2, 3 and 5). The increased levels of NPQ accompanied lower φII signals, particularly during sinusoidal and fluctuating days. This implies a synchronized role for *kea3* in photosynthetic acclimation to fluctuating light.

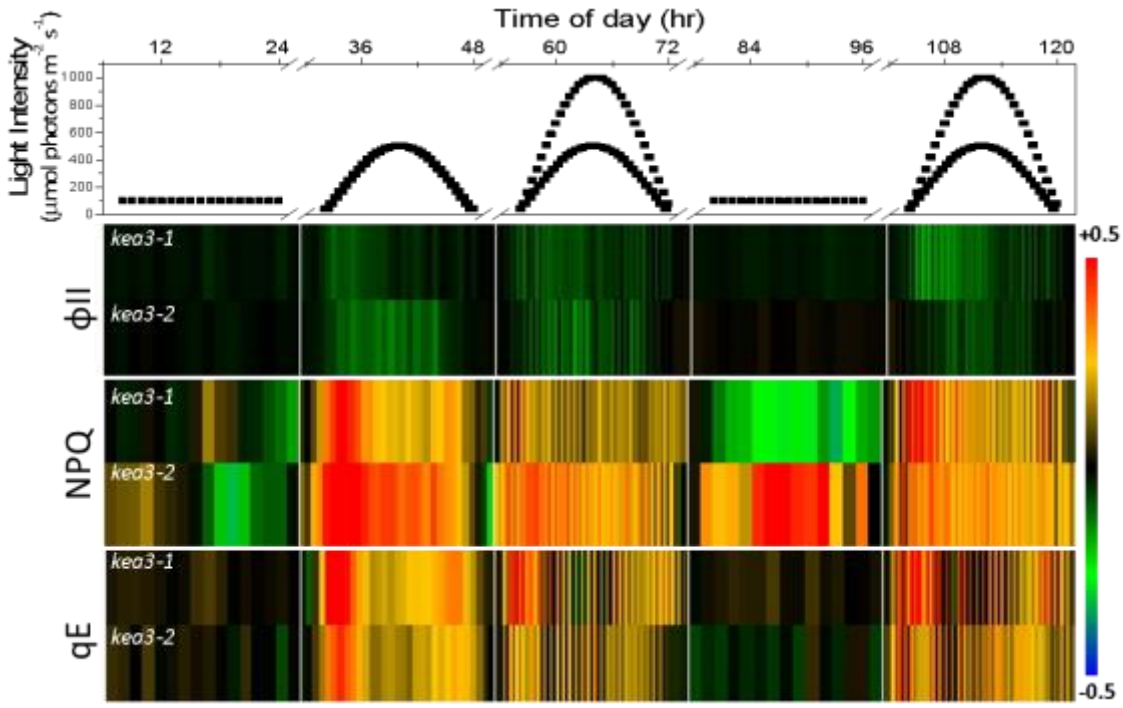

Supplemental Figure 2. Dynamic photosynthetic response in *kea3* revealed through DEPI. Three photosynthetic parameters: φII, NPQ and qE were measured using a 5-day light regime (flat day, sinusoidal day, fluctuating light, flat day, fluctuating light) via the DEPI chambers. Within each panel displays the log-fold expression differences of both *kea3-1* (top) and *kea3-2* (bottom) normalized to the respective wild type (Col-0 and WS). Signal intensities is according to the false color scale on the right (log-fold expression) of the corresponding panels, n≥3.

In order to verify if the increased NPQ response was induced specifically by an increase in light intensity or by the rapid change in intensities we used IDEAspec (Hall et al., 2013) fluorimeter to perform longer NPQ induction studies. Both *kea3* mutants appeared to have increased levels of NPQ upon transitioning from dark to low light conditions (Supplemental Figure 3A). Under low irradiance (50 µmol photons m^2 s^{-1}) the WT NPQ partially recovered with basal levels after 5 min, while the response in *kea3* followed similar trends to the WT at the onset of light exposure, the NPQ response

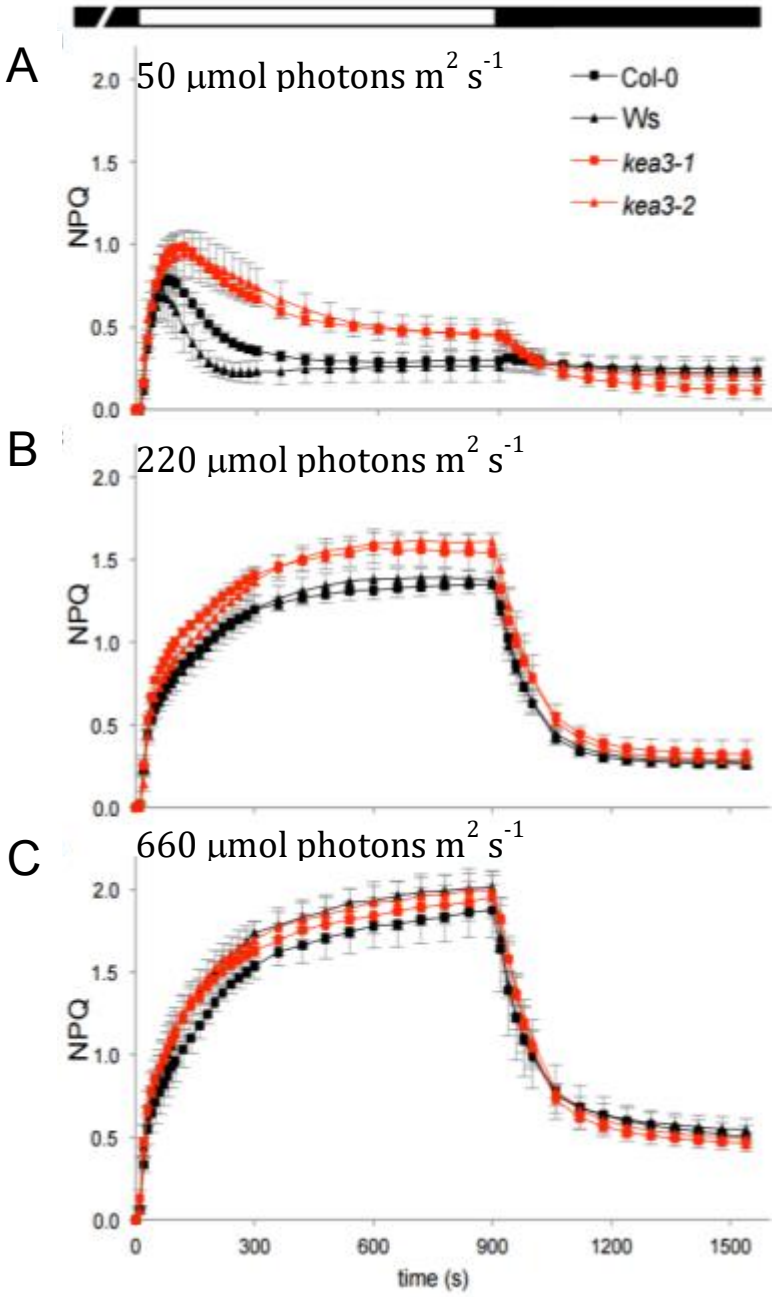

Supplemental Figure 3. Transient NPQ- induction and relaxation- response in *kea3*. Wild type (Col-0 and WT) and kea3 (*kea3-1* and *kea3-2*) leaves were dark-adapted for 30-min before illuminating at increasing light intensities of 50 µmol photons m^2 s^{-1} (A), 220 µmol photons m^2 s^{-1}, and 660 µmol photons m^2 s^{-1}. The NPQ induction phase consisted of a 15-min light period followed by a 10-min dark relaxation period. Mean values represented (n=4) ± SEM.

exceeded WT at ~1.5 minutes and remained consistently higher. The increased photosynthetic acclimation response was less apparent with increasing light intensities, as illustrated with 220 μmol photons m^2 s^{-1} (Supplemental Figure 3B) and 660 μmol photons m^2 s^{-1} (Supplemental Figure 3C). Yet for all light intensities the increased stress indicator-NPQ in *kea3* exceeded that of WT and delayed in relaxation (Supplemental Figure 3).

KEA3 NPQ response is associated with the proton motive force

In order to determine whether the increased NPQ response in KEA3 is associated with its role as a K^+/H^+ antiporter effecting the proton motive force (*pmf*), we performed near-simultaneous measurements of NPQ and dark interval relaxation kinetics (DIRK) using the carotenoid electrochromic shift (ECS) measurements, as done in (Sacksteder and Kramer, 2000). We predicted that as an antiporter, it could alter the proton concentration (ΔpH) and/or electric potential ($\Delta\psi$) components of the *pmf* to alleviate backpressures. Despite KEA3's role as an antiporter, the overall *pmf* or total ECS (ECS_t) was only slightly lower in *kea3* compared to WT upon transitioning from dark to low light conditions and indistinguishable in the dark (Supplemental Figure 4A). This implies that the increase NPQ response is not directly linked to the capacity of *pmf*.

Nonetheless, by also extracting information on both parameters simultaneously, allowed us to correlate the relationship between the overall *pmf* and NPQ response, seen in Supplemental Figures 2 and 3. As shown in Supplemental Figure 4B, despite the dynamics of the *pmf* being largely unchanged in *kea3*, the sensitivity of NPQ to ECS_t was higher than in WT, suggesting that KEA3 transiently decreases the contribution of ΔpH to the *pmf*.

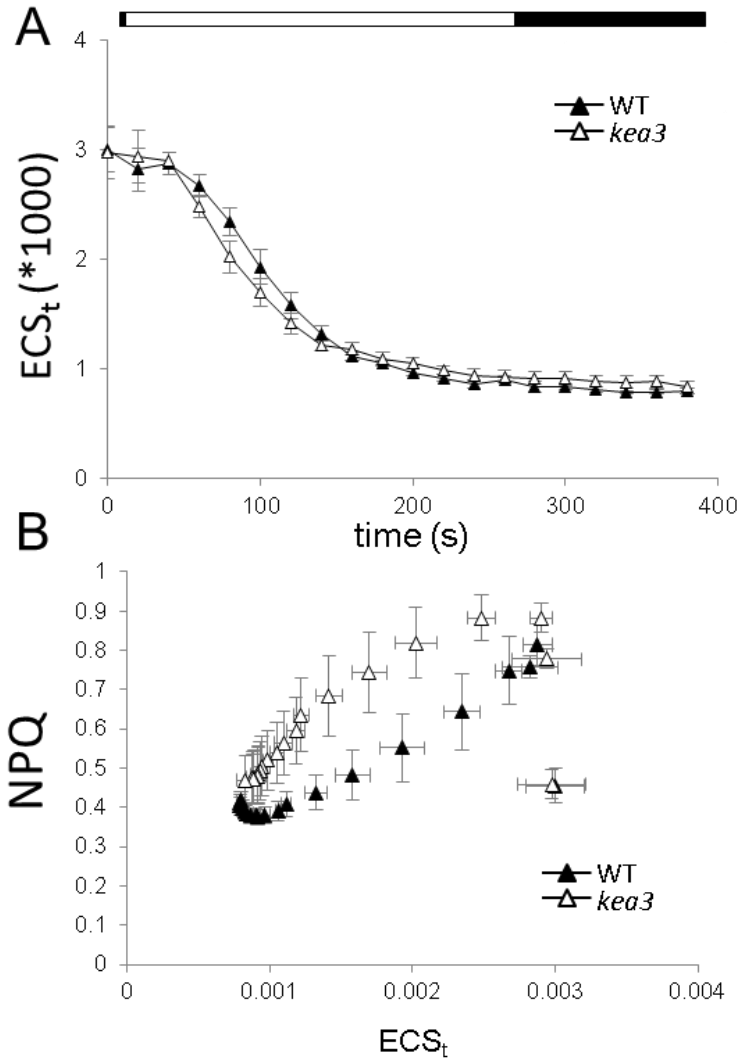

Supplemental Figure 4. Enhanced NPQ response is associated with a decrease in *pmf* (ECS_t). Chlorophyll a fluorescence and DIRK measurements were simultaneously taken from single leaves using the IDEAspec at an actinic light intensity of 70 µmol m^2 s^{-1} by applying saturating light flashes. (A) Shown is ECS_t of two-week-old wild type (Col-0, WS) and *kea3* mutant (*kea3-1* and *kea3-2*) plants that had been dark adapted for 30 min and were then exposed to 70 µmol m^2 s^{-1} for several minutes followed by a dark relaxation period. (B) Plot of NPQ versus ECS_t derived from simultaneous measurement of fluorescence and ECS DIRK. Error bars represent standard error (n ≥ 6).

Parsing the two components of *pmf* in *kea3*

We measured both *pmf* components, Δψ and ΔpH, after 100s of illumination at different intensities followed by a dark period in order to determine the extended kinetics of ECS, as previously performed (Cruz et al., 2001). As predicted, the *pmf* partitioning was altered in the *kea3* mutant under low light conditions with a 1.8-fold greater ΔpH compared to WT (Supplemental Figure 5, $p<0.04$, Student's t-test). At the same time interval, the partitioning phenotype was consistent with the observed increase in transient

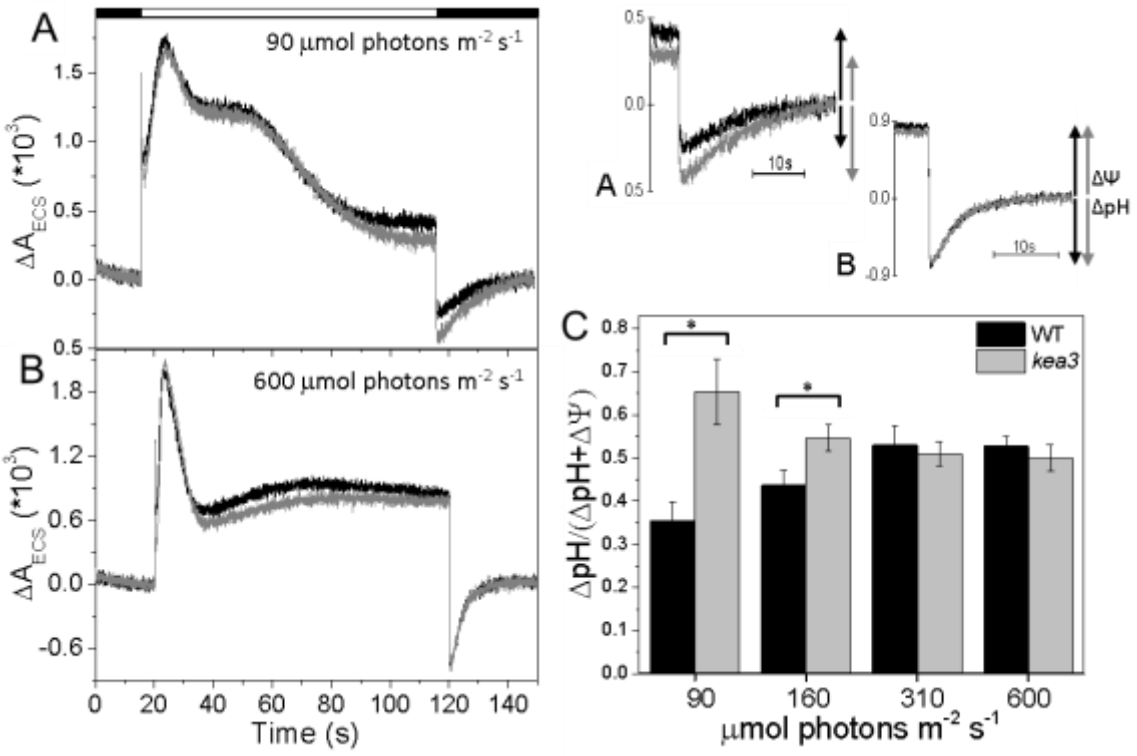

Supplemental Figure 5. KEA3 modulates the partitioning of *pmf*. LIRK measurements were performed at increasing light intensities (90, 160, 310 and 600 µmol photons m^2 s^{-1}) with the lowest (A) and highest (B) light intensity ECS traces displayed. Insets of both (A, B) traces illustrate the ECS kinetic response after dark adaptation, partitioning into ΔΨ and ΔpH components of *pmf*. (C) Plotted graph representation of the fraction of *pmf* contributed by ΔpH for wild type (Col-0 and WS) and *kea3* (*kea3-1* and *kea3-2*) mutants at increasing light intensities. Asterisks indicate the measurements that were significantly different between WT and *kea3* (*P<0.04, Student's t-test). Error bars represent SEM. (n=6).

NPQ for *kea3* (Supplemental Figure 4). While under light-saturating conditions (600 and even 310 μmol photon m^2 s^{-1}) the ECS inverse, ΔpH component, had no difference. This data further supports the role that KEA3 in buffering the lumenal pH by decreasing the contribution of ΔpH and increasing the contribution of Δψ to *pmf*. Furthermore, the role of KEA3 is more apparent under low-light intensities (Supplemental Figure 5C).

KEA3 displays lower H^+ membrane conductance after MV treatment

The *pmf* is controlled by ionic strength and the lumen buffering capacity (Cruz et al., 2001), therefore, the estimations of ECS_{inv} or ΔpH from the parsing traces performed (Supplemental Figure 5) could be underestimated based on the ionic strength of the thylakoid membrane permeable ions. As an additional evaluation, we assessed the partitioning of *pmf* upon inducing an acidified thylakoid lumen. Addition of MV acts as an alternative electron acceptor to PSI, offsetting the ATP/NADPH pools and presumably inhibiting the H^+ consumption by ATP synthase. Based on the results (Supplemental Figure 6), the *kea3* has a decreased ATP synthase conductivity (g_H+) (Supplemental Figure 6B) and recovery of H^+ influx after transitioning from light to dark (Supplemental Figure 6C), possibly owing to higher ΔpH in *kea3*. This leads us to propose three possible hypotheses for the behavior: 1) a change in ion fluxes from alteration in thylakoid permeabilities or stromal/lumenal ion content; 2) an increased consumption of ATP; or 3) proton "slippage" or partial uncoupling of the thylakoid, where KEA3 could act as a H^+/K^+ antiporter coupled to a K^+ channel i.e., TPK.

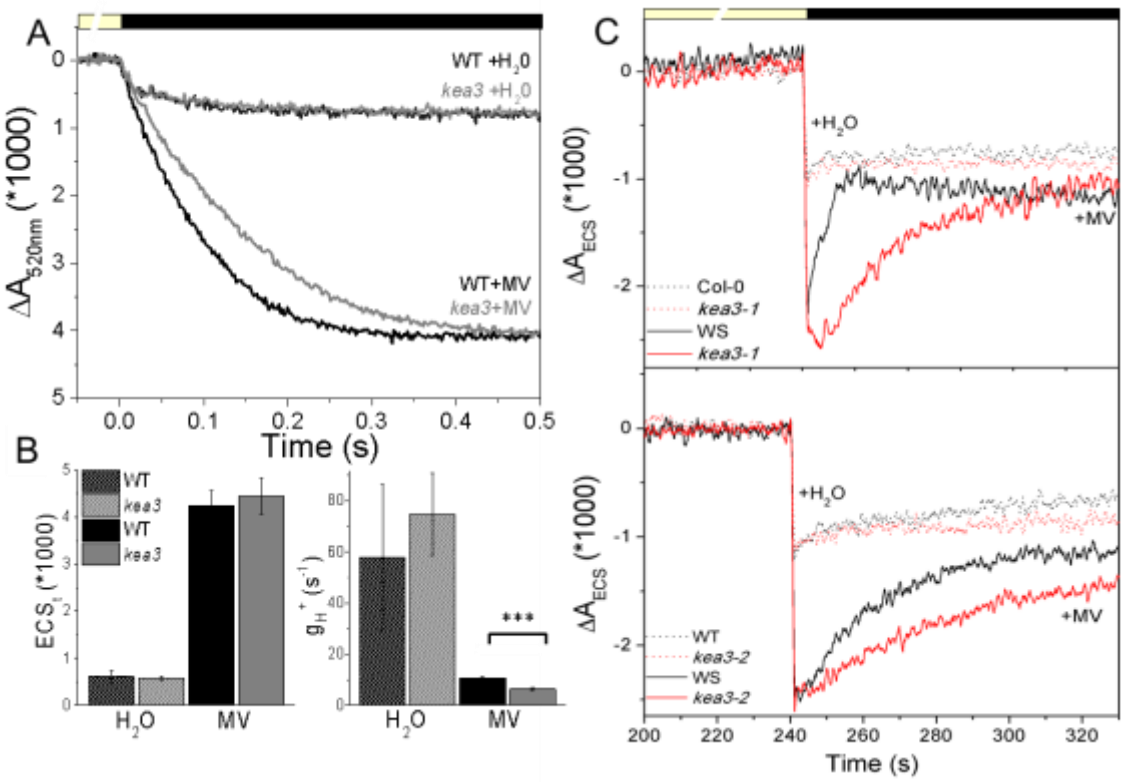

Supplemental Figure 6. ATP synthase kinetic responses of *kea3* to MV. (A) Averaged DIRK (*Δ*A520 nm) measurements after transitioning from light to dark period for WT (Col-0) and *kea3-1* MV treated leaves. (B) ATP synthase parameters, amplitude of ECS (ECS_t) representative of overall *pmf* and the conductivity of ATP synthase (g_{H^+}) derived from (A) kinetics. (C) *Pmf* parsing response from leaves of both kea3 (*kea3-1* and *kea3-2*) mutants and WT (Col-0 and WS) infiltrated with MV. Leaves were infiltrated with 100 mM MV and water (as the control) to determine the ECS kinetic responses after transitioning from light to dark. Asterisks indicate the measurements that were significantly different between Col-0 and *kea3-1* (*P<0.001, Student's t-test). Error bars represent SEM. (n ≥ 4).

Discussion

KEA3 transports protons out of the lumen in exchange for K^+ and thereby we propose accelerates the relaxation of the energy dependent quenching mechanism (qE) resulting in a more rapid photosynthetic acclimation system under fluctuating light (Supplemental Figure 2) (Armbruster et al., 2014). The mechanism of KEA3 plays a role in

aiding plants by sensing a decrease in ΔpH and acting as a safety valve to alleviate the qE (Supplemental Figures 2 and 3) response to better cope with the dynamics of fluctuating light. This prediction agrees with the overexpressing KEA3 mutant displaying a higher φII compared to WT, presumably by allowing qE relaxation to occur more rapidly and thus decreasing excitation pressures at PSII (Armbruster et al., 2014). Furthermore, small concentrations (0.03 μM) of the electroneutral K^+/H^+ molecule nigericin rescues the qE and NPQ phenotype, confirming the role of the KEA3 antiporter directly influences these reversible photosynthetic stress responses (Armbruster et al., 2014).

As illustrated with Supplemental Figure 4, the overall *pmf* or ECS_t is like that of WT but the NPQ relationship to ECS_t is elevated in the mutant, thus alleviating pressures on ATP synthase by increasing *pmf* sensitivity, also displayed in Supplemental Figure 6. The *pmf* partitioning has been proposed by previous work as a flexibility mechanism that alleviates pressures on ATP synthase without affecting the ATP/NADPH ratios, via 'type II flexibility mechanism' (Kanazawa and Kramer, 2002; Kramer et al., 2004a; Kramer et al., 2004b)

Recently, it was shown that the K^+ channel TPK3 is localized to the thylakoid and activated by a low pH (Carraretto et al., 2013). This agrees with our third hypothesis for the *kea3* behavior following MV infiltration (Supplemental Figure 6), where a K^+ channel can be voltage gated and assist in alleviating the Δφ accumulated by KEA3. We believe that both, TPK3 and KEA3, can cooperatively modulate the proton concentration of the thylakoid lumen when it reaches below a critical threshold, thus acting as a safety valve. This work supports an added tool for photosynthetic efficiency and flexibility induced under rapid changes in light intensity, particularly to low-light.

Experimental Procedures

Plant material and growth conditions

Two KEA3 mutant lines were used in these studies, *kea3-1* (Gabi_170G09) in the Col-0 background and *kea3-2* (FLAG_493_C01) in the Wassilewskija (WS) background. Plants were grown on soil in light-controlled chambers ~100 μmol photons m^2 s^{-1} with a 16:8 photoperiod at 23°C. The majority of the measurements (if not noted otherwise) were obtained from 3-week old plants.

Photosynthetic spectroscopic analysis

The photosynthetic *in vivo* spectroscopy measurements were made on ~3 week old intact Arabidopsis leaves clamped into a measuring chamber. The spectrophotometer/ chlorophyll fluorimeter chamber made in-house with non-focusing optics using 3 different wavelengths (505 nm. 520 nm, and 535 nm) for deconvoluted measurements of the electrochromic shift (ECS) kinetics (Sacksteder et al., 2000; Sacksteder et al., 2001). Prior to the experiments leaves were dark adapted for 30 min. The dark interval relaxation kinetic (DIRK) measurements and *pmf* parsing trace were made by perturbing the steady-state (70-80 μmol photon m^2 s^{-1}) with a rapid dark period ~400 ms and 45 sec, respectively and preventing proton efflux (Sacksteder et al., 2000; Avenson et al., 2005).The components of *pmf* partitioning, ECS steady-state (Δψ) and ECS inverse (ΔpH), were measured as described previously (Cruz et al., 2001; Takizawa et al., 2007). The initial proton flux (vH+) was calculated based on the initial decay of the DIRK kinetics (Avenson et al., 2005; Kohzuma et al., 2009b). The ATP synthase conductivity (g_{H+}) which is based on the conductivity of protons across the thylakoid membrane is calculated using the inverse

value of the first-order exponential decay kinetics of DIRK (Avenson et al., 2005; Kohzuma et al., 2009b).

MV Infiltrations

Infiltrations were performed using newly extracted leaves incubated on a damp kimwipes floating with 100 μM MV solution (and water as the control) under low light (~5uE) for 1 hour, similar to previous work (Livingston et al., 2010). Prior to spectroscopic measurements leaves were cleaned of excess solution by gently blotting with kimwipes.

REFERENCES

REFERENCES

Allen JF (2002) Photosynthesis of ATP—electrons, proton pumps, rotors, and poise. Cell 110: 273–276

Amthor JS (2010) From sunlight to phytomass: on the potential efficiency of converting solar radiation to phyto-energy. New Phytol 188: 939–959

Armbruster U, Carrillo, LR, Venema K, Pavlovic L, Schmidtmann E, Kornfield A, Jahns P, Berry JA, Kramer DM, Jonikas MC (2014) Ion antiport accelerates photosynthetic acclimation in fluctuating light environments. Nat Commun 5: 5439

Arnon DL, Whatley FR, Allen MB (1958) Assimilatory power in photosynthesis. Science 127: 1026–1034

Aro EM, Virgin I, Andersson B (1993) Photoinhibition of photosystem II. Inactivation, protein damage and turnover. Biochim Biophys Acta BBA 1143: 113–134

Asada K (1999) The water-water cycle in chloroplasts: scavenging of active oxygens and dissipation of excess photons. Annu Rev Plant Physiol Plant Mol Biol 50: 601–639

Asada K (2006) Production and scavenging of reactive oxygen species in chloroplasts and their functions. Plant Physiol 141: 391–396

Avenson TJ, Cruz JA, Kanazawa A, Kramer DM (2005) Regulating the proton budget of higher plant photosynthesis. Proc Natl Acad Sci 102: 9709–9713

Baker NR (2008) Chlorophyll fluorescence: a probe of photosynthesis *in vivo*. Annu Rev Plant Biol 59: 89–113

von Ballmoos C, Wiedenmann A, Dimroth P (2009) Essentials for ATP synthesis by F1F0 ATP synthases. Annu Rev Biochem 78: 649–672

Bassham JA, Benson AA, Kay LD, Harris AZ, Wilson AT, Calvin M (1954) The path of carbon in photosynthesis. XXI. The cyclic regeneration of carbon dioxide acceptor. J Am Chem Soc 76: 1760–1770

Bendall DS, Manasse RS (1995) Cyclic photophosphorylation and electron transport. Biochim Biophys Acta BBA - Bioenerg 1229: 23–38

Bernal-Bayard P, Ojeda V, Hervás M, Cejudo FJ, Navarro JA, Velázquez-Campoy A, Pérez-Ruiz JM (2014) Molecular recognition in the interaction of chloroplast 2-Cys peroxiredoxin with NADPH-thioredoxin reductase c (NTRC) and thioredoxin x. FEBS Lett 588: 4342–4347

Boekema EJ, van Heel M, Gräber P (1988) Structure of the ATP synthase from chloroplasts studied by electron microscopy and image processing. Biochim Biophys Acta BBA - Bioenerg 933: 365–371

Buchanan BB (1980) Role of light in the regulation of chloroplast enzymes. Annu Rev Plant Physiol 31: 341–374

Buchanan BB, Balmer Y (2005) Redox regulation: a broadening horizon. Annu Rev Plant Biol 56: 187–220

Cape JL, Bowman MK, Kramer DM (2006) Understanding the cytochrome bc complexes by what they don't do. The Q-cycle at 30. Trends Plant Sci 11: 46–55

Capitani G, Marković-Housley Z, DelVal G, Morris M, Jansonius JN, ürmann P (2000) Crystal structures of two functionally different thioredoxins in spinach chloroplasts. J Mol Biol 302: 135–154

Carraretto L, Formentin E, Teardo E, Checchetto V, Tomizioli M, Morosinotto T, Giacometti GM, Finazzi G, Szabó I (2013) A thylakoid-located two-pore K+ channel controls photosynthetic light utilization in plants. Science 342: 114–118

Carrillo LR, Froehlich JE, Cruz JA, Savage L, Kramer DM (2016) Multi-level regulation of the chloroplast ATP synthase: The chloroplast NADPH thioredoxin reductase c (NTRC) is required for redox modulation specifically under low irradiance. Plant J 87: 654–663

Cejudo FJ, Ferrández J, Cano B, Puerto-Galán L, Guinea M (2012) The function of the NADPH thioredoxin reductase C-2-Cys peroxiredoxin system in plastid redox regulation and signalling. FEBS Lett 586: 2974–2980

Clarke JE, Johnson GN (2001) *In vivo* temperature dependence of cyclic and pseudocyclic electron transport in barley. Planta 212: 808–816

Collin V, Issakidis-Bourguet E, Marchand C, Hirasawa M, Lancelin J-M, Knaff DB, Miginiac-Maslow M (2003) The Arabidopsis plastidial thioredoxins new functions and new insights into specificity. J Biol Chem 278: 23747–23752

Croce R, van Amerongen H (2014) Natural strategies for photosynthetic light harvesting. Nat Chem Biol 10: 492–501

Crofts AR, Meinhardt SW, Jones KR, Snozzi M (1983) The role of the quinone pool in the cyclic electron-transfer chain of Rhodopseudomonas sphaeroides a modified Q-cycle mechanism. Biochim Biophys Acta BBA - Bioenerg 723: 202–218

Cruz JA, Avenson TJ, Kanazawa A, Takizawa K, Edwards GE, Kramer DM (2005a) Plasticity in light reactions of photosynthesis for energy production and photoprotection. J Exp Bot 56: 395–406

Cruz JA, Kanazawa A, Treff N, Kramer DM (2005b) Storage of light-driven transthylakoid proton motive force as an electric field (Δψ) under steady-state conditions in intact cells of Chlamydomonas reinhardtii. Photosynth Res 85: 221–233

Cruz JA, Sacksteder CA, Kanazawa A, Kramer DM (2001) Contribution of electric field (Δψ) to steady-state transthylakoid proton motive force (*pmf*) *in vitro* and *in vivo*. control of *pmf* parsing into Δψ and ΔpH by ionic strength. Biochemistry 40: 1226–1237

Cséke C, Buchanan BB (1986) Regulation of the formation and utilization of photosynthate in leaves. Biochim Biophys Acta BBA - Rev Bioenerg 853: 43–63

Dai S, Friemann R, Glauser DA, Bourquin F, Manieri W, Schürmann P, Eklund H (2007) Structural snapshots along the reaction pathway of ferredoxin-thioredoxin reductase. Nat Lond 448: 92–6

Demmig-Adams B, Adams III WW (1996) The role of xanthophyll cycle carotenoids in the protection of photosynthesis. Trends Plant Sci 1: 21–26

Eberhard S, Finazzi G, Wollman F-A (2008) The dynamics of photosynthesis. Annu Rev Genet 42: 463–515

Fischer S, Gräber P (1999) Comparison of ΔpH- and Δφ-driven ATP synthesis catalyzed by the H+-ATPases from Escherichia coli or chloroplasts reconstituted into liposomes. FEBS Lett 457: 327–332

Fischer S, Gräber P, Turina P (2000) The activity of the ATP synthase from Escherichia coli is regulated by the transmembrane proton motive force. J Biol Chem 275: 30157–30162

Foyer CH, Harbinson J (1994) Oxygen metabolism and the regulation of photosynthetic electron transport. Causes Photooxidative Stress Amelior. Def. Syst. Plants. CRC press, Londres (Royaume Uni), p 42

Foyer CH, Lelandais M, Harbinson J (1992) Control of the quantum efficiencies of photosystems I and II, electron flow, and enzyme activation following dark-to-light transitions in pea leaves relationship between NADP/NADPH ratios and NADP-malate dehydrogenase activation state. Plant Physiol 99: 979–986

Furbank RT, Horton P (1987) Regulation of photosynthesis in isolated barley protoplasts: the contribution of cyclic photophosphorylation. Biochim Biophys Acta BBA - Bioenerg 894: 332–338

Genty B, Briantais J-M, Baker NR (1989) The relationship between the quantum yield of photosynthetic electron transport and quenching of chlorophyll fluorescence. Biochim Biophys Acta BBA 990: 87–92

Gilmore AM (1997) Mechanistic aspects of xanthophyll cycle-dependent photoprotection in higher plant chloroplasts and leaves. Physiol Plant 99: 197–209

Govindjee, Shevela D, Björn LO (2017) Evolution of the Z-scheme of photosynthesis: a perspective. Photosynth Res 1–11

Gräber P, Junesch U, Schatz GH (1984) Kinetics of proton transport coupled ATP synthesis in chloroplasts. activation of the ATPase by an artificially generated ΔpH and Δψ. Berichte Bunsenges Für Phys Chem 88: 599–608

Gross EL, Pan B, Li B, Brown L (1994) Stability of plastocyanin to acid pH. Biophysical J 66: 272

Gütle DD, Roret T, Hecker A, Reski R, Jacquot J-P (2017) Dithiol disulphide exchange in redox regulation of chloroplast enzymes in response to evolutionary and structural constraints. Plant Sci 255: 1–11

Hall CC, Cruz J, Wood M, Zegarac R, DeMars D, Carpenter J, Kanazawa A, Kramer D (2013) Photosynthetic measurements with the idea spec: an integrated diode emitter array spectrophotometer/fluorometer. Photosynth. Res. Food Fuel Future. Springer Berlin Heidelberg, pp 184–188

Hangarter RP, Good NE (1982) Energy thresholds for ATP synthesis in chloroplasts. Biochim Biophys Acta BBA - Bioenerg 681: 397–404

Hartman FC, Harpel MR (1994) Structure, Function, Regulation, and Assembly of D-Ribulose-1,5-Bisphosphate Carboxylase/Oxygenase. Annu Rev Biochem 63: 197–232

Heldt HW (1969) Adenine nucleotide translocation in spinach chloroplasts. FEBS Lett 5: 11–14

Hill R, Bendall F (1960) Function of the two cytochrome components in chloroplasts: a working hypothesis. Nature 186: 136–137

Hisabori T, Ueoka-Nakanishi H, Konno H, Koyama F (2003) Molecular evolution of the modulator of chloroplast ATP synthase: origin of the conformational change dependent regulation. FEBS Lett 545: 71–75

Hogg PJ (2003) Disulfide bonds as switches for protein function. Trends Biochem Sci 28: 210–214

Horton P, Hague A (1988) Studies on the induction of chlorophyll fluorescence in isolated barley protoplasts. IV. Resolution of non-photochemical quenching. Biochim Biophys Acta BBA - Bioenerg 932: 107–115

Joët T, Genty B, Josse E-M, Kuntz M, Cournac L, Peltier G (2002) Involvement of a plastid terminal oxidase in plastoquinone oxidation as evidenced by expression of the *Arabidopsis thaliana* enzyme in tobacco. J Biol Chem 277: 31623–31630

Johnson MP, Ruban AV (2011) Restoration of rapidly reversible photoprotective energy dissipation in the absence of PsbS protein by enhanced ΔpH. J Biol Chem 286: 19973–19981

Joliot P, Johnson GN (2011) Regulation of cyclic and linear electron flow in higher plants. Proc Natl Acad Sci 108: 13317–13322

Junesch U, Gräber P (1987) Influence of the redox state and the activation of the chloroplast ATP synthase on proton-transport-coupled ATP synthesis/hydrolysis. Biochim Biophys Acta BBA - Bioenerg 893: 275–288

Junesch U, Gräber P (1991) The rate of ATP-synthesis as a function of ΔpH and Δψ catalyzed by the active, reduced H+-ATPase from chloroplasts. FEBS Lett 294: 275–278

Junge W, Nelson N (2015) ATP synthase. Annu Rev Biochem 84: 631–657

Kampfenkel K, Möhlmann T, Batz O, Montagu MV, Inzé D, Neuhaus HE (1995) Molecular characterization of an *Arabidopsis thaliana* cDNA encoding a novel putative adenylate translocator of higher plants. FEBS Lett 374: 351–355

Kanazawa A, Kramer DM (2002) *In vivo* modulation of nonphotochemical exciton quenching (npq) by regulation of the chloroplast atp synthase. Proc Natl Acad Sci 99: 12789–12794

Ketcham SR, Davenport JW, Warncke K, McCarty RE (1984) Role of the gamma subunit of chloroplast coupling factor 1 in the light-dependent activation of photophosphorylation and atpase activity by dithiothreitol. J Biol Chem 259: 7286–7293

Kohzuma K, Cruz JA, Akashi K, Hoshiyasu S, Munekage YN, Yokota A, Kramer DM (2009) The long-term responses of the photosynthetic proton circuit to drought. Plant Cell Environ 32: 209–219

Kramer D, Avenson T, Edwards G (2004a) Dynamic flexibility in the light reactions of photosynthesis governed by both electron and proton transfer reactions. Trends Plant Sci 9: 349–357

Kramer DM, Avenson TJ, Kanazawa A, Cruz JA, Ivanov B, Edwards GE (2004b) The relationship between photosynthetic electron transfer and its regulation. In GC Papageorgiou, Govindjee, eds, Chlorophyll Fluoresc. Springer Netherlands, pp 251–278

Kramer DM, Crofts AR (1989) Activation of the chloroplast ATPase measured by the electrochromic change in leaves of intact plants. Biochim Biophys Acta BBA - Bioenerg 976: 28–41

Kramer DM, Cruz JA, Kanazawa A (2003) Balancing the central roles of the thylakoid proton gradient. Trends Plant Sci 8: 27–32

Kramer DM, Evans JR (2011) The importance of energy balance in improving photosynthetic productivity. Plant Physiol 155: 70–78

Kramer DM, Sacksteder CA, Cruz JA (1999) How acidic is the lumen? Photosynth Res 60: 151–163

Kramer DM, Wise RR, Frederick JR, Alm DM, Hesketh JD, Ort DR, Crofts AR (1990) Regulation of coupling factor in field-grown sunflower: a redox model relating coupling factor activity to the activities of other thioredoxin-dependent chloroplast enzymes. Photosynth Res 26: 213–222

Krause GH (1988) Photoinhibition of photosynthesis. An evaluation of damaging and protective mechanisms. Physiol Plant 74: 566–574

Krieger-Liszkay A (2005) Singlet oxygen production in photosynthesis. J Exp Bot 56: 337–346

Krieger A, Moya I, Weis E (1992) Energy-dependent quenching of chlorophyll a fluorescence: effect of pH on stationary fluorescence and picosecond-relaxation kinetics in thylakoid membranes and Photosystem II preparations. Biochim Biophys Acta BBA - Bioenerg 1102: 167–176

Leegood RC, Walker DA (1980) Regulation of fructose-1,6-bisphosphatase activity in intact chloroplasts. Studies of the mechanism of inactivation. Biochim Biophys Acta BBA - Bioenerg 593: 362–370

Lemaire SD, Michelet L, Zaffagnini M, Massot V, Issakidis-Bourguet E (2007) Thioredoxins in chloroplasts. Curr Genet 51: 343–365

Lepistö A, Pakula E, Toivola J, Krieger-Liszkay A, Vignols F, Rintamäki E (2013) Deletion of chloroplast NADPH-dependent thioredoxin reductase results in inability to regulate starch synthesis and causes stunted growth under short-day photoperiods. J Exp Bot 64: 3843–3854

Li X-P, Gilmore AM, Caffarri S, Bassi R, Golan T, Kramer D, Niyogi KK (2004) Regulation of photosynthetic light harvesting involves intrathylakoid lumen pH sensing by the PsbS protein. J Biol Chem 279: 22866–22874

Li Z, Wakao S, Fischer BB, Niyogi KK (2009) Sensing and Responding to Excess Light. Annu Rev Plant Biol 60: 239–260

Lichtenthaler HK (1987) Chlorophylls and carotenoids: pigments of photosynthetic biomembranes. Methods Enzymol 148: 350–382

Lilley RM, Stitt M, Mader G, Heldt HW (1982) Rapid fractionation of wheat leaf protoplasts using membrane filtration. Plant Physiol 70: 965–970

Livingston AK, Cruz JA, Kohzuma K, Dhingra A, Kramer DM (2010) An Arabidopsis mutant with high cyclic electron flow around photosystem i (hcef) involving the NADPH dehydrogenase complex. Plant Cell Online 22: 221–233

Michalska J, Zauber H, Buchanan BB, Cejudo FJ, Geigenberger P (2009) NTRC links built-in thioredoxin to light and sucrose in regulating starch synthesis in chloroplasts and amyloplasts. Proc Natl Acad Sci 106: 9908–9913

Michelet L, Zaffagnini M, Morisse S, Sparla F, Pérez-Pérez ME, Francia F, Danon A, Marchand CH, Fermani S, Trost P, et al (2013) Redox regulation of the Calvin–Benson cycle: something old, something new. Front Plant Sci. doi: 10.3389/fpls.2013.00470

Mitchell P (1961) Coupling of phosphorylation to electron and hydrogen transfer by chemi-osmotic type of mechanism. Nature 141–145

Mitchell P (1976) Possible molecular mechanisms of the protonmotive function of cytochrome systems. J Theor Biol 62: 327–367

Mitchell P (1966) Chemiosmotic coupling in oxidative and photosynthetic phosphorylation. Biol Rev 41: 445–501

Müller P, Li X-P, Niyogi KK (2001) Non-photochemical quenching. a response to excess light energy. Plant Physiol 125: 1558–1566

Naranjo B, Mignée C, Krieger-Liszkay A, Hornero-Méndez D, Gallardo-Guerrero L, Cejudo FJ, Lindahl M (2016) The chloroplast NADPH thioredoxin reductase C, NTRC, controls non-photochemical quenching of light energy and photosynthetic electron transport in Arabidopsis. Plant Cell Environ 39: 804–822

Nelson DL, Nelson DL, Lehninger AL, Cox MM (2008) Lehninger principles of biochemistry. W.H. Freeman, New York

Neuhaus HE, Emes MJ (2000) Nonphotosynthetic metabolism in plastids. Annu Rev Plant Physiol Plant Mol Biol 51: 111–140

Neuhaus HE, Thom E, Möhlmann T, Steup M, Kampfenkel K (1997) Characterization of a novel eukaryotic ATP/ADP translocator located in the plastid envelope of *Arabidopsis thaliana* L. Plant J 11: 73–82

Nevo R, Charuvi D, Tsabari O, Reich Z (2012) Composition, architecture and dynamics of the photosynthetic apparatus in higher plants. Plant J 70: 157–176

Nicholls DG, Ferguson SSJ (2002) Bioenergetics 3. Harcourt Academic

Nikkanen L, Toivola J, Rintamäki E (2016) Crosstalk between chloroplast thioredoxin systems in regulation of photosynthesis. Plant Cell Environ 39: 1691–1705

Noctor G, Foyer (2000) Homeostasis of adenylate status during photosynthesis in a fluctuating environment. J Exp Bot 51: 347–356

Ort DR, Baker NR (2002) A Photoprotective Role for O2 as an Alternative Electron Sink in Photosynthesis? Curr Opin Plant Biol 5: 193–198

Ort DR, Yocum CF (1996) Oxygenic Photosynthesis: The Light Reactions. Springer

Pascual MB, Mata-Cabana A, Florencio FJ, Lindahl M, Cejudo FJ (2010) Overoxidation of 2-Cys peroxiredoxin in prokaryotes. J Biol Chem 285: 34485–34492

Pearcy RW (1990) Sunflecks and photosynthesis in plant canopies. Annu Rev Plant Physiol Plant Mol Biol 41: 421–453

Pérez-Ruiz JM, Guinea M, Puerto-Galán L, Cejudo FJ (2014) NADPH thioredoxin reductase c Is involved in redox regulation of the mg-chelatase I subunit in *Arabidopsis thaliana* chloroplasts. Mol Plant 7: 1252–1255

Pérez-Ruiz JM, Spinola MC, Kirchsteiger K, Moreno J, Sahrawy M, Cejudo FJ (2006) Rice NTRC Is a high-efficiency redox system for chloroplast protection against oxidative damage. Plant Cell 18: 2356–2368

Petersen J, Förster K, Turina P, Gräber P (2012) Comparison of the H+/ATP ratios of the H+-ATP synthases from yeast and from chloroplast. Proc Natl Acad Sci 109: 11150–11155

Quick WP, Neuhaus HE (1997) regulation and control of photosynthetic carbon assimilation. Mol. Approach Prim. Metab. High. Plants

Raines CA (2003) The Calvin cycle revisited. Photosynth Res 75: 1–10

Reinhold T, Alawady A, Grimm B, Beran KC, Jahns P, Conrath U, Bauer J, Reiser J, Melzer M, Jeblick W, et al (2007) Limitation of nocturnal import of ATP into Arabidopsis chloroplasts leads to photooxidative damage. Plant J 50: 293–304

Reiser J, Linka N, Lemke L, Jeblick W, Neuhaus HE (2004) Molecular physiological analysis of the two plastidic ATP/ADP transporters from Arabidopsis. Plant Physiol 136: 3524–3536

Richter AS, Peter E, Rothbart M, Schlicke H, Toivola J, Rintamäki E, Grimm B (2013) Posttranslational influence of NADPH-dependent thioredoxin reductase c on enzymes in tetrapyrrole synthesis. Plant Physiol 162: 63–73

Richter ML (2004) Gamma–epsilon interactions regulate the chloroplast ATP synthase. Photosynth Res 79: 319–329

Richter ML, Gao F (1996) The chloroplast ATP synthase: Structural changes during catalysis. J Bioenerg Biomembr 28: 443–449

Rott M, Martins NF, Thiele W, Lein W, Bock R, Kramer DM, Schöttler MA (2011) ATP synthase repression in tobacco restricts photosynthetic electron transport, CO2 assimilation, and plant growth by overacidification of the thylakoid lumen. Plant Cell Online 23: 304–321

Ruban AV, Johnson MP, Duffy CDP (2012) The photoprotective molecular switch in the photosystem II antenna. Biochim Biophys Acta BBA - Bioenerg 1817: 167–181

Sacksteder CA, Jacoby ME, Kramer DM (2001) A portable, non-focusing optics spectrophotometer (NoFOSpec) for measurements of steady-state absorbance changes in intact plants. Photosynth Res 70: 231–240

Sacksteder CA, Kanazawa A, Jacoby ME, Kramer DM (2000) The proton to electron stoichiometry of steady-state photosynthesis in living plants: a proton-pumping Q cycle is continuously engaged. Proc Natl Acad Sci U S A 97: 14283–14288

Sacksteder CA, Kramer DM (2000) Dark-interval relaxation kinetics (DIRK) of absorbance changes as a quantitative probe of steady-state electron transfer. Photosynth Res 66: 145–158

Scheibe R (2004) Malate valves to balance cellular energy supply. Physiol Plant 120: 21–26

Schürmann P, Buchanan BB (2008) The Ferredoxin/Thioredoxin System of Oxygenic Photosynthesis. Antioxid Redox Signal 10: 1235–1274

Seelert H, Poetsch A, Dencher NA, Engel A, Stahlberg H, Müller DJ (2000) Structural biology: Proton-powered turbine of a plant motor. Nature 405: 418–419

Serrato AJ, Pérez-Ruiz JM, Spínola MC, Cejudo FJ (2004) A novel NADPH thioredoxin reductase, localized in the chloroplast, which deficiency causes hypersensitivity to abiotic stress in *Arabidopsis thaliana*. J Biol Chem 279: 43821–43827

Sharkey TD (1990) Feedback limitation of photosynthesis and the physiological role of ribulose bisphosphate carboxylase carbamylation. Bot Mag Tokyo 2: 87–105

Sivak MN, Walker DA (1986) Photosynthesis *in vivo* can be limited by phosphate supply. New Phytol 102: 499–512

Strand DD, Kramer DM (2014) Control of non-photochemical exciton quenching by the proton circuit of photosynthesis. Non-Photochem. Quenching Energy Dissipation Plants Algae Cyanobacteria. pp 387–408

Streb P, Josse E-M, Gallouët E, Baptist F, Kuntz M, Cornic G (2005) Evidence for alternative electron sinks to photosynthetic carbon assimilation in the high mountain plant species Ranunculus glacialis. Plant Cell Environ 28: 1123–1135

Strelow F, Rumberg B (1993) Kinetics and energetics of redox regulation of ATP synthase from chloroplasts. FEBS Lett 323: 19–22

Strotmann H, Berger S (1969) Adenine nucleotide translocation across the membrane of isolated acetabularia chloroplasts. Biochem Biophys Res Commun 35: 20–26

Takahashi S, Murata N (2008) How do environmental stresses accelerate photoinhibition? Trends Plant Sci 13: 178–182

Takizawa K, Cruz JA, Kanazawa A, Kramer DM (2007) The thylakoid proton motive force *in vivo*. Quantitative, non-invasive probes, energetics, and regulatory consequences of light-induced *pmf*. Biochim Biophys Acta BBA - Bioenerg 1767: 1233–1244

Thormählen I, Zupok A, Rescher J, Leger J, Weissenberger S, Groysman J, Orwat A, Chatel-Innocenti G, Issakidis-Bourguet E, Armbruster U, et al (2017) Thioredoxins play a crucial role in dynamic acclimation of photosynthesis in fluctuating light. Mol Plant 10: 168–182

Trentmann O, Horn M, van Scheltinga ACT, Neuhaus HE, Haferkamp I (2007) Enlightening energy parasitism by analysis of an ATP/ADP transporter from Chlamydiae. PLoS Biol 5: e231

Trentmann O, Jung B, Neuhaus HE, Haferkamp I (2008) Nonmitochondrial ATP/ADP transporters accept phosphate as third substrate. J Biol Chem 283: 36486–36493

Triantaphylidès C, Krischke M, Hoeberichts FA, Ksas B, Gresser G, Havaux M, Breusegem FV, Mueller MJ (2008) Singlet oxygen Is the major reactive oxygen species involved in photooxidative damage to plants. Plant Physiol 148: 960–968

Turina P, Melandri BA, Gräber P (1991) ATP synthesis in chromatophores driven by artificially induced ion gradients. Eur J Biochem 196: 225–229

Turina P, Petersen J, Gräber P (2016) Thermodynamics of proton transport coupled ATP synthesis. Biochim Biophys Acta BBA - Bioenerg 1857: 653–664

Vallejos RH, Arana JL, Ravizzini RA (1983) Changes in activity and structure of the chloroplast proton ATPase induced by illumination of spinach leaves. J Biol Chem 258: 7317–7321

Van Walraven HS, Strotmann H, Schwarz O, Rumberg B (1996) The H+/ATP coupling ratio of the ATP synthase from thiol-modulated chloroplasts and two cyanobacterial strains is four. FEBS Lett 379: 309–313

Varco-Merth B, Fromme R, Wang M, Fromme P (2008) Crystallization of the c14-rotor of the chloroplast ATP synthase reveals that it contains pigments. Biochim Biophys Acta BBA - Bioenerg 1777: 605–612

Watt IN, Montgomery MG, Runswick MJ, Leslie AGW, Walker JE (2010) Bioenergetic cost of making an adenosine triphosphate molecule in animal mitochondria. Proc Natl Acad Sci 107: 16823–16827

Way DA, Pearcy RW (2012) Sunflecks in trees and forests: from photosynthetic physiology to global change biology. Tree Physiol 32: 1066–1081

Weber AP (2004) Solute transporters as connecting elements between cytosol and plastid stroma. Curr Opin Plant Biol 7: 247–253

Weber APM, Facchinelli F (2011) The metabolite transporters of the plastid envelope: an update. Front Plant Physiol 2: 50

Weber APM, Fischer K (2007) Making the connections – The crucial role of metabolite transporters at the interface between chloroplast and cytosol. FEBS Lett 581: 2215–2222

Wilson AT, Calvin M (1955) The photosynthetic cycle. CO_2 dependent transients. J Am Chem Soc 77: 5948–5957

Yano H, Kuroda S, Buchanan BB (2002) Disulfide proteome in the analysis of protein function and structure. PROTEOMICS 2: 1090–1096

Yoshida K, Hisabori T (2016) Two distinct redox cascades cooperatively regulate chloroplast functions and sustain plant viability. Proc Natl Acad Sci 113: e3967–e3976

Yoshida K, Hisabori T (2017) Distinct electron transfer from ferredoxin-thioredoxin reductase to multiple thioredoxin isoforms in chloroplasts. Biochem J 474: 1347–1360

Yoshida K, Matsuoka Y, Hara S, Konno H, Hisabori T (2014) Distinct redox behaviors of chloroplast thiol enzymes and their relationships with photosynthetic electron transport in *Arabidopsis thaliana*. Plant Cell Physiol 55: 1415–1425

CHAPTER 2

MULTI-LEVEL REGULATION OF THE CHLOROPLAST ATP SYNTHASE: THE CHLOROPLAST NADPH THIOREDOXIN REDUCTASE C (NTRC) IS REQUIRED FOR REDOX MODULATION SPECIFICALLY UNDER LOW IRRADIANCE

Work presented in this chapter has been published:

L. Ruby Carrillo, John E. Froehlich, Jeffrey A. Cruz, Linda Savage and David M. Kramer

(2016)

The Plant Journal doi: 10.1111/tpj.13226

Abstract

The chloroplast ATP synthase is known to be regulated by redox modulation of a disulfide bridge on the γ-subunit through the ferredoxin-thioredoxin regulatory system. We show that a second enzyme, the recently identified chloroplast NADPH thioredoxin reductase C (NTRC), plays a role specifically at low irradiance. Arabidopsis mutants lacking NTRC (*ntrc*) displayed a striking photosynthetic phenotype in which feedback regulation of the light reactions was strongly activated at low light, but returned to wild-type levels as irradiance was increased. This effect was caused by an altered redox state of the γ-subunit under low, but not high, light. The low light-specific decrease in ATP synthase activity in *ntrc* resulted in a buildup of the thylakoid proton motive force with subsequent activation of nonphotochemical quenching and downregulation of linear electron flow. We conclude that NTRC provides redox modulation at low light using the relatively oxidizing substrate NADPH, whereas the canonical ferredoxin-thioredoxin system can take over at higher light, when reduced ferredoxin can accumulate. Based on these results, we reassess previous models for ATP synthase regulation and propose that NTRC is most likely regulated by light. We also find that *ntrc* is highly sensitive to rapidly changing light intensities that probably do not involve the chloroplast ATP synthase, implicating this system in multiple photosynthetic processes, particularly under fluctuating environmental conditions.

Introduction

Photosynthesis powers life by converting light energy to chemical energy that can be used to drive downstream chemical reactions. Simultaneously, photosynthesis generates potentially harmful reactive intermediates (e.g., especially ROS that can damage the cell) which require fine-tuning of the photosynthetic reactions to balance the efficient conversion of energy while allowing the organism to avoid deleterious side reactions (Apel and Hirt, 2004).

The Trx regulatory system was first identified in plastids, but found in a wide range of biological systems (Buchanan and Wolosiuk, 1976; Montrichard et al., 2009); it is now recognized as a central regulatory system for photosynthesis, adjusting the activity of key enzymes in response to changes in the redox state of the stromal electron carriers (Buchanan, 1980). Trxs are thiol/disulfide oxidoreductases that contain redox active cysteine residues and catalyze the reversible transfer of reducing potential from the photosystems to regulatory thiol enzymes. In chloroplasts of higher plants there are three Trx isoforms: f, m and x, all of which appear to be reduced by FTR but function with different sets of target enzymes (Schürmann and Jacquot, 2000; Collin et al., 2003). In the light, electron flow from PSI leads to reduction of Fd, which can reduce Trx via FTR and in turn reduce the disulfides on target enzymes. In the dark, free thiols are re-oxidized, possibly through the action of specific enzymes such as the chloroplastic atypical thioredoxin (ACHT4), reversing the regulatory processes (Eliyahu et al., 2015).

Here we focus on the redox regulation of the chloroplast CF_0-CF_1 ATP synthase, which catalyzes the synthesis of ATP from ADP and P_i, coupled to the transfer of protons from the thylakoid lumen to the stroma. During photosynthesis, the light-induced *pmf*

drives the endergonic synthesis of ATP. The reaction is also reversible in the dark, forming a *pmf* from ATP hydrolysis (Junesch and Gräber, 1991a; Seelert et al., 2003). The ATP synthase complex is composed of two major subcomplexes: CF_0 and CF_1, consisting of four (I_1, II_1, III_{14}, IV_1 or a_1, b_2, c_n in bacterial systems) and five (α_3, β_3, γ_1, δ_1 and ε_1) subunits, respectively. The CF_0 is a transmembrane complex that couples the movement of protons across the membrane to rotational motion, while CF_1 couples this rotation to ATP synthesis (Groth and Strotmann, 1999; Richter et al., 2000; Seelert et al., 2003).

The ATP synthase is regulated through the Trx system so that it is active in the light during photosynthesis and inactivate in the dark, presumably to prevent wasteful ATP hydrolysis (Ketcham et al., 1984; Hangarter et al., 1987; Junesch and Gräber, 1987). The γ-subunit on the CF_1 subcomplex contains the regulatory cysteine residues (Cys^{199} and Cys^{205} in *Arabidopsis thaliana*) (Junesch and Gräber, 1991a; Evron and McCarty, 2000; Richter, 2004). Redox modulation of the ATP synthase operates in conjunction with an additional activation mechanism that involves energization by the *pmf* (Junesch and Gräber, 1987). The enzyme is latent (i.e. cannot catalyze synthesis or hydrolysis of ATP) in the absence of *pmf*, but can be activated upon application of a *pmf* above certain threshold values. A considerably higher threshold *pmf* is needed to activate the enzyme when the γ -subunit thiols are oxidized compared to reduced, leading to inactivation in the dark (Ketcham et al., 1984; Hangarter et al., 1987; Junesch and Gräber, 1987). The rate and extent of the γ-subunit reduction is also modulated by *pmf* (Ort and Oxborough, 1992; Evron and McCarty, 2000; Hisabori et al., 2002), suggesting that reduction and activation are linked through common conformational changes in the γ-subunit.

In contrast to other thiol modulated enzymes, which tend to be incrementally reduced as light is varied over a broad range, ATP synthase becomes rapidly activated at only a few μmol photons m^2 s^{-1}, perhaps to prevent the harmful buildup of *pmf* during dark-light induction of photosynthesis (Quick and Mills, 1986; Kramer et al., 1990). It was proposed that the prominent sensitivity is due to the relatively high (and thus more easily reduced) redox potential of the regulatory thiols (Kramer et al., 1990), but this proposal has not been directly tested.

The NADPH-dependent thioredoxin reductase C (NTRC) is part of a related, but more recently discovered, chloroplast thiol-regulatory system (Serrato et al., 2004). Unlike FTR, NTRC uses NADPH as its reductant and appears to deliver electrons to target proteins via a tethered thioredoxin domain (Serrato et al., 2004). NTRC has been shown to be involved in a range of redox processes, including the antioxidant 2-Cys peroxiredoxin system, chlorophyll biosynthesis and the activation of ADP-glucose pyrophosphorylase to regulate starch synthesis (Lepistö et al., 2009; Michalska et al., 2009; Cejudo et al., 2012). In contrast to the FTR-Trx redox system, NTRC appears to primarily function in the dark or under limited irradiance, likely because it derives its reducing potential from NADPH, which can be produced independently of photosynthesis through the oxidative pentose phosphate pathway (Neuhaus and Emes, 2000).

Recently, mutants lacking NTRC were found to display high NPQ responses (Naranjo et al., 2015; Thormählen et al., 2015; Naranjo et al., 2016). Based on our previous work showing that lumen pH is modulated by regulation of the chloroplast ATP synthase (Kanazawa and Kramer, 2002), we further investigated the possibility that NTRC is directly involved in the regulation of the ATP synthase and if so, under what conditions this

regulation is important. This hypothesis, that NTRC might regulate ATP synthase, was also mentioned in recent papers by (Naranjo et al., 2016; Nikkanen et al., 2016).

Results and Discussion

NADPH redox regulator displays strong photosynthetic phenotypes specifically under low light

Figure 11 shows responses of photosynthetic parameters of wild-type (Col-0) and two independent *Arabidopsis thaliana* T-DNA knockout lines of NTRC (*ntrc1* and *ntrc2*) to

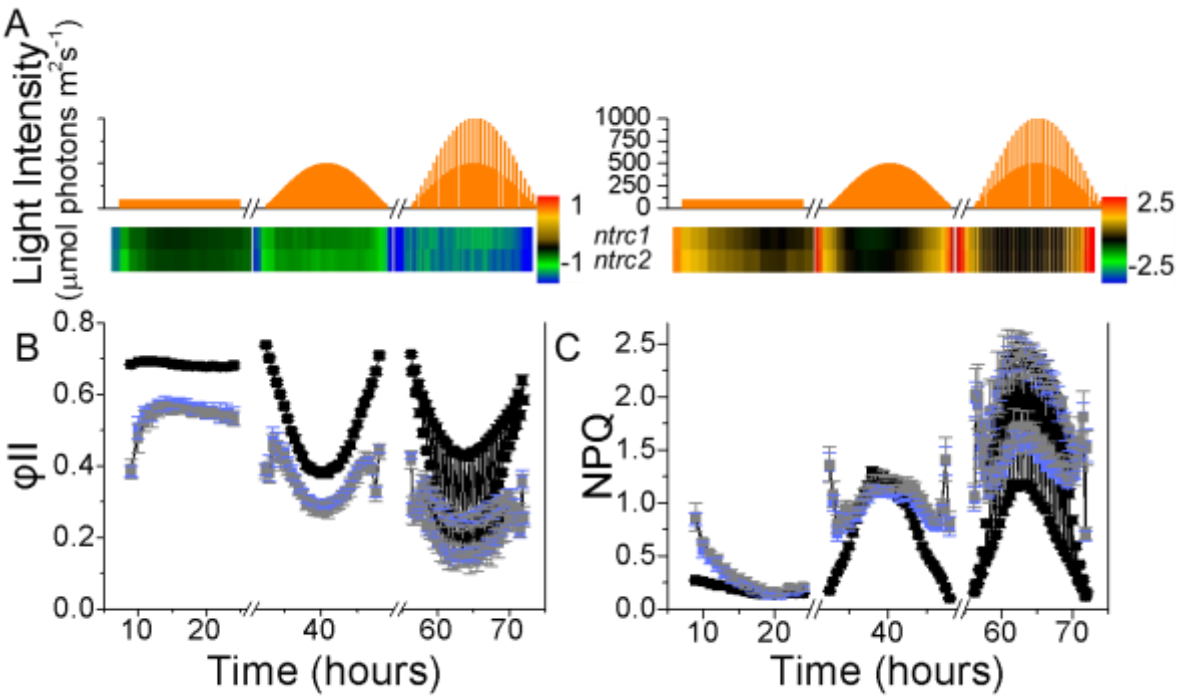

Figure 11. Three-day photosynthetic screen of *Atntrc* mutants. The screen consisted of three varying light regimes: constant, sinusoidal and fluctuating (A). Photosynthetic efficiency (φ_{II}) (B) and NPQ (C) of *ntrc1* (blue), *ntrc2* (grey) and Col-0 (black). The heat maps, illustrating the photosynthetic parameters and placed above their respective graphs, correspond to the log-fold differences of *ntrc1* and *ntrc2* compared to Col-0. The light cycles consisted of a 16-hour light period and 8-hour dark period where the intensities ranged from constant light (100 µmol photons m^2 s^{-1}), sinusoidal (39-500 µmol photons m^2 s^{-1}) and fluctuating light (39-1,000 µmol photons m^2 s^{-1}) (n=4 and error bars represent SD).

three, 16-hour light regimes (Figure 11A). The light regimes consisted of: 1) constant irradiance of 100 μmol photons m^2 s^{-1}; 2) a sinusoidal gradient of light, mimicking a natural day with peak light intensity of 500 μmol photons m^2 s^{-1}; and 3) and a sinusoidal profile with superimposed rapid light fluctuations and light intensities as high as 1,000 μmol photons m^2 s^{-1}, with alternatively doubling and halving intensity every 10 min. From chlorophyll fluorescence video streams, we calculated fluorescence of photosystem II (PSII) quantum efficiency (φ_{II}, Figure 11B) and NPQ (Figure 11C). Log_2-fold changes of these parameters in the *ntrc* mutants compared to Col-0, shown in heat maps just below Figure 11A, emphasize the comparative responses. In Col-0, photosynthetic parameters were relatively constant throughout continuous illumination (Figure 11B), with φ_{II} remaining at about 0.7, close to the maximal quantum efficiency measured in the dark (0.8 ± 0.038), and NPQ remained near zero, indicating very low engagement of photoprotection or photoinhibition. In contrast, the *ntrc* lines showed lower φ_{II} throughout the day, but were most severely affected at the earliest time points. Initially upon application of continuous illumination, φ_{II} for *ntrc1* and *ntrc2* (Figure 11B) was about half that of Col-0 (0.38 ± 0.02 and 0.39 ± 0.03, respectively) while NPQ (Figure 11C) was substantially higher (0.85 ± 0.06 and 0.87 ± 0.13). These effects were not caused by previous photodamage because maximal PSII quantum efficiency (F_v/F_m) was only marginally decreased for *ntrc1* and *ntrc2* compared to Col-0 (0.77 ± 0.03 and 0.77 ± 0.02, respectively), but are consistent with a rate-limitation downstream from PSII, leading to buildup of ΔpH with subsequent activation of qE and slowing of linear electron flow (LEF) (Figure 12AB). Over the following 6 hours of illumination, φ_{II} values for both *ntrc* recovered to a steady-state level of about 0.55 (compared to 0.68 for Col-0), while NPQ decreased to levels very similar to those in

Col-0, indicating that the limitation in photosynthesis imposed by loss of NTRC was partially overcome over the course of the day.

During the sinusoidal illumination regime, Col-0 showed typical photosynthetic responses to changing light. At low light, during the earliest time points, φ_{II} values were high (near or above 0.7), but gradually decreased as light intensity increased (reaching a minimum of about 0.38 at 500 μmol photons m^2 s^{-1}, near mid-day), followed by a smooth recovery as the light decreased at the end of the day. The NPQ responded in tandem with changes in light intensity, with very low levels in the morning, the highest levels at mid-day, and declining levels as light decreased in the evening. There was little residual NPQ at the end of the day, indicating that the accumulation of photoinhibition was minimal. Photosynthesis in both *ntrc*, by contrast, showed complex dependence on sinusoidal light, with stronger effects observed at lower light intensities, in the morning and evening. The differential light effects of *ntrc1* and *ntrc2* versus Col-0 are clearly represented in the log-fold heat maps (Figure 11, below light regimes). Initially upon illumination, φ_{II} was strongly suppressed in *ntrc*, while NPQ was much higher compared to Col-0. Contrary to our expectations, however, as light was increased from ~40 to 150 μmol photons m^2 s^{-1}, φ_{II} increased and NPQ decreased (opposite from the behavior seen in Col-0, as demonstrated in the heat maps).

Above 150 μmol photons m^2 s^{-1}, the photosynthetic parameters showed more classical behaviors, with φ_{II} decreasing and NPQ increasing with increased light intensities. The surprising "reverse dependence" of photosynthetic behaviors on light intensity returned in the evening as light decreased below 150 μmol photons m^2 s^{-1}, with φ_{II} decreasing and NPQ increasing in accordance with decreasing light intensities. Importantly,

neither NPQ nor φ_{II} fully recovered by the end of the day, likely indicating accumulation of photoinhibition.

During fluctuating light, on day 3, the differences in φ_{II} and NPQ between Col-0 and the *ntrc* mutants at low light were similar to those seen during sinusoidal illumination. However, the fluctuations at higher light induced stronger effects in the *ntrc* on both φ_{II} and NPQ that appeared to accumulate over the day and persisted, even as the light intensity decreased at the end of the day, likely reflecting strong accumulation of PSII photoinhibition. Agreeably, increased photoinhibition is anticipated for mutants lacking NTRC particularly under fluctuating and demanding light conditions, since NTRC is an efficient reductant for 2-Cys peroxiredoxins, a chloroplast antioxidant system (Pérez-Ruiz et al., 2006). These results indicate that NTRC affects photosynthesis at both low light and high or fluctuating light, but probably through different mechanisms.

The low light effects of *ntrc* are attributable to altered ATP synthase activity at low light

We then performed more detailed photosynthetic measurements on attached leaves using the IDEAspec kinetic spectrophotometer/fluorimeter, to better understand the mechanistic bases of the observed effects. Consistent with the results obtained from the imaging system, the extents of NPQ, in this case the energy-dependent NPQ component, q_E, were over 8-fold higher in *ntrc* compared to Col-0 at irradiance ≤ 120 μmol photons m^2 s^{-1} (Figure 12B), but the difference largely disappeared at irradiance above ~300 μmol photons m^2 s^{-1}. These results likely indicate that at low (but not higher) light the thylakoid lumen in the mutants became strongly acidified, triggering q_E and slowing LEF. Consistent

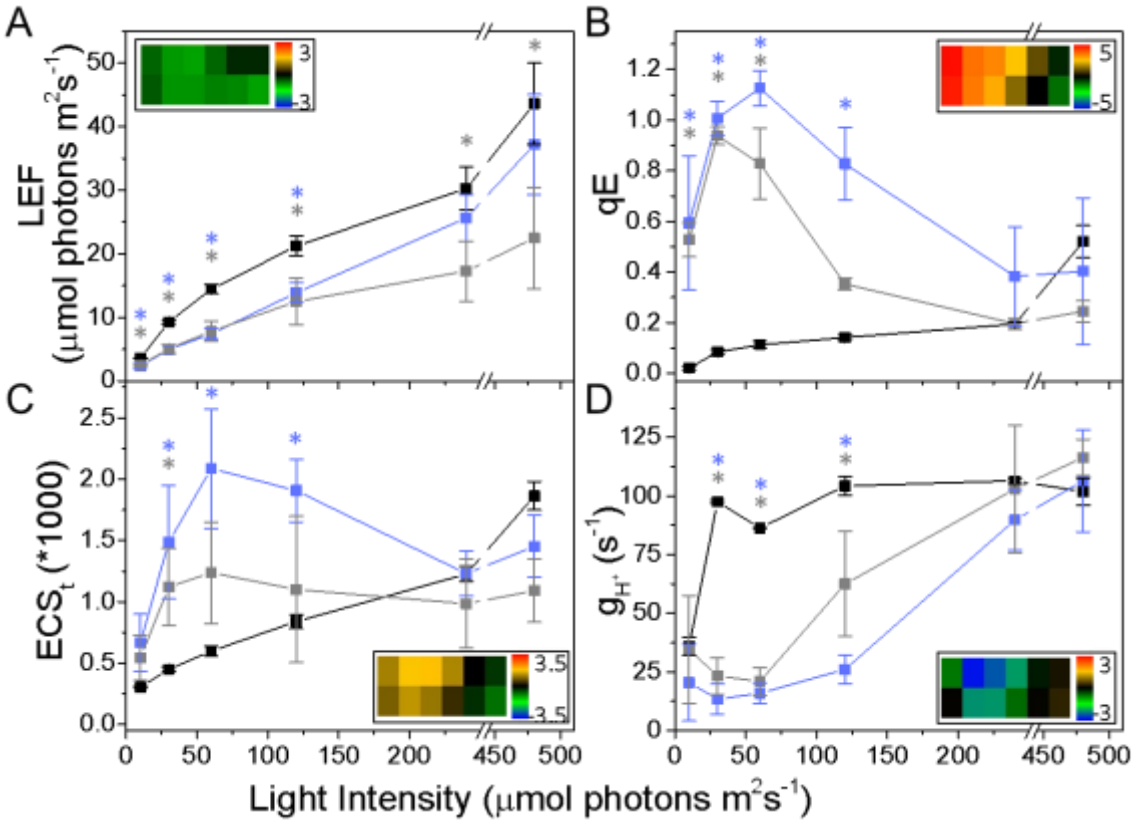

Figure 12. The relationship between light intensity-dependence and photosynthesis. The photosynthetic parameters tested were LEF (A), qE (B), total amplitude of the electrochromic shift (ECS_t) (C) and the conductivity of ATP synthase (g_{H^+}) (D). Col-0 (black), *ntrc1* (blue) and *ntrc2* (grey) measurements were taken from attached leaves (n≥3 and error bars represent SD). The inset heat maps represent the log-fold differences of *ntrc1* (top row) and *ntrc2* (bottom row) in relation to Col-0. Statistically significant differences to Col-0 are denoted with an asterisk (P values <0.05, as calculated by Student's *t*-test).

with this interpretation, we observed a strong increase in light-driven thylakoid *pmf*, as measured by the total electrochromic shift amplitude (ECS_t) parameter, in both *ntrc1* and *ntrc2* under low, but not high, irradiances (Figure 12C). There were some quantitative differences between *ntrc1* and *ntrc2*, with the former showing increased qE and ECS_t (compared to Col-0) that persisted over higher irradiance.

Linear electron flow (LEF) was lower in both *ntrc* lines compared to Col-0 at all irradiances, but significantly different ($p < 0.005$, Student's t-test) for both mutants at lower light intensities (Figure 12A). In *ntrc1*, LEF nearly recovered to wild type rates at above 300 μmol photons m^2 s^{-1}, whereas in *ntrc2*, the suppression of LEF continued over higher light intensities (Figure 12A, and inset heat maps expressing the log-fold difference of LEF in *ntrc1* and *ntrc2* versus Col-0), suggesting that the two alleles had different secondary effects at high light (see also Conclusions).

Increased thylakoid *pmf* can, in principle, be caused by either increased proton flux into the lumen from LEF or cyclic electron flow (CEF), or decreased proton efflux by slowing the chloroplast ATP synthase (Kanazawa and Kramer, 2002). The rate of light-driven proton flux, estimated using the ECS decay parameter (v_{H^+}), closely mirrored changes in LEF throughout the experiments (see Appendix, Supplemental Figure 7), implying that neither increased LEF nor increased CEF could explain the elevated *pmf*. On the other hand, the conductivity of the thylakoid membrane to proton efflux (g_{H+}) (Figure 12D), which is primarily controlled by the activity of the chloroplast ATP synthase (Kanazawa and Kramer, 2002), was strongly suppressed (2-4-fold) in *ntrc1* and *ntrc2* compared to Col-0 at low light (≤100 μmol photons m^2 s^{-1}), but indistinguishable at higher light (as demonstrated in the inset heat map). The *pmf* (ECS_t) behavior was quantitatively reproduced by considering effects of LEF on g_{H+} (Supplemental Figure 7), implying that changes in ATP synthase activity, by itself, could account for the low light phenotypes in *ntrc*. Moreover, the light intensity-dependence of the photosynthetic effects (expressed as log-fold differences between *ntrc* and Col-0, Figure 12 insets) were similar for all parameters, where the strongest effect was specifically at lower irradiance. These results

suggest that decreased ATP synthase activity at low light led to increased *pmf* and acidification of the lumen, subsequently activating q_E and slowing of LEF. Thus, we hypothesize that NTRC is essential for regulation of the ATP synthase, specifically at low light.

The *ntrc* mutants display altered redox regulation of the chloroplast ATP synthase

To test whether NTRC is involved in the redox regulation of the ATP synthase, we probed its activation and de-activation using flash-induced relaxation kinetics (FIRK) of the ECS signal, which was previously shown to reflect redox- and *pmf*-modulation of the γ-subunit thiols (Kramer and Crofts, 1989; Kramer et al., 1990). The excitation flashes were kept at low intensity to minimize the buildup of *pmf* or the reduction of Fd that could lead to the activation of the ATP synthase. Fully dark-adapted leaves showed very slow ECS decay kinetics (lifetime of about 800 ms, see Appendix), consistent with inactive ATP synthases containing oxidized γ-subunit. Pre-exposure of Col-0 plants, even to very low light intensity (10 μmol photons m^2 s^{-1}), resulted in rapid ECS decay (lifetime of about 20 ms, Supplemental Figure 8) indicating activation of the ATP synthase.

To assess the redox effects on the γ-subunit of ATP synthase, FIRK measurements were taken at specific time points in the dark following a short pre-illumination of 10, 100 and 300 μmol photons m^2 s^{-1}. As expected, the rapid ECS decay kinetics persisted for at least 10 min in the dark (Figure 13C, for Col-0), whereas pre-illumination-induced increases in the *pmf* under the oxidized state should have decayed in about 2 min (Kramer and Crofts, 1989), implying that the increased ATP synthase activation was most likely caused by reduction of the γ-subunit regulatory thiols. The γ-subunit re-oxidation kinetics, as reflected in the slowing of the flash-induced ECS signal (Supplemental Figure 8 and

Figure 13), showed characteristic sigmoidal kinetics, with a lag phase that increased with the intensity of the pre-illumination (Figure 13); this followed a recovery phase with a half-time of about 12 minutes, nearly identical to that seen previously (Kramer and Crofts, 1989; Kramer et al., 1990).

The FIRK responses in *ntrc* were distinct from those in Col-0 (Figure 13), showing a strong dependence on pre-illumination intensity. The decay kinetics in *ntrc* immediately after pre-illumination were just as rapid as Col-0 (lifetime of about 20 ms); however, the response to dark adaptation were much more immediate, especially at low irradiance with a halftime of about 3 min (Figure 13A). This suggest that the weak pre-illumination (10 μmol photons m^2 s^{-1}) activated ATP synthase by building up the thylakoid *pmf* (which decays on the time scale of a few min), rather than the reduction of the γ-subunit thiols. At higher pre-illumination intensities (Figures 13B and 13C), the ECS decay kinetics remained rapid (active) at a longer time scale compared to *pmf* dissipation, signifying that ATP synthase was activated by reduction. However, the de-activation kinetics of the *ntrc* mutants were much shorter when compared to Col-0, suggesting that the γ-subunit redox state equilibrates with a much smaller pool of reductants. We thus propose a model for *ntrc*, where the normal redox equilibrium between the γ-subunit thiols and NADPH pool is blocked, but at high light, the reduction of thiols can occur via a smaller pool of reductants (i.e., Trxs).

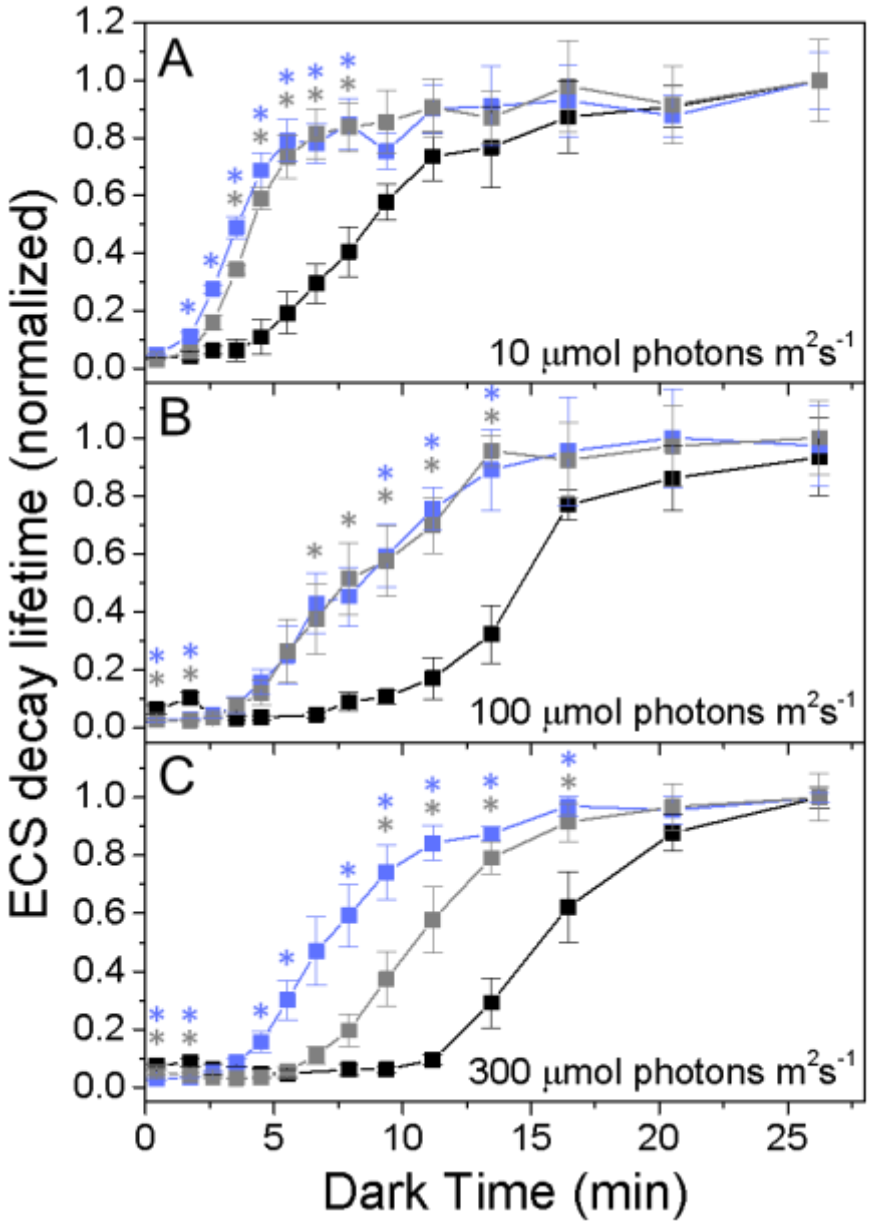

Figure 13. Mis-regulated relaxation kinetics of ATP synthase in *Atntrc*. Effects of dark re-adaptation on the decay kinetics of a flash-induced ECS (FIRK) take at 520 nm. Plants were pre-illuminated for 3 min at 10 (A), 100 (B), or 300 µmol photons m^2 s^{-1} (C) and measurements were made upon dark adapting >26 minutes. The FIRK decay kinetics represent averaged (n≥3) measurements normalized for Col-0 (black), *ntrc1* (blue) and *ntrc2* (grey) at increasing dark period (error bars represent SEM). The lifetime for fully dark-adapted leaves was ~800 ms. Statistically significant differences to Col-0 were calculated at each time point and denoted with an asterisk (P values <0.05, as calculated by Student's t-test).

Altered γ-subunit redox state under low irradiance in *ntrc*

To test our redox model we probed the light-induced changes in γ-subunit of ATP synthase redox state using 4-acetamido-4'-maleimidylstilbene-2,2'-disulfonate (AMS) labeling followed by SDS-PAGE and immunodetection (Konno et al., 2004). Experiments were performed under the sinusoidal day conditions described in Figure 11, with simultaneous measurements of φ_{II} (see representative images in Figure 14, left panel) and the γ-subunit redox state (Figure 14, right panel). Figure 14 (right panel) shows photo-reduction patterns of both *ntrc* lines and Col-0 under increasing light intensities. Consistent with previous, the ATP synthase in wild type plants is activated at relatively low light intensity (Kramer and Crofts, 1989; Yoshida et al., 2014), essentially all of the γ-subunit in Col-0 were reduced at 40 μmol photons m^2 s^{-1} and above. In contrast, ATPC1 from *ntrc1* and *ntrc2* remained partially oxidized even at light intensities as high as 120 μmol photons m^2 s^{-1}, but fully reduced at 500 μmol photons m^2 s^{-1}, closely paralleling the observed ATP synthase activity assays seen in Figures 12D and 13. These results are consistent with the ECS decay kinetics (Figure 13) and directly implicate the involvement of NTRC in modulating the reduction of ATP synthase at lower light intensities.

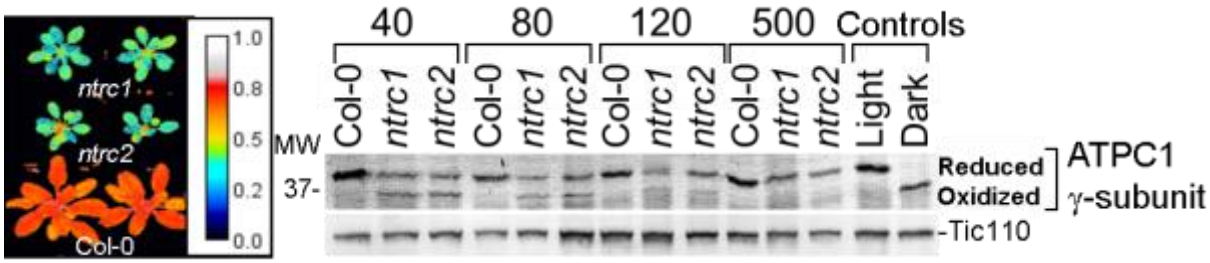

Figure 14. Analyzing the redox state of CF1-ATP synthase *in vitro* using AMS. Near simultaneous *in vivo* chlorophyll fluorescence imaging was performed at increasing light intensities prior to quenching the redox state of CF_1-ATP synthase. The chlorophyll fluorescence measurement (left panel) indicated decreased levels of φII for duplicates of both *ntrc1* (top row) and *ntrc2* (middle row) compared to Col-0 (bottom row) at 40 µmol photons m^2 s^{-1}. Upon confirming φII levels at designated light intensities (40, 80, 120, and 500 µmol photons m^2 s^{-1}), leaves were extracted and quenched with AMS, as described in materials and methods. Following AMS-labeling, samples were visualized by SDS-PAGE and probed using ATPC1 antibody, specific for γ-subunit of ATP synthase (right panel). The light and dark controls, right, demonstrate the wild-type redox shift. The same immunoblot was probed with Tic110 antibody to show the relative protein amount, bottom of right panel.

NTRC is not responsible for "metabolism-related" regulation of the ATP synthase

It has been proposed that, in addition to the established redox and *pmf* regulation, ATP synthase is regulated in response to metabolic status, e.g. in response to CO_2 levels or environmental stresses (Kanazawa and Kramer, 2002; Kohzuma et al., 2009; Kohzuma et al., 2013). The mechanism of this secondary regulation is unknown, though it has been proposed to involve substrates (e.g. inorganic phosphate) or metabolic intermediates (Kanazawa and Kramer, 2002; Kohzuma et al., 2013). To test whether NTRC is involved in this "metabolism-related" regulation, we assayed the effects of varying irradiance and CO_2 levels on ATP synthase activity, probed using the g_H+ parameter (Figure 15A) and NPQ (Figure 15B). The mutants required much higher light intensities (200 and 100 µmol photons m^2 s^{-1} for *ntrc1* and *ntrc2*, respectively compared to 55 µmol photons m^2 s^{-1} for

Col-0) to achieve maximal g_{H+}. However, in all but the lowest light intensities, for both *ntrc* and Col-0, lowering the levels of CO_2, 50 ppm (filled symbols) versus 1,000 ppm (open symbols), resulted in decreases of g_{H+} (Figure 15A), with concomitant increases in the NPQ responses (Figure 15B), indicating that NTRC is most likely not responsible for metabolism-related regulation of ATP synthase.

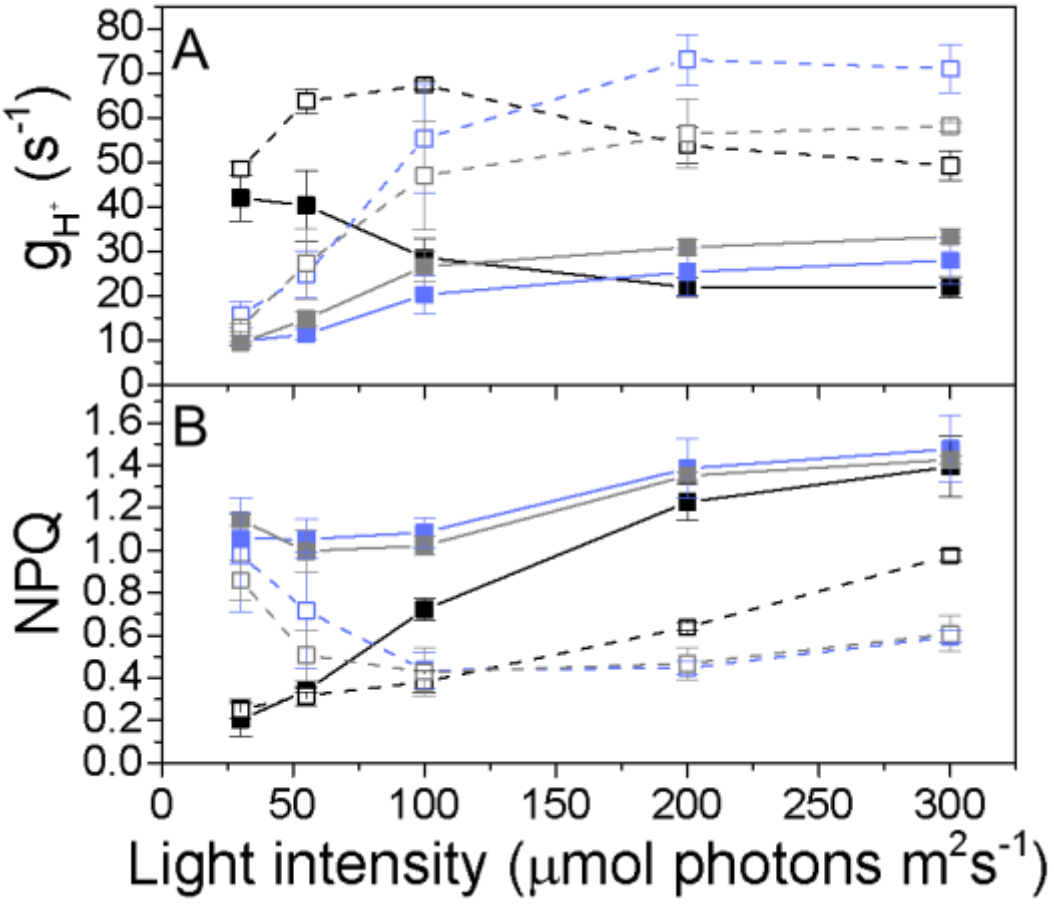

Figure 15. Effects of CO_2 levels on ATP synthase activity. Measurements were taken at atmospheric CO_2 levels and increasing light intensities. ATP synthase activity was probed by ECS decay kinetics through the g_{H^+} parameter (A) and NPQ (B) using standard chlorophyll *a* fluorescence assays, as described in Materials and Methods. Col-0 (black), *ntrc1* (blue) and *ntrc2* (grey) were exposed to increasing irradiance, from 0 to 300 µmol photons m^2 s^{-1}, with 50 (filled symbols) and 1,000 ppm atmospheric CO_2 (open symbols). Data is for attached leaves with n=3-4 and error bars represent SEM.

Conclusions

NTRC modulates the chloroplast ATP synthase specifically at low light

The ATP synthase is perhaps the most rapidly light-activated thiol-modulated enzyme in the chloroplast (Kramer and Crofts, 1989; Kramer et al., 1990). The previous model proposed that this redox modulation occurred through the FTR-Trx system, and that its unusual redox behavior could be explained by the relationship of the redox midpoint potential of the γ-subunit thiols with respect to the large NADPH redox buffering pool (Kramer et al., 1990; Ort and Oxborough, 1992). Our results challenge this model, showing that the low-light behavior is highly dependent on NTRC. Our results are consistent with those of recent work from Naranjo et al. (2106) who showed a direct effect of NADPH and NTRC on ATP synthase activity *in vitro*. The present study shows that the rapid and highly sensitive redox modulation of ATP synthase was lost in *ntrc1* and *ntrc2* (Figures 13 and 14), resulting in the suppression of ATP synthase activity specifically at low light (Figure 12D), leading to high *pmf*, lumen acidification (Figure 12C), elevated q_E (Figures 11C and 12B), and suppression of LEF (Figure 12A). Together with Naranjo et al. (2016), our findings warrant a significant revision of the canonical model for ATP synthase redox modulation.

The effects of *ntrc* on all these processes were observed specifically at irradiance lower than 100-150 μmol photons m^2 s^{-1} (as illustrated in the log-fold heat maps from Figures 11 and 12) but most (see below) of these effects were reversed at higher light, implying the participation of two separate redox regulatory systems for ATP synthase. Most likely, NTRC is responsible for the modulation at low light, while the canonical FTR-Trx system operates at higher light. Such parallel 'dual mode' light modulation of ATP

synthase, can also explain the transient NPQ response specifically induced upon the transition from dark to low-light (Kalituho et al., 2007). The increased transient qE response dissipates in less than 150 seconds, which was attributed to the consumption of ATP and NADPH by light-activated reactions, i.e., Calvin-Benson-Bassham cycle (Slovacek and Hind, 1981; Horton, 1983). However, it is also plausible that the low light increase of the NADPH pool is depleted by reducing NTRC and results in the rapid activation of ATP synthase.

Evidence for secondary regulation of the NTRC-related redox modulation

The *ntrc* mutants also show more rapid, and less sigmoidal, ATP synthase inactivation kinetics in the dark (Figure 13), likely reflecting a loss of redox equilibration between the γ-subunit thiols and the large stromal pool of NADPH (Kramer and Crofts, 1989; Kramer et al., 1990). This is consistent with the enzymology of NTRC (Spínola et al., 2008; Cejudo et al., 2012), in which electrons are transferred from the relatively high potential (compared to Fd) NADPH pool to disulfide pairs on target enzymes. The availability of electrons from NADPH (both in the light and dark) (Usuda, 1988) would allow NTRC to rapidly activate ATP synthase, particularly at low light (Kramer et al., 1990). In contrast, the FTR system requires higher light intensities to substantially produce the more reducing Fd. The sigmoidal re-oxidation behavior (Supplemental Figure 8 and Figure 13) was previously recognized as reflecting the equilibration of γ-subunit redox state with a large redox buffering pool (Kramer et al., 1990), and this model is supported by the fact that the sigmoidicity is altered in *ntrc*, as expected if the pool of reductants in equilibrium with the γ-subunit was altered.

However, the fact that NTRC appears to act as a conduit for equilibration of the NAPDH pool with the γ-subunit may lend credibility to an alternative model where NTRC is regulated at a secondary level. According to work from several labs (Stitt et al., 1982; Heber et al., 1986; Heineke et al., 1991), the NADPH redox state is relatively constant under steady state conditions, varying little between light and dark conditions, with the exception of rapid fluctuations in light (Foyer et al., 1992). Indeed, work from Thormählen et al. (2015) demonstrates that NADPH pool can be further reduced after extensive dark acclimation compared to steady-state illumination, and this effect is greater in *ntrc*. With a constitutively active NTRC and given the range of reported redox potentials for the γ-subunit thiols, ranging from -270 mV to -327 (at pH 7.0) (Kohzuma et al., 2013; Kohzuma et al., 2012; Wu et al., 2007; Kramer and Crofts, 1989), we would expect ATP synthase to remain partly reduced in the dark, at odds with our (Figure 14) and other (Ort & Oxborough 1992; Hisabori, Konno, Ichimura, Strotmann & Bald 2002) observations. We thus propose a model where NTRC is, itself, modulated between light and dark conditions. In the 'active' state, NTRC would allow for equilibration of the NADPH pool with the γ-subunit, but in the dark, NTRC would be inactivated, resulting in the inactivation of the ATP synthase. Thus, this model thus explains the perplexing issue whereby the γ-subunit tends to be oxidized after prolonged dark acclimation, despite that the NADPH pool has been shown to be partly reduced. Although this model is currently speculative, it could also explain the sigmoidal oxidation kinetics, by allowing for a time-dependent inactivation of NTRC in the dark would explain the lag phase in ATP synthase re-oxidation.

We also tested the hypothesis that, by connecting the NADPH redox state to ATP synthase, NTRC may contribute for the "metabolism-related" regulation of ATP synthase

that occurs at low CO_2 levels or in certain metabolic mutants (Gabrys et al., 1994; Kanazawa and Kramer, 2002; Kohzuma et al., 2013). However, in our experimental conditions with varying CO_2 levels showed that, while NTRC alters the low light activation of ATP synthase, it does not affect secondary regulation in response to changing CO_2 levels (Figure 15). These results are also consistent with recent findings on the photosynthetic efficiency of NTRC mutants as a function of CO_2 fixation with similar responses of deficiencies, specifically under low-light, while improvements of CO_2 assimilation rates were accounted for in the NTRC overexpression lines (Pérez-Ruiz et al., 2006; Nikkanen et al., 2016). Thus, these observations support earlier work on ATP synthase mutants (Kohzuma et al., 2013), showing that redox- and metabolism-related ATP synthase regulation occur through distinct mechanisms.

Studies on *ntrc* null mutants have been reported to have effects on photosynthetic metabolism and are especially pronounced at low light (Pérez-Ruiz et al., 2006; Naranjo et al., 2015; Thormählen et al., 2015; Nikkanen et al., 2016). Our results, showing a highly distinct low-light effect on ATP synthase suggest that some of these effects may be caused by, or accentuated by lack of activation of the chloroplast ATP synthase, which in turn could affect chloroplast metabolism by modulating the availability of inorganic phosphate and the ratio of ATP-ADP (Kiirats et al., 2009). A growing body of work implicates NTRC in regulation of a range of chloroplast enzymes, from assimilation (Lepistö et al., 2009; Cejudo et al., 2012), starch biosynthesis (Michalska et al., 2009; Lepistö et al., 2013) and oxidative damage (Serrato et al., 2004; Pérez-Ruiz et al., 2006), as well as playing a cooperative role with the canonical chloroplast thioredoxin redox regulator. Studies on double mutants of *ntrc* with Trx-f1, exhibited effects in regulating the Calvin-Benson-Bassham cycle activity

(Supplemental Figure 1), specifically affecting FBPase and AGPase activity along with impairments in NAPH-$NADP^+$ and ATP-ADP ratio (Thormählen et al., 2015; Nikkanen et al., 2016).

Such effects, beyond those on the ATP synthase, may account for the decreases in LEF at higher light (Figure 12A), which cannot be explained by redox modulation of the ATP synthase. Contrary to recent speculations regarding the lack of involvement of NTRC in relation to high-light stress (Toivola et al., 2013; Naranjo et al., 2016), both *ntrc* lines showed strong photo-inhibition at high light following rapid fluctuations in light intensities (Figure 11C). Under the above-mentioned conditions, ATP synthase is expected to be fully reduced, implying that NTRC is involved in processes beyond the modulation of the ATP synthase that are critical for maintaining photosynthetic efficiency and resilience. The photo-inhibitory responses, especially under rapidly fluctuating light conditions, may be related to the proposed role of NTRC in ROS detoxification through 2-Cys Prx system (Pérez-Ruiz et al., 2006).

Experimental procedures

Plant and growth conditions

Arabidopsis thaliana wild-type (ecotype Columbia-0) and two alleles of NTRC (At2G41680) T-DNA knockout lines (SAIL_115_E08: *ntrc1* and SALK_114293: *ntrc2*), were obtained from the Arabidopsis Biological Resource Center (USA) and identified by PCR analysis (Alonso et al., 2003). Both alleles were confirmed previously (Lepistö et al., 2009; Chae et al., 2013) and had similar phenotype to the first identified *ntrc* (SALK_012208) mutant (Serrato et al., 2004). Plants were grown on soil for a 16:8 day-night cycle in growth chambers with 125 μmol photons m^2 s^{-1} for 3-4 weeks.

Chlorophyll fluorescence imaging

In situ chlorophyll fluorescence imaging was performed in plant growth chambers (Bigfoot FLXC-19, Biochambers, Winnipeg, Canada; or Percival AR41L2, Geneva Scientific, http://www.geneva-scientific.com) outfitted as Dynamic Environment Photosynthesis Imager (DEPI) (Kramer et al., 2015). For large-scale screening, plants were typically assayed after 16-18 days of growth under standard conditions, as described above. Processing was performed using custom software developed in the laboratory and based on, ImageJ (http://rsbweb.nih.gov/ij/) to produce images of maximum photosynthetic efficiency of PSII (F_v/F_m), quantum yield of photosynthesis (φII), linear electron flow (LEF), non-photochemical quenching (NPQ) and its derivatives (qE and qI) for a three-day different light cycle. The light regimes consisted of a 16:8 photoperiod with the light intensities ranging from flat (100 μmol photons m^2 s^{-1}), sinusoidal (0-500 μmol photons m^2 s^{-1}) and fluctuating (0-1,000 μmol photons m^2 s^{-1}).

In vivo spectroscopy assays

Individual plants were non-invasively assayed for photosynthetic parameters using the integrated diode emitter array spectrophotometer/fluorimeter (IDEAspec) (Hall et al., 2013). Attached Arabidopsis leaves from 3-4 week-old plants were dark-adapted for 30 minutes prior to measurements and kept humid by bubbling room air (~372 ppm CO_2/21% O_2) through water onto the leaves. Chlorophyll a fluorescence measurements yield information on the photosynthetic parameters described above by using a compilation of ≥10 individual fluorescence traces and either blue-green light (505nm) for measuring pulses and/or red light (625nm) for actinic and saturation pulses. The sequence of the saturation pulses and measurements made yield information on the dark-adapted, steady-state and dark-recovery state of the photosynthetic parameters, mentioned above.

Estimates on ATP synthase parameters were also calculated based on the dark interval relaxation kinetics (DIRK) derived from the absorbance changes of the electrochromic shift (ECS) (Sacksteder et al., 2000; Sacksteder and Kramer, 2000). A deconvolution of three wavelengths: 505 nm, 520 nm, and 535 nm, was used in sequence with a light-dark transition to derive information on the initial flux of H^+ (ν_{H+}) across the thylakoid membrane, overall *pmf*, also termed ECS_t, and the conductivity of ATP synthase (g_{H+}) derived from the time constant of the ECS decay (Cruz et al., 2001a).

Estimates of ATP synthase re-oxidation by FIRK

A flash-induced relaxation kinetic (FIRK) measurement was made based on the ECS at 520 nm, as described previously (Kramer and Crofts, 1989; Kramer et al., 1990). Intact leaves were pre-illuminated at three different light intensities: 10 μmol photons m^2 s^{-1}, 100 μmol photons m^2 s^{-1} and 300 μmol photons m^2 s^{-1}, for 3 minutes followed by a dark-

adaptation period (0-26 min). The activity was monitored by applying short (100 μs) non-saturating flashes to generate a thylakoid *pmf* and measure the time constants of the ECS decay rate at 520 nm using a first-order exponential curve fit (Kramer and Crofts, 1989; Morita et al., 1982). The time constants (τ) of the individual ECS curves were measured at increasing dark period to estimate the rate of re-oxidation of the thiols on the γ-subunit of ATP synthase (Kramer and Crofts, 1989; Kramer et al., 1990; Morita et al., 1982). The mean values (n≥3) were normalized to the maximum value to better compare the redox differences between samples.

AMS Labelling and Protein Work

The redox state of CF_1 ATP synthase was probed using 4-acetamido-4'-maleimidylstilbene-2,2'-disulfonate (AMS), resulting in a MW redox shift based the covalent binding of AMS to the reduced thiols, as described previously with some modifications (Motohashi et al., 2001; Kohzuma et al., 2012). Upon confirming the photosynthetic phenotypes using DEPI, the redox states were quenched by freezing leaves in liquid nitrogen followed by grinding and 10% trichloroacetic acid treatment. Protein precipitates were washed twice in ice-cold acetone solution, centrifuged at maximum speed for 10 minutes in room temperature and pellets were resuspended in AMS labelling solution (1% SDS, 50mM Tris-HCl, pH 8.0 and 15mM AMS). Protein amounts were estimated using a Bradford assay (Bio-Rad) and separated with non-reducing 12% SDS-PAGE. Proteins were transferred onto polyvinylidene difluoride (PVDF) membrane (Invitrogen) and probed with anti-ATPC1, a CF_1-specific ATP synthase antibody (Agrisera), as described in(Livingston et al., 2010). The membranes were incubated with anti-rabbit conjugated to alkaline phosphatase (AP) (KLP,Inc) at 1:5,000 dilution for 1 hour in

5%DM/TBST. The blots were developed using a standard AP detection system with BCIP/NBT as substrates (Sigma).

Acknowledgements

The authors would like to thank Dr. Nicholas Fisher for helpful discussions and Dolores M. Alvarez for maintenance and technical assistance. This work was supported by the U.S. Department of Energy (DOE), Office of Science, and Basic Energy Sciences (BES) under Award number DE-FG02-91ER20021 with additional support for phenotyping instrumentations and analyses provided by the MSU Center for Advanced Algal and Plant Phenotyping (CAAPP)

APPENDIX

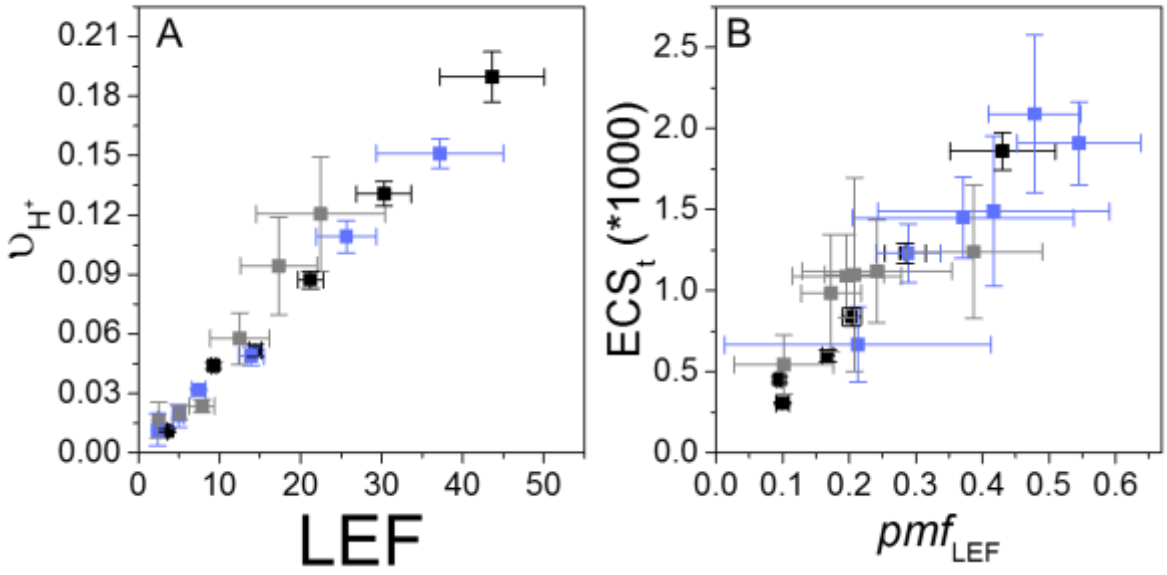

Supplemental Figure 7. Consistent proton and electron reactions in *ntrc.* The relationship between LEF and light-driven proton flux (v_{H^+}) across the thylakoid membrane and light-induced *pmf* versus *pmf* generated by LEF alone. Chlorophyll *a* fluorescence and ECS_t measurements were taken, as described in Materials and Methods, to calculate the steady-state proton flux into the lumen (v_{H^+}) (A), light-induced *pmf* (ECS_t) and LEF. From this data, we estimated pmf_{LEF} (i.e., pmf_{LEF}= LEF/g_{H^+}) in relation to ECS_t (B). Col-0 (black), *ntrc1* (blue) and *ntrc2* (grey) measurements were taken from attached leaves (n≥3) and error bars represent SEM.

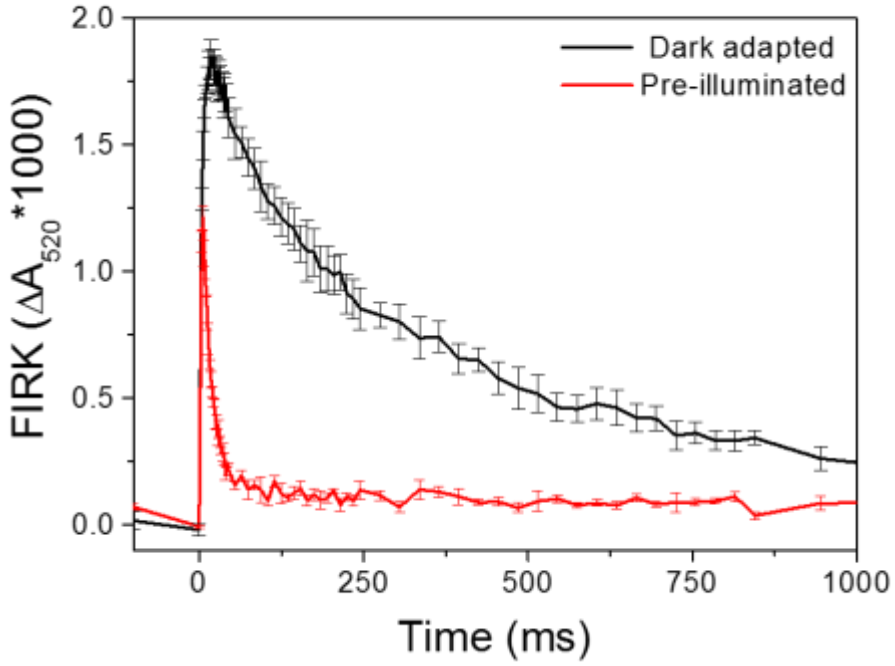

Supplemental Figure 8. ATP synthase kinetic response to light. Flash-induced relaxation kinetics (FIRK) response upon dark re-adaptation using intact *Arabidopsis* Col-0 leaves. The 520 nm FIRK response depicts the ATP synthase kinetics after dark adapting plants that were pre-illuminated for 3-min at very low light intensities (10 µmol photons m^2 s^{-1}). The red trace is the rapid response following 1 min dark adaptation and black trace is after dark adapting >30 min. The FIRK decay kinetics represent averaged (n≥3) measurements for Col-0 with error bars representing SEM.

REFERENCES

REFERENCES

Alonso JM, Stepanova AN, Leisse TJ, Kim CJ, Chen H, Shinn P, Zimmerman J, Barajas P, Cheuk R, Gadrinab C, et al (2003) Genome-wide insertional mutagenesis of *Arabidopsis thaliana*. Science 301: 653–657

Apel K, Hirt H (2004) Reactive oxygen species: metabolism, oxidative stress, and signal transduction. Annu Rev Plant Biol 55: 373–399

Buchanan BB (1980) Role of light in the regulation of chloroplast enzymes. Annu Rev Plant Physiol 31: 341–374

Buchanan BB, Wolosiuk RA (1976) Photosynthetic regulatory protein found in animal and bacterial cells. Nature 264: 669–670

Cejudo FJ, Ferrández J, Cano B, Puerto-Galán L, Guinea M (2012) The function of the NADPH thioredoxin reductase C-2-Cys peroxiredoxin system in plastid redox regulation and signalling. FEBS Lett 586: 2974–2980

Chae HB, Moon JC, Shin MR, Chi YH, Jung YJ, Lee SY, Nawkar GM, Jung HS, Hyun JK, Kim WY, et al (2013) Thioredoxin reductase type c (NTRC) orchestrates enhanced thermotolerance to arabidopsis by its redox-dependent holdase chaperone function. Mol Plant 6: 323–336

Collin V, Issakidis-Bourguet E, Marchand C, Hirasawa M, Lancelin J-M, Knaff DB, Miginiac-Maslow M (2003) The Arabidopsis plastidial thioredoxins new functions and new insights into specificity. J Biol Chem 278: 23747–23752

Cruz JA, Sacksteder CA, Kanazawa A, Kramer DM (2001b) Contribution of electric field (Δψ) to steady-state transthylakoid proton motive force (*pmf*) *in vitro* and *in vivo*. Control of *pmf* parsing into Δψ and ΔpH by ionic strength. Biochemistry 40: 1226–1237

D R Ort, Oxborough K (1992) In situ regulation of chloroplast coupling factor activity. Annu Rev Plant Physiol Plant Mol Biol 43: 269–291

Eliyahu E, Rog I, Inbal D, Danon A (2015) ACHT4-driven oxidation of APS1 attenuates starch synthesis under low light intensity in Arabidopsis plants. Proc Natl Acad Sci 112: 12876–12881

Evron Y, McCarty RE (2000) Simultaneous measurement of ΔpH and electron transport in chloroplast thylakoids by 9-aminoacridine fluorescence. Plant Physiol 124: 407–414

Foyer CH, Lelandais M, Harbinson J (1992) Control of the quantum efficiencies of photosystems I and II, electron flow, and enzyme activation following dark-to-light

transitions in pea leaves relationship between NADP/NADPH ratios and NADP-malate dehydrogenase activation state. Plant Physiol 99: 979–986

Gabrys H, Kramer DM, Crofts AR, Ort DR (1994) Mutants of chloroplast coupling factor reduction in Arabidopsis. Plant Physiol 104: 769–776

Groth G, Strotmann H (1999) New results about structure, function and regulation of the chloroplast ATP synthase (CF0CF1). Physiol Plant 106: 142–148

Hall CC, Cruz J, Wood M, Zegarac R, DeMars D, Carpenter J, Kanazawa A, Kramer D (2013) Photosynthetic measurements with the idea spec: an integrated diode emitter array spectrophotometer/fluorometer. Photosynth. Res. Food Fuel Future. Springer Berlin Heidelberg, pp 184–188

Hangarter RP, Grandoni P, Ort DR (1987) The effects of chloroplast coupling factor reduction on the energetics of activation and on the energetics and efficiency of ATP formation. J Biol Chem 262: 13513–13519

Heber U, Neimanis S, Dietz KJ, Viil J (1986) Assimilatory power as a driving force in photosynthesis. Biochim Biophys Acta BBA - Bioenerg 852: 144–155

Heineke D, Riens B, Grosse H, Hoferichter P, Peter U, Flügge U-I, Heldt HW (1991) Redox transfer across the inner chloroplast envelope membrane. Plant Physiol 95: 1131–1137

Hisabori T, Konno H, Ichimura H, Strotmann H, Bald D (2002) Molecular devices of chloroplast F1-ATP synthase for the regulation. Biochim Biophys Acta BBA - Bioenerg 1555: 140–146

Horton P (1983) Effects of changes in the capacity for photosynthetic electron transfer and photophosphorylation on the kinetics of fluorescence induction in isolated chloroplasts. Biochim Biophys Acta BBA - Bioenerg 724: 404–410

Junesch U, Gräber P (1987) Influence of the redox state and the activation of the chloroplast ATP synthase on proton-transport-coupled ATP synthesis/hydrolysis. Biochim Biophys Acta BBA - Bioenerg 893: 275–288

Junesch U, Gräber P (1991b) The rate of ATP-synthesis as a function of ΔpH and Δψ catalyzed by the active, reduced H+-ATPase from chloroplasts. FEBS Lett 294: 275–278

Kalituho L, Beran KC, Jahns P (2007) The transiently generated nonphotochemical quenching of excitation energy in Arabidopsis leaves is modulated by zeaxanthin. Plant Physiol 143: 1861–1870

Kanazawa A, Kramer DM (2002) *In vivo* modulation of nonphotochemical exciton quenching (NPQ) by regulation of the chloroplast ATP synthase. Proc Natl Acad Sci 99: 12789–12794

Ketcham SR, Davenport JW, Warncke K, McCarty RE (1984) Role of the gamma subunit of chloroplast coupling factor 1 in the light-dependent activation of photophosphorylation and ATPase activity by dithiothreitol. J Biol Chem 259: 7286–7293

Kiirats O, Cruz JA, Edwards GE, Kramer DM (2009) Feedback limitation of photosynthesis at high CO2 acts by modulating the activity of the chloroplast ATP synthase. Funct Plant Biol 36: 893–901

Kohzuma K, Bosco CD, Kanazawa A, Dhingra A, Nitschke W, Meurer J, Kramer DM (2012) Thioredoxin-insensitive plastid ATP synthase that performs moonlighting functions. Proc Natl Acad Sci 109: 3293–3298

Kohzuma K, Bosco CD, Meurer J, Kramer DM (2013) Light- and metabolism-related regulation of the chloroplast ATP synthase has distinct mechanisms and functions. J Biol Chem 288: 13156–13163

Kohzuma K, Cruz JA, Akashi K, Hoshiyasu S, Munekage YN, Yokota A, Kramer DM (2009) The long-term responses of the photosynthetic proton circuit to drought. Plant Cell Environ 32: 209–219

Konno H, Suzuki T, Bald D, Yoshida M, Hisabori T (2004) Significance of the epsilon subunit in the thiol modulation of chloroplast ATP synthase. Biochem Biophys Res Commun 318: 17–24

Kramer D, Cruz J, Hall C, Kovac WK, Zegarac R (2015) Plant phenometrics systems and methods and devices related thereto.

Kramer DM, Crofts AR (1989a) Activation of the chloroplast ATPase measured by the electrochromic change in leaves of intact plants. Biochim Biophys Acta BBA - Bioenerg 976: 28–41

Kramer DM, Crofts AR (1989b) Activation of the chloroplast ATPase measured by the electrochromic change in leaves of intact plants. Biochim Biophys Acta BBA - Bioenerg 976: 28–41

Kramer DM, Wise RR, Frederick JR, Alm DM, Hesketh JD, Ort DR, Crofts AR (1990) Regulation of coupling factor in field-grown sunflower: a redox model relating coupling factor activity to the activities of other thioredoxin-dependent chloroplast enzymes. Photosynth Res 26: 213–222

Lepistö A, Kangasjärvi S, Luomala E-M, Brader G, Sipari N, Keränen M, Keinänen M, Rintamäki E (2009) Chloroplast NADPH-thioredoxin reductase interacts with photoperiodic development in Arabidopsis. Plant Physiol 149: 1261–1276

Lepistö A, Pakula E, Toivola J, Krieger-Liszkay A, Vignols F, Rintamäki E (2013) Deletion of chloroplast NADPH-dependent thioredoxin reductase results in inability to regulate starch synthesis and causes stunted growth under short-day photoperiods. J Exp Bot 64: 3843–3854

Livingston AK, Cruz JA, Kohzuma K, Dhingra A, Kramer DM (2010) An Arabidopsis mutant with high cyclic electron flow around photosystem i (hcef) involving the NADPH dehydrogenase complex. Plant Cell Online 22: 221–233

Michalska J, Zauber H, Buchanan BB, Cejudo FJ, Geigenberger P (2009) NTRC links built-in thioredoxin to light and sucrose in regulating starch synthesis in chloroplasts and amyloplasts. Proc Natl Acad Sci 106: 9908–9913

Montrichard F, Alkhalfioui F, Yano H, Vensel WH, Hurkman WJ, Buchanan BB (2009) Thioredoxin targets in plants: the first 30 years. J Proteomics 72: 452–474

Morita S, Itoh S, Nishimura M (1982) Correlation between the activity of membrane-bound ATPase and the decay rate of flash-induced 515-nm absorbance change in chloroplasts in intact leaves, assayed by means of rapid isolation of chloroplasts. Biochimica et Biophysica Acta BBA - Bioenergetics 679: 125–130

Motohashi K, Kondoh A, Stumpp MT, Hisabori T (2001) Comprehensive survey of proteins targeted by chloroplast thioredoxin. Proc Natl Acad Sci 98: 11224–11229

Naranjo B, Mignée C, Krieger-Liszkay A, Hornero-Méndez D, Gallardo-Guerrero L, Cejudo FJ, Lindahl M (2016) The chloroplast NADPH thioredoxin reductase C, NTRC, controls non-photochemical quenching of light energy and photosynthetic electron transport in Arabidopsis. Plant Cell Environ 39: 804–822

Neuhaus HE, Emes MJ (2000) Nonphotosynthetic metabolism in plastids. Annu Rev Plant Physiol Plant Mol Biol 51: 111–140

Nikkanen L, Toivola J, Rintamäki E (2016) Crosstalk between chloroplast thioredoxin systems in regulation of photosynthesis. Plant Cell Environ 39: 1691–1705

Ort DR, Oxborough K (1992) In Situ Regulation of Chloroplast Coupling Factor Activity. Annu Rev Plant Physiol Plant Mol Biol 43: 269–291

Pérez-Ruiz JM, Spinola MC, Kirchsteiger K, Moreno J, Sahrawy M, Cejudo FJ (2006) Rice NTRC Is a high-efficiency redox system for chloroplast protection against oxidative damage. Plant Cell 18: 2356–2368

Quick WP, Mills JD (1986) Thiol modulation of chloroplast CF0-CF1 in isolated barley protoplasts and its significance to regulation of carbon dioxide fixation. Biochim Biophys Acta BBA - Bioenerg 851: 166–172

Richter ML (2004) Gamma–epsilon interactions regulate the chloroplast ATP synthase. Photosynth Res 79: 319–329

Richter ML, Hein R, Huchzermeyer B (2000) Important subunit interactions in the chloroplast ATP synthase. Biochim Biophys Acta BBA - Bioenerg 1458: 326–342

Sacksteder CA, Kanazawa A, Jacoby ME, Kramer DM (2000) The proton to electron stoichiometry of steady-state photosynthesis in living plants: a proton-pumping Q cycle is continuously engaged. Proc Natl Acad Sci U S A 97: 14283–14288

Sacksteder CA, Kramer DM (2000) Dark-interval relaxation kinetics (DIRK) of absorbance changes as a quantitative probe of steady-state electron transfer. Photosynth Res 66: 145–158

Schürmann P, Jacquot J-P (2000) Plant Thioredoxin Systems Revisited. Annu Rev Plant Physiol Plant Mol Biol 51: 371–400

Seelert H, Dencher NA, Müller DJ (2003) Fourteen protomers compose the oligomer III of the proton-rotor in spinach chloroplast ATP synthase. J Mol Biol 333: 337–344

Serrato AJ, Pérez-Ruiz JM, Spínola MC, Cejudo FJ (2004) A novel NADPH thioredoxin reductase, localized in the chloroplast, which deficiency causes hypersensitivity to abiotic stress in *Arabidopsis thaliana*. J Biol Chem 279: 43821–43827

Slovacek RE, Hind G (1981) Correlation between photosynthesis and the transthylakoid proton gradient. Biochim Biophys Acta 635: 393–404

Spínola MC, Pérez-Ruiz JM, Pulido P, Kirchsteiger K, Guinea M, González M, Cejudo FJ (2008) NTRC new ways of using NADPH in the chloroplast. Physiol Plant 133: 516–524

Stitt M, Lilley RM, Heldt HW (1982) Adenine nucleotide levels in the cytosol, chloroplasts, and mitochondria of wheat leaf protoplasts. Plant Physiol 70: 971–977

Thormählen I, Meitzel T, Groysman J, Öchsner AB, Roepenack-Lahaye E von, Naranjo B, Cejudo FJ, Geigenberger P (2015) Thioredoxin F1 and NADPH-dependent thioredoxin reductase C have overlapping functions in regulating photosynthetic metabolism and plant growth in response to varying light conditions. Plant Physiol 169: 1766–1786

Toivola J, Nikkanen L, Dahlstrom KM, Salminen TA, Lepisto A, Vignols hb F, Rintamaki E (2013) Overexpression of chloroplast NADPH-dependent thioredoxin reductase in

Arabidopsis enhances leaf growth and elucidates *in vivo* function of reductase and thioredoxin domains. Front Plant Sci 4: 389

Usuda H (1988) Adenine nucleotide levels, the redox state of the NADP system, and assimilatory force in nonaqueously purified mesophyll chloroplasts from maize leaves under different light intensities. Plant Physiol 88: 1461–1468

Wu G, Ortiz-Flores G, Ortiz-Lopez A, Ort DR (2007) A point mutation in atpC1 raises the redox potential of the Arabidopsis chloroplast ATP synthase gamma-subunit regulatory disulfide above the range of thioredoxin modulation. J Biol Chem 282: 36782–36789

Yoshida K, Matsuoka Y, Hara S, Konno H, Hisabori T (2014) Distinct redox behaviors of chloroplast thiol enzymes and their relationships with photosynthetic electron transport in *Arabidopsis thaliana*. Plant Cell Physiol 55: 1415–1425

CHAPTER 3
EVIDENCE FOR RAPID ATP EXCHANGE ACROSS THE CHLOROPLAST ENVELOPE

Work presented in preparation for publication:

L. Ruby Carrillo, John E. Froehlich, and David M. Kramer

(2017)

Abstract

Efficient and sustainable oxygenic photosynthesis requires the fine balancing of energy storage in the forms of ATP and NADPH to match the needs of metabolism. Several mechanisms, e.g. cyclic electron flow and the Mehler reaction (water-water cycle), have been proposed to alleviate imbalances between the production and consumption of ATP and NADPH. However, these mechanisms assume a closed adenylate system and fail to account for cytoplasmic flux. Early work suggested that exchange of ATP and ADP between the chloroplast and cytoplasm were slow, and thus the compartments likely have functionally independent adenylate pools; at least in the shorter time scale (i.e., under fluctuating light intensities), thus requiring a self-contained photosynthetic regulatory system. This view appeared to be consistent with work on mutants defective in expression of the chloroplast ATP/ADP+P_i nucleotide triphosphate transporters (NTT1 and NTT2), which suggested that these transporters function mainly in supplying energy to the chloroplast at night when photosynthesis is inactive. Surprisingly, our results show that isolated intact chloroplasts of spinach and Arabidopsis could export ATP almost as rapidly as intact thylakoids. We propose that the observed export was not caused by disruption of the chloroplast envelope, but represents a capacity for ATP/ADP transport that is within a factor of the maximal ATP synthesis rate. Expression analyses showed residual expression of both *ntt1* and *ntt2* in the individual and double mutant lines. Further segregation analysis showed that a complete (double-mutant) null line is lethal, presumably at germination, as seeds fail to grow. However, the leaky double knockdown mutant (NTTdKD) shows slower rates of ATP export from the chloroplast compared to the wild type, suggesting a role for NTT in this process. A closer examination of the photosynthetic

properties of NTTdKD line in Arabidopsis show substantial phenotypes, particularly under rapid fluctuating light conditions, which result in lowering of chloroplast ATP synthase activity, buildup of thylakoid proton motive force (*pmf*) and activation of the q_E response. Overall, these results suggest that NTT, in addition to supplying ATP at night, may help to balance the ATP/NADPH by connecting the stromal and cytosolic ATP pools.

Introduction

The compartmentalization of metabolic networks within cellular compartments allows for the communication among evolutionarily-distinct organelles, or the establishment of local environments optimized for specialized functions. The essential components that allow these compartments to function in this manner include highly selective, transport of metabolites, ions, and signaling molecules, across their membranes (Weber and Fischer, 2007).

The chloroplast is also enclosed by two distinct membranes or "envelopes." The outer envelope contains pore-forming proteins and is considered highly permeable to small molecules (<10kDa) (Flügge and Benz, 1984); while the inner envelope membrane contains a large number of transporters specific for substrates that are required to maintain distinct metabolic pools both in the chloroplasts and the cytoplasm (Heldt and Sauer, 1971; Neuhaus and Wagner, 2000; Flügge et al., 2011). The control of metabolic flow across these compartments may thus allow for the fine-tuning of local environments (e.g., pH, ionic balance, the presence or absence of certain chemical species) while avoiding the release of potentially toxic intermediates (Noctor and Foyer, 2000; Kramer and Evans, 2011). Balancing the requirement to control and compartmentalize processes is equally as important as the rapid and efficient flux of metabolites. In the case of photosynthesis, this balancing also requires that the ratio of ATP and NADPH produced during photosynthesis must perfectly match the needs of metabolism. The light-driven reactions of photosynthesis linear electron flow (LEF) produces a fixed stoichiometry of ATP and reductant (NADPH) insufficient to meet the demand necessary for carbon assimilation under static conditions alone (Allen, 2002). Given the relatively low pool sizes for these

energy carriers, and the high rates of energy flowing through them, even a small imbalance will lead to the accumulation of one form or another, causing metabolic congestion (Noctor and Foyer, 2000).

It has been generally assumed that the exchange of ATP and ADP across the chloroplast envelope is quite slow. This view came from early transport studies that suggested the chloroplast envelope had very low nucleotide exchange capacity (~5 μmoles per mg Chl^{-1} hr^{-1}) (Heldt, 1969; Stitt et al., 1982; Kampfenkel et al., 1995; Neuhaus et al., 1997). This led to the view that the chloroplast inner envelope nucleotide triphosphate transporter (NTT) mainly functions as an ATP importer, providing energy when photophosphorylation inactive, thus maintaining metabolic reactions in darkness (Heldt, 1969; Schunemann et al., 1993; Neuhaus et al., 1997).

On the other hand, studies of metabolites in plant cell compartments suggest that the adenylate status of the chloroplast stroma and cytoplasm are highly synchronized in response to rapid changes in light intensity and CO_2 levels (Santarius et al., 1964; Heber and Santarius, 1970; Heber, 1974; Flügge and Hinz, 1986). It has also been shown that disrupting mitochondrial respiration directly effects plastid ATP/NADPH levels (Bailleul et al., 2015), suggesting energetic communication or crosstalk between chloroplast and mitochondria.

A truly isolated chloroplast adenylate pool thus implies that not only must the photosynthetic "energy budget" be balanced by adjusting processes within the chloroplast, but also coordinated to that of the rest of the cell. Several, non-exclusive, processes have been proposed to balance the ATP/NADPH production and consumption ratio, including: 1) alternative electron transport processes in the chloroplast, such as cyclic electron flow

(CEF), the water-water cycle, and the plastid terminal oxidase that can modulate the output of ATP and NADPH to meet demand (Cruz et al., 2005; Eberhard et al., 2008; Kramer and Evans, 2011); 2) Malate valve, in which reducing equivalents are exported from the chloroplast through the exchange of malate and oxaloacetate, allowing production of ATP by oxidative phosphorylation in the mitochondrion (Flügge and Heldt, 1991; Scheibe, 2004). How these processes could be regulated to maintain both the stromal and cytosolic adenylate pools is not known, but could involve metabolic exchange or inter-organelle signaling, similar to the proposed anterograde and retrograde signaling processes (Eberhard et al., 2008).

In our recent work on CEF (described below), we serendipitously found evidence for much more rapid exchange of ATP and ADP across the chloroplast envelope, leading us to re-evaluate the isolated adenylate pool model. The exchange of ATP and ADP across the chloroplast envelope, a question that has been studied for some decades, at a very interesting time in bioenergetics, when many groups were making big strides by comparing the energy coupling of mitochondrial oxidative phosphorylation with that of photosynthesis. Mitochondria generate ATP and export through the ATP/ADP carrier protein (AAC). AAC catalyzes the electrogenic exchange of ATP for ATP (see review by (Klingenberg, 2008). Inorganic phosphate (P_i) is transported through a separate Pi carrier in its neutral (protonated form). Both these reactions are driven forward towards ATP export and P_i import by coupling to the electric potential across the membrane, fulfilling the role of supplying energy to the cell.

In contrast, the chloroplast expresses an evolutionarily distinct system, NTT (Reiser et al., 2004), with high sequence similarity (>66%) to the ATP/ADP transporters of obligate

intracellular parasites, including *Rickettsia prowazekii* and *Chlamydia psittaci* (Winkler, 1976; Hatch et al., 1982; Kampfenkel et al., 1995; Möhlmann et al., 1998; Neuhaus and Winkler, 1999), where they parasitically extract energy from other organisms (Trentmann et al., 2008). The NTT transporters are thought to catalyze an electroneutral exchange of ATP for both ADP and P_i (Trentmann et al., 2007). The lack of coupling to the membrane potential implies that, energetically, the NTT reaction should be reversible, perhaps acting to supply ATP to the chloroplast with ATP under some conditions, but export it under others. The ATP/ADP transport kinetics of the pathogenic bacteria, as well as for the chloroplasts NTT, are highly P_i-dependent and required as a co-substrate with ADP for optimal exchange of ATP (Trentmann et al., 2008), consistent with the NTT electroneutral mode of exchange.

In *Arabidopsis thaliana* there are two isoforms of NTT- NTT1 and NTT2, that share nearly identical structural and functional properties, but previous work suggested that NTT2 has a more prominent role given that *ntt2* knockout mutants display stronger effects than *ntt1* on plant development (Neuhaus et al., 1997; Tjaden et al., 1998; Reiser et al., 2004). Although NTT is electroneutral, transport studies using spinach have classified it mainly as an ATP importer, providing energy when photophosphorylation is inactive, thus maintaining metabolic reactions in the dark. However, many of the earlier studies failed to account for integral components required for optimal exchange, e.g., the co-substrate, P_i was excluded, possibly resulting in erroneous interpretations (Heldt, 1969; Stitt et al., 1982).

While performing controlled experiments to assess the mechanisms of CEF we serendipitously found evidence for much higher rates of ATP exchange across the

chloroplast envelope. This led us to the work described here, that reexamines NTT and its potential mechanism and role in balancing the energy budget of the chloroplast.

Results

Integrity of the chloroplasts envelope

To investigate chloroplast transport mechanisms, it is important to assess the integrity of the chloroplast envelope. Several methods were used to determine if the chloroplast inner envelope presented a sealed, physical barrier to diffusion. First, centrifugation of our spinach chloroplast preparation on a Percoll density gradient, showed a migration pattern consistent with the majority being intact chloroplasts. Second, we assessed the fraction of chloroplasts that were intact based on the index of refraction of the intact stroma, as visualized using contrast microscopy (Walker et al., 1987).

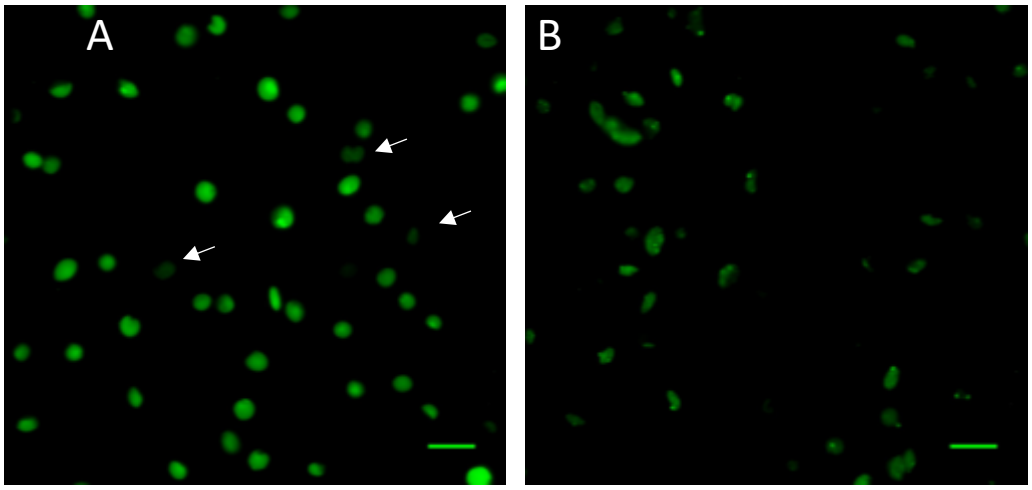

Figure 16. Assessing chloroplasts intactness with CFDA staining. Representative images of isolated chloroplasts (A) and thylakoids (B) labelled with CFDA staining and visualized by epifluorescence microscopy. Arrows indicate damaged and/or out of focus plastids. Scale bars are 10 μm.

To confirm this assessment, we examined chloroplasts stained with the fluorescent supravital stain carboxyfluorescein diacetate (CFDA) (Figure 16). CFDA is used to differentiate intact and damaged chloroplasts, as it strongly fluoresces when de-esterified by carboxylesterases, which are found specifically in the intact chloroplast stroma (Schulz et al., 2004). Figure 16 shows representative microscope images of our chloroplasts preparation (Figure 16A) and osmotically shocked chloroplasts or broken thylakoids (Figure 16B). An issue encountered with this method was the difficulty in distinguishing decreased fluorescence with cells at different phase of alignments, as depicted in white arrows.

Chloroplasts have been classified into an array of categories based on the biochemical properties following isolation, with "type A" being the only category verified to contain both inner and outer undisrupted membranes and rapid rates of CO_2 fixation (50-250 μmol mg Chl^{-1} hr^{-1}) without the addition of exogenous substrate (Hall, 1972a). Type A is also differentiated by its impermeability to NADP and ferricyanide (Hall, 1972a; Lilley et al., 1975). As a third method, the membrane integrity was verified by monitoring the rates of membrane-impermeable ferricyanide reduction via electrons from PSI using intact and osmotically shocked chloroplasts suspensions, as performed previously (Hill, 1951). As shown in Figure 17, only the thylakoid sample resulted in an absorbance decrease upon light-activation of the photosystems with less than 3% of the chloroplasts layer appearing leaky or disrupted.

As a further verification, we assessed the intactness of our chloroplast preparations by measuring the ability to import proteins across the chloroplast membranes. Using the methods described in (Froehlich, 2011), we found that ribulose bisphosphate carboxylase

oxygenase (Rubisco) small subunit (SSU) with intact transit peptide was readily imported into chloroplast (Figure 17B), whereas luciferase, a large (60 kDa protein) with no chloroplast transit peptide, was not. These results imply that the chloroplasts possess a complete, functional envelope that is able to actively transport native proteins. In addition, this assay demonstrates that the non-native protein luciferase, is not transported, consistent with the impermeability of the chloroplast envelopes to proteins of this size (Flügge and Benz, 1984), nor does it associate with the chloroplast envelope.

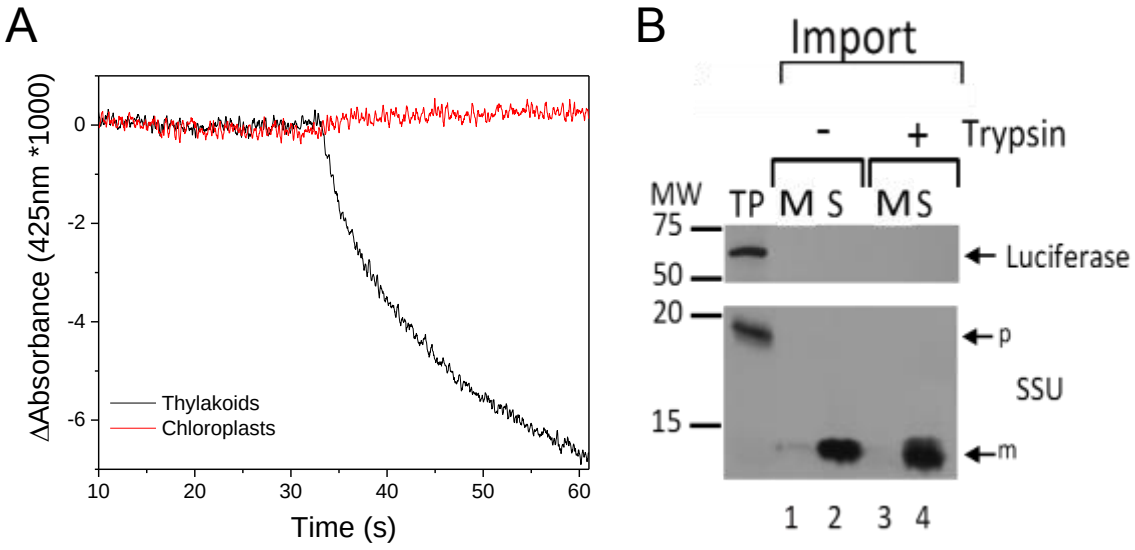

Figure 17. Confirming the integrity of intactness via ferricyanide and import assays. Confirmation of ferricyanide impermeability in intact chloroplasts was assessed by light induced ferricyanide reduction (A) measured at 425 mm using thylakoids (black) and chloroplasts (red) preparations. Import assays confirmed rubisco small subunit (SSU), but not Luciferase, is imported into isolated chloroplasts (B). Import assays using either [3H]-labeled Luciferase or [3H]-labeled precursor to the SSU was performed according to Froehlich (2011). Image depicts membrane (M) and soluble (S) fractions following the import assay, as well as the total protein (TP), precursor (p), and mature (m) portions.

Analysis of ATP transport kinetics

Assays were performed following confirmation of membrane intactness for each chloroplast preparation using the ferricyanide assay (Figure 17A). ATP export rates were measured using luciferase luminescence, which we have demonstrated (Figure 17B) cannot penetrate the chloroplast envelope over this time scale. The exclusion of luciferase from the stromal compartment allowed for real-time detection of photosynthesis-generated ATP external to the stroma. Two sets of conditions were used. In LEF conditions, methyl viologen (MV) was added as an electron acceptor for PSI. Under CEF conditions, LEF was inhibited at PSII by the addition of DCMU (dichloromethyl urea). ATP production in thylakoids was negligible in the presence of DCMU, 1.3 μmol ATP mg Chl^{-1} hr^{-1} ±0.86 (Figure 18A, grey trace), consistent with the rupture-induced loss of stromal components including ferredoxin, which is required for CEF (Munekage et al., 2002). In contrast, thylakoids showed elevated rates of ATP production under LEF conditions (129 μmol ATP mg Chl^{-1} hr^{-1} ±22, Figure 18A black trace), indicating that the thylakoids were chemiosmotically intact. Addition of the uncoupler gramicidin, which should dissipate the light-induced *pmf*, completely inhibited light-induced ATP production (Nishio and Whitmarsh, 1991). The drastic loss of ATP production in thylakoids under CEF conditions alone, imply the lack of a stromal component(s), down-regulation or disruption of a CEF-specific process upon isolation.

In the presence of DCMU, ATP production was 5-fold higher in chloroplasts compared to thylakoids (7.3 μmol ATP mg Chl^{-1} hr^{-1} ±1.1, Figure 18B, grey trace), likely indicating that all stromal components needed for CEF-related ATP production were present (Alric, 2014; Strand et al., 2016) supporting our assessment of chloroplast

envelope intactness. The most surprising result was that in chloroplast preparations under LEF conditions showed ATP production rates (92.6 μmol ATP mg Chl^{-1} hr^{-1} ±1.1., Figure 18B, black trace) that were only slightly slower than thylakoids, suggesting that ATP was able to diffuse through the chloroplast envelope and react with luciferase at rates near those of its production at the thylakoid membrane.

Rates under LEF simulated conditions ranged from 50-200 μmol ATP mg-Chl^{-1} hr^{-1}, possibly due to differences in the age of the plant, time and duration of extraction. However, even when taking error into account, rate of exchange between ATP with ADP + P_i was estimated to be 20-fold higher than previously suggested (Heldt, 1969; Stitt et al., 1982; Neuhaus et al., 1997), and imply the presence of a highly active ATP transport system. In reference to photosynthesis, the rates are highly significant and account for 50% of the rate required for CO_2 assimilation (Jensen and Bassham, 1966), which can be a contributing factor in offsetting photosynthetic metabolic pools.

Deciphering the two Arabidopsis *ntt* mutant isoforms

To assess the potential roles of NTT1 (locus AT1G80300) and NTT2 (locus AT1G15500) in the observed rapid ATP transport, we investigated the effects of a series of Arabidopsis T-DNA mutant lines affecting the expression of these genes. Our initial work focused on several isoforms of the two mutant lines. Four of the five single mutants were confirmed homozygous by PCR: *Atntt1-1* (Salk_023159), *Atntt2-1* (Salk_016353), *Atntt2-2* (Salk_081179), and *Atntt2-3* (Salk_016244). To verify if homozygous lines were true null mutants, the gene expression was analyzed via qRT-PCR using glyceraldehyde 3-phosphate dehydrogenase (GADPH) as the housekeeping gene. Our results (Table 1) show differences in the expression response compared to wild type for the individual T- DNA lines,

particularly in *Atntt1-1* and *Atntt2-1* demonstrating the greatest decrease in expression compared to Col-0 with a ~5-fold and ~4-fold decrease, respectively.

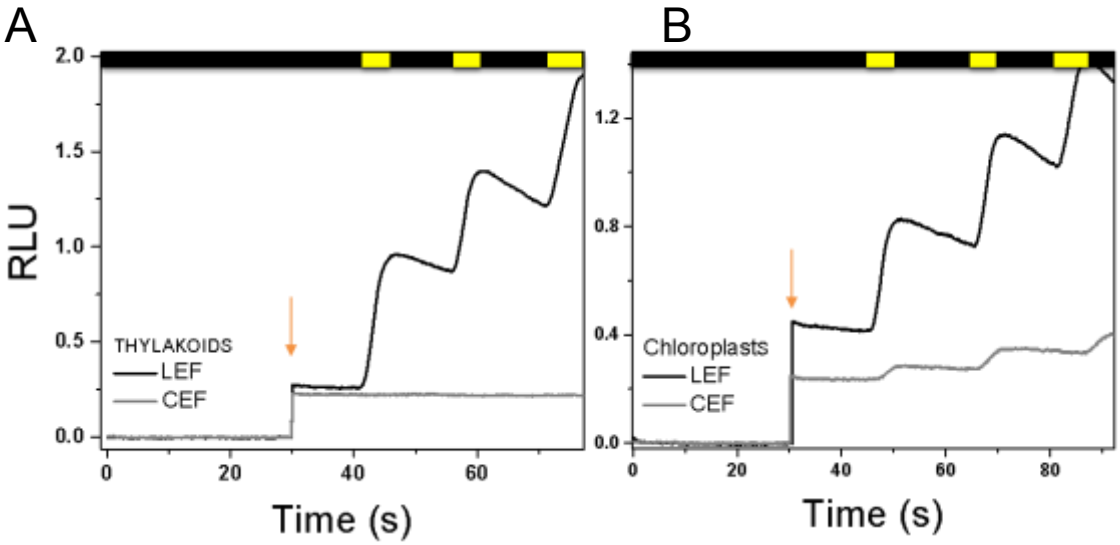

Figure 18. ATP detection assay using a Becquerel phosphoroscope and luciferase/luciferin. reaction. Rates were calculated using CEF (grey) and LEF (black) simulated conditions for both thylakoids (A) and chloroplasts (B). Luciferase reagent was added at the 30 s time-point (designated with an arrow). Rates were averaged (n>3) based on light-activated positive slopes (top bar illustrates light and dark portions).

Table 1. *Atntt1* and *Atntt2* gene expression levels compared to Col-0

Mutant	LOG_2-FOLD CHANGE (compared to wild type)
Atntt1-1	-4.74
Atntt1-2	-0.156
Atntt2-1	-3.70
Atntt2-2	0.847
Atntt2-3	-1.181
Atntt2-4	-0.835

Shortly after, we acquired the double NTT mutant seeds *Atntt1-2* (Salk_013530) x *Atntt2-4* (GARLIC_288_EO8.b.1a.Lb3Fa) previously studied (Reiser et al., 2004) and confirmed to be homozygous by PCR. Gene expression levels (Table 1) of the *Atntt1-2 x Atntt2-4* double-mutant confirmed a decrease in the expression levels for both *ntt1* and *ntt2* (-0.156 and -0.835 $\log_2$ fold-change compared to Col-0, respectively), however, to a much lesser extent compared to *Atntt1-1* and *Atntt2-1*. This implies that the previously assumed "null NTT double-knockout mutant" may be leaky and should more accurately be classified as a knock-down (KD) rather than knock-out. Herein the *Atntt1-2 x Atntt2-4* double-mutant will be referred to as NTTdKD.

Given that the previously reported mutant lines were leaky, we attempted to generate a true double null line using the workflow described in (Bolle et al., 2013). Crossing of the two single-mutants (*Atntt1-1* and *Atntt2-1*), which exhibited the largest reduction in gene expression, was performed, resulting with a heterozygous double mutant F1 generation. However, the offspring (selfing) of F1 generation only produced a homozygous-heterozygous F2 double mutant population. Additional selfing and propagation of proceeding homozygous-heterozygous populations (F3 and F4) only resulted in seeds that failed to germinate and lines that were either homozygous for *ntt1* or heterozygous for *ntt2*. When seeds were grown on MS plates supplemented with sucrose, 55% of the seeds failed to grow in the F4 generation compared to 18% in Col-0 ($p = 0.0079$, n=10). As predicted by other researchers, if segregation of F2-F4 populations failed to produce homozygous double mutants, we can presume that the *Atntt1xAtntt2* double mutants are embryo lethal.

Photosynthetic responses of Arabidopsis mutants defective in NTT expression

The strongest need for rapid energy balance will most likely occur during rapid changes in light input. We thus screened our mutant lines using the recently developed DEPI (Dynamic Environmental Photosynthetic Imaging) chambers (Cruz et al., 2016a). After growth under standard laboratory conditions, plants were subjected to a 3-day light regimen (as illustrated in Figure 19A) consisting of: 1) flat day at 100 μmol photons m^2 s^{-1}, 2) sinusoidal day where light increased to 500 μmol photons m^2 s^{-1} at mid-day and 3) fluctuating light day, with a pattern of doubling light intensity superimposed on the sinusoidal waveform. Several photosynthetic parameters were computed from the fluorescence images (see Appendix), including maximal PSII quantum efficiency (F_V/F_m), the realized PSII quantum efficiency during illumination (φ_{II}), and nonphotochemcial quenching (NPQ) with its rapidly (qE) and slowly (qI) decaying forms. It should be noted that, to avoid long-term dark acclimation, which we found to disrupt photosynthesis, we did not distinguish in the imaging experiments qI and other slowly-relaxing forms of NPQ, e.g. qZ or qT.

Table 2. The maximal quantum efficiency of PSII (Fv/Fm) values

Line	Fv/Fm prior to Flat day (100 μmol photons m^2 s^{-1})	Fv/Fm prior to Sinusoidal day (0-500 μmol photons m^2 s^{-1})	Fv/Fm prior to Fluctuating day (0-1,00 μmol photons m^2 s^{-1})
Col-0	0.79 ± 0.003	0.79 ± 0.004	0.77 ± 0.005
NTTdKD	0.77 ± 0.011	0.77 ± 0.011	0.76 ± 0.005

Values are means ± SD of n ≥ 5. The slight decrease in φ_{II} with increasing days was not significantly different in the wild-type compared to the mutant (P = 0.4827) as determined by the student's T-test.

Prior to illumination on each experimental day, the F_V/F_m values were recorded (Table 2), showing the double *ntt* mutant exhibited marginally lower values, perhaps reflecting a slight increase in long-term photoinhibition. Larger phenotypes appeared during illumination, in particular, at higher and fluctuating light intensities (Figure 19). On day 1, with constant low light, the *ntt* double mutant only showed slight (about 5%) but a consistent decreased PSII photosynthetic efficiency (φ_{II}), however the extent of NPQ (Figure 19B) was highly elevated (about 1.5-fold) and attributable to increases in both qE (Figure 19D) and qI (Figure 19E).

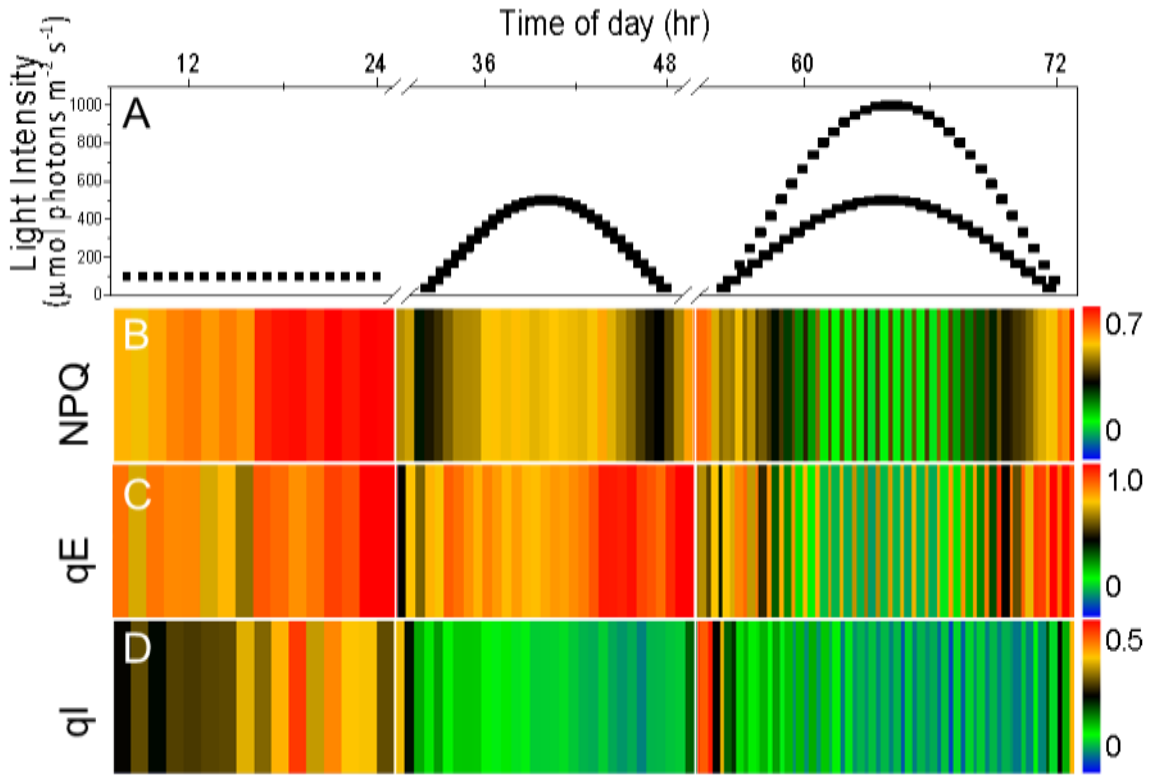

Figure 19. NTTdKD mutant displays hysteretic behavior to fluctuating light. Chlorophyll *a* fluorescence imaging was performed on 2-week old Arabidopsis plants using the DEPI system to capture three distinct 16-hr photoperiods (constant, sinusoidal and fluctuating light) over a three-day light cycle (A). The measured parameters include NPQ (B) and the associated qE (C) and qI (D) response. Data represents log2-fold changes normalized to wild type with legend and values displayed on the right of each row (n>5).

On day 2, during the sinusoidal illumination, the large increase in NPQ (Figure 19B) appeared be attributed to a larger increase (over 2-fold compared to Col-0) in qE (Figure 19C) and a smaller increase in qI (Figure 19D). The most interesting phenotype occurred on day 3, during fluctuating light. Although the difference in qI was similar to the previous day, the qE response in the mutant fluctuated dramatically, exceeding that of Col-0 during the high light periods, but falling below during the lower light intervals. This hysteretic behavior, easily observed in the log_2-fold heat maps (Figure 19C), suggest a strong impact of low NTT expression on the thylakoid *pmf*, with higher extents during the high light, and lower extents during the intermediate intensities.

In vivo assessment of ATP photosynthetic responses of NTTdKD to CO_2

In order to assess the photosynthetic responses of the mutants under more demanding pressures, particularly on the stromal adenylate pools, we used the IDEA (Idea Diode Emitter Array) spectrophotometer/ fluorimeter, to capture information on both the light reactions of PSII via chlorophyll a fluorescence and ATP synthase through the electrochromic shift (ECS) (description of measurements found in Appendix) (Baker, 2008; Hall et al., 2013). The NTTdKD mutants were measured under minimal CO_2 (<1ppm) concentrations, to create an environment of excess ATP and reductant (NADPH) while perturbing the system with fluctuating light periods. Estimations of the transthylakoid H^+ flux (v_{H^+}) are based on the initial decay rates of the ECS signal and compared to LEF, given that the H^+ and electron reactions are highly coupled and produce a fixed (H^+/e^-) stoichiometric ratio. Figure 20A, illustrates the response of the proton circuit to LEF in wild-type (black trace) and NTTdKD (red trace) revealing an increased v_{H^+} per LEF, as previously demonstrated with hcef2, high cyclic mutants (Strand et al., 2017). There was

nearly a 2-fold increase in NTTdKD slope (0.0016 ± 0.006) compared to Col-0 (0.0009 ± 0.007, p<0.0001 ANCOVA, n>3). An increase in CEF would supplement photosynthesis by

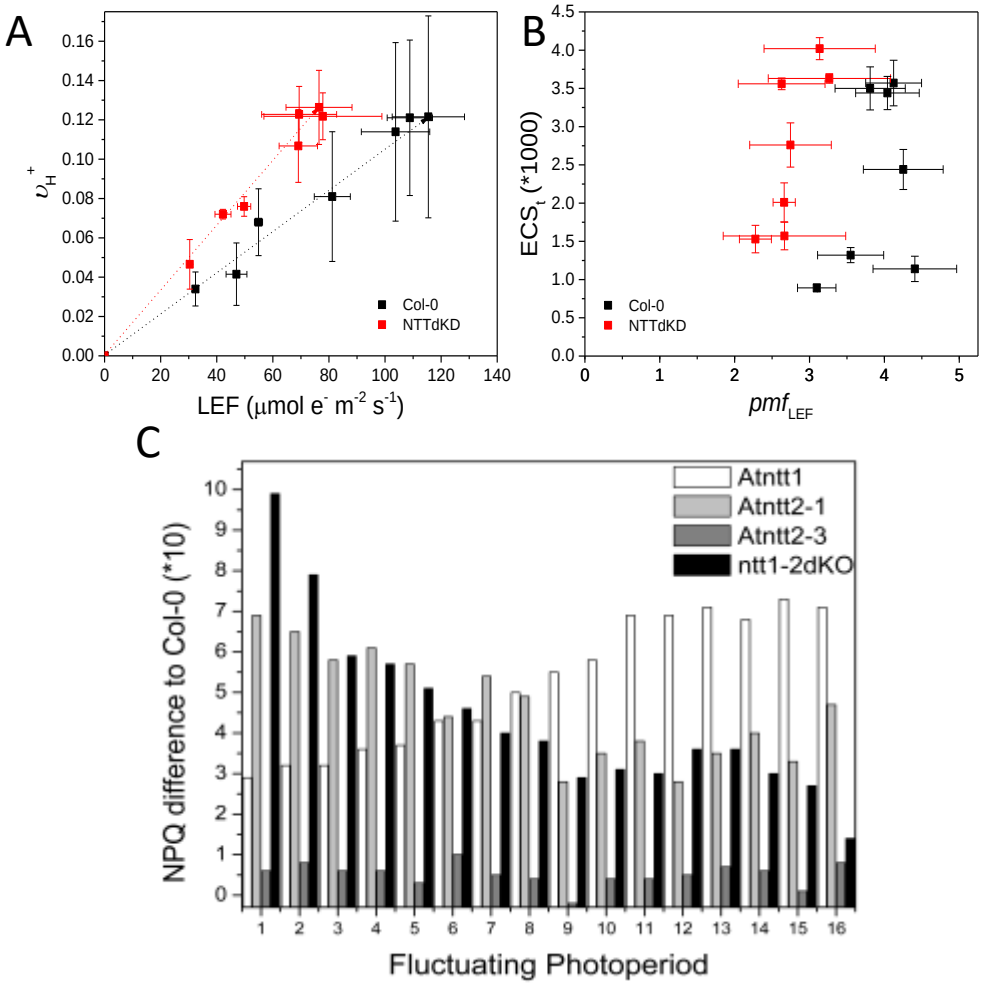

Figure 20. Photosynthetic responses to minimal CO_2 levels. The relationship between fluorescence and ATP synthase in NTTdKD to minimal CO2 levels is illustrated (A-B). Graph (A) describes the relationship between electron flow of LEF to the initial flux of protons (νH+). Graph (B) shows the pmf associated with LEF reactions in relation to the total ECS amplitude in NTTdKD mutants (red) compared to wild-type (black). n>3 and error bars illustrate SEM. Graph (C) shows the differences in NPQ levels for the single *ntt* mutants as well as NTTdKO compared to wild type under fluctuating light with lower (300 ppm) CO2 conditions. Light conditions pertain to the fluctuating light regime described in the methods. n≥3.

supplying additional H^+ to the *pmf* independent of PSII, thus offsetting a misbalance between the ATP/NADPH ratio.

In addition, we investigated the overall *pmf*, estimated by the total ECS amplitude (ECS_t), and compared it to the *pmf* attributed to LEF alone (pmf_{LEF}) (Figure 20B). As described in Avenson, Cruz, Kanazawa & Kramer (2005a), the method complements the initial assessment (Figure 20A) and takes into account the kinetics related to ATP synthase turnover by measuring the difference in LEF versus the conductivity of ATP synthase (g_{H^+}). Once again, there was an apparent difference in the NTTdKD mutant compared to Col-0 (Figure 20B) with a consistently lower pmf_{LEF} associated with higher ECS amplitudes.

The surprising result was obtained using the DEPI system described above to assess the NPQ response under lower (~300 ppm) CO_2 concentrations. As shown in Figure 20C, the response for NTTdKD resembled the accumulated response for the individual *ntt1* and *ntt2* lines. In addition, the strongest differences in NPQ response compared to wild type was initially present in the ntt2 and NTTdKD lines. The levels slowly decreased to a consistent basal level after ~8 hours of increasing fluctuating light, while *ntt1* levels alone started to increase. These results reveal contrasting differences in the expression response for *ntt1* versus *ntt2*, possibly associated with the evolutionary reason for maintaining two isoforms of the NTT gene.

Rapid rates of ATP efflux diminished in NTTdKD

To test the hypothesis that NTT is involved in the rapid efflux of ATP in isolated chloroplasts, we assayed the rates of ATP production and transport in the Arabidopsis NTTdKD mutants using the luciferase assay described above (Figure 18). As shown in Figure 21, the rate of ATP appearance after the addition of luciferase in the wild type

thylakoids was like that of NTTdKD (47.4 and 41.1 μmol ATP mg Chl^{-1} hr^{-1}, respectively) and around 2.7-fold lower than spinach. However, the more meaningful finding was between the NTTdKD mutant and wild type for the isolated chloroplasts (Figure 21, p=0.0007 Students t-test, n=3), with rates of ATP efflux 3-fold higher in Col-0. This implies that the decreased expression levels in the *ntt* double mutant specifically prevented the

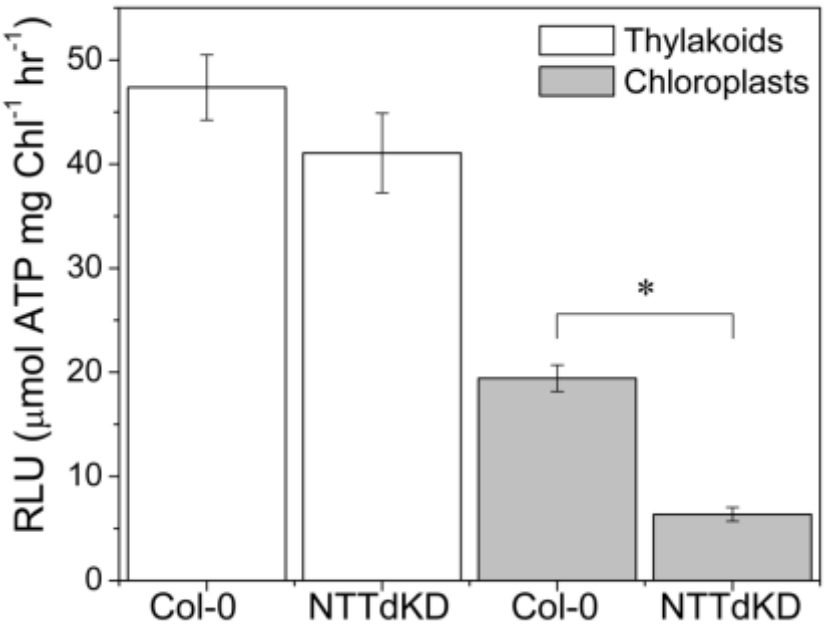

Figure 21. ATP efflux rates via luciferase assay. The graph represents the rates of ATP synthesized and quantified in both thylakoid (white bars) and intact chloroplasts (grey bars) preparations of *A. thaliana* using wild-type and NTTdKD plants. Error bars represent SEM with n>3 and the significant difference (P-value=0.0007), as determined by the student's T-test

rapid rates of ATP efflux from intact chloroplasts and not thylakoids, confirming the rapid appearance of detectable ATP is attributed to NTT.

Discussion

It is assumed that the adenylate pools of the chloroplast are kinetically isolated from those in the cytosol, so any discrepancies in the photosynthetic energy budget must be balanced solely by chloroplast reactions (Asada, 1999; Joët et al., 2002; Kramer et al., 2004; Scheibe, 2004). This concept was mainly influenced by earlier work showing slow rates of ATP transport across the inner envelope membrane (Heldt, 1969; Stitt et al., 1982). ATP is assumed to equilibrate between the stroma and cytosol at slow rates, possibly through indirect methods, e.g., via the triose phosphate shuttle where it is converted to sucrose and aids in the ATP/NADPH offset by only requiring ATP rather than reductant (Heber and Heldt, 1981). However, our results of rapid rates of ATP efflux (Figures 18 and 21) suggest otherwise. Opening the possibility that ATP energy balancing could encompass reactions within other compartments, such as cytosolic and mitochondrial reactions. Two major electron transport coupled systems that synthesize ATP are photophosphorylation in chloroplasts, during the day, and oxidative phosphorylation in mitochondria, both day and night (Raghavendra and Padmasree, 2003). Both compartments, along with the cytosol, yield adenylates at different rates and it seems essential for pools to metabolically exchange for a well-balanced system (Stitt et al., 1982; Heineke et al., 1991).

With the current advancements in the field, we can now account for the missing and contributing factors that were excluded during the initial assessments of plastidial ATP transport. For instance, early work failed to include the adenylate kinase inhibitor i.e., DAPP, which prevent the conversion of ATP and AMP to ADP (Heldt, 1969). By incorporating DAPP we can more accurately account for precise concentration differences between ATP and ADP without interconversion. Additionally, assays neglected to account

for the redox regulation of ATP synthase, e.g., exclusion of DTT, and most importantly the required ADP co-substrate, P_i (Heldt, 1969; Stitt et al., 1982). The chloroplast ATP transporter was originally compared to the well-studied AAC of mitochondria, but studies have now confirmed that the two systems are phylogenetically, structurally, and physiologically different (Fiore et al., 1998; Saier, 2000; Nury et al., 2006). Recent findings have confirmed the high-sequence homology of the NTT from Arabidopsis more closely resembles the human parasitic NTT bacterium and the kinetics of both are highly P_i -dependent for optimal exchange of ATP (Trentmann et al. 2008; J. Tjaden et al. 1999; Trentmann et al. 2007). The rates of ATP exchange increased by 4-fold with the addition of P_i and ADP rather than ADP alone (Trentmann et al., 2008), consistent with the electroneutral mode of exchange for NTT. In agreement, *in vitro* studies using the *Atntt1* x *Atntt2* double knockdown lines demonstrate slower rates of ATP export when compared to wild type. The hampered rates of ATP efflux pertained to intact chloroplast systems alone, with comparable rates of export in thylakoids.

The work presented in this paper considers the appropriate buffering conditions with the addition of DAPP, DTT and P_i to optimally quantify the rapid rates of ATP export using thylakoids and chloroplasts for both spinach (Figure 18) and Arabidopsis (Figure 21). Previous work classified NTT as a nocturnal import of ATP (Neuhaus et al., 1997) based on the sluggish rates (Heldt, 1969; Stitt et al., 1982) and the lack of ATP produced during the night cycle via the photosynthetic light reactions. We agree that NTT can possess a role during the night cycle when reactions are depleted of ATP; however, we propose that it also functions to aid in ATP homeostasis between the stroma and cytosol, particularly in stressful or energy-depleted conditions. In agreement with this hypothesis, the

photosynthetic responses were most adverse under more dynamic and stressful conditions, e.g. rapid alterations in light intensities (Figure 19) and limiting CO_2 concentrations (Figure 20), which would be expected if a major source of stromal adenylate pool is restricted (Sharkey, 1990).

According to Armisén et al. (2008), within the Arabidopsis genome over 90% of the protein-coding genes contain homologues and are usually influenced by functional selection, rather than gene duplication. The redundancy of NTT can have an evolutionary purpose related to adenylate transport, possibly induced under varying stress conditions. This is demonstrated with the differences in the isoform-specific responses under low CO_2 concentration and fluctuating light. It appears that the overall NTTdKD response is the accumulation of both individual *Atntt1* and *Atntt2* responses (Figure 20C). Furthermore, NTTdKD appears to have reduced expression levels (Table 1) but to a much lesser extent than the single mutant lines, *Atntt1-1* and *Atntt2-1* which were unable to successfully produce a double mutant. These findings implicate a more essential role for NTT, not only in supplying ATP at night, but also in balancing the inconstant system by connecting the stromal and cytosolic ATP pools.

Materials and Methods

Plant and Growth Conditions

Arabidopsis thaliana single NTT mutant lines were obtained from the Arabidopsis Biological Resource Center (USA) and four were confirmed homozygous: *ntt1-1* (Salk_023159), *ntt2-1* (Salk_016353), *ntt2-2* (Salk_081179), and *ntt2-3* (Salk_016244) by PCR analysis (Alonso et al., 2003). NTT double-knockdown mutant (NTTdKD) consist of a T-DNA insertion at *ntt1-2* (Salk_013530) and *ntt2-4* (GARLIC_288_E08.b.1a.Lb3Fa), which

were provided courtesy of Dr. H. Ekkehard Neuhaus. NTTdKD mutant was confirmed by PCR using primers previously described (Reiser et al., 2004). Plants were grown on soil for a 16:8 day-night cycle in growth chambers with 125 μmol photons m^2 s^{-1} for ≥3 weeks. Generation of additional double-mutants was attempted by crossing homozygous *ntt1-1* with *ntt2-3* lines, as they both demonstrated the greatest reduction in gene expression via qRT-PCR. F1 crosses successfully yielded heterozygous mutants of both *ntt1* and *ntt2*. However, F2-F4 crosses only produced homozygous NTT1 lines and heterozygous NTT2 lines. As performed by Bolle et al. 2013, additional assessment of double-mutants was made by plating F2-F4 seeds on MS plates supplemented with sucrose.

Quantitative gene expression studies

Total RNA was extracted from 100 mg plant material using the RNeasy Plant Mini Kit (Qiagen). RNA (1 μg) was then reverse transcribed to produce cDNA using Superscript III reverse transcriptase (Invitrogen) primed with random hexamers. The expression levels were calculated using SYBR Green I (Thermo Fisher Scientific) via qRT-PCR at The Research Technology Support Facility (RTSF) at Michigan State University.

Table 3. qRT-PCR primers for NTT gene expression studies.

Gene	Locus	Forward primer	Reverse primer
NTT1	AT1G80300	5'-TGGGAACGATGGAAAGCTTG-3'	5'-CGTGCAGGTTGAGAAGTCT-3'
NTT2	AT1G15500	5'-GGGAACAATGGAGAGCTTGA-3'	5'-CTGTGCAGGTTGAGAAGTCG-3'
GAPDH	AT1G13440	5'-TGAGGGATGGCAACACTTTCCC-3'	5'-ACCACTGTCCACTCTATCACTGC-3'

Chloroplast Intactness Assays

The extraction of chloroplast and thylakoids from spinach and Arabidopsis was performed as described in Current Protocols in Cell Biology, with slight modifications (Seigneurin-Berny et al., 2008). The final centrifugation step involving a 40% and 80% density Percoll gradient was repeated following resuspension as a preliminary confirmation. Phase contrast microscopy was also used to visually confirm intactness. Since there are a number of intact chloroplast classifications, based on the biochemical properties succeeding isolation (Hall, 1972a), we confirmed the "type A" isolated chloroplasts with a ferricyanide assay. The integrity of the chloroplast membranes was assessed by monitoring the rates of membrane-impermeable ferricyanide reduction at 420nm, as performed previously (Lilley et al. 1975), in comparison with an osmotically shocked chloroplasts suspension (Figure 17).

The import assay used [3H] labeled protein that was incubated with isolated pea chloroplasts for 30 minutes, at room temperature with 5 mM Mg-ATP. After import, reactions were divided in half and treated without (-) or with (+) Trypsin for 20 minutes one ice and then quenched with Trypsin inhibitor for 5 minutes. Intact chloroplasts were recovered by centrifugation through a 40% Percoll cushion and the resulting pellet was resuspended in lysis buffer and fractionated into total membrane or soluble fraction. All fractions were analyzed by SDS-PAGE and fluography.

ATP Bioluminescence Assay

The Becquerel phosphoroscope and Enliten ATP Detection Kit (Promega) was used to allow for real-time *in vitro* measurements of ATP. The detector was filtered with a 550 BP 25 yellow filter to prevent non-specific contaminating light and biolumenscence was

detected in the same manner as described before with slight modifications (Lundin and Thore, 1975; Livingston et al., 2010). The assays consisted of 30 μg chlorophyll/mL of the sample resuspended in a buffer containing 25 mM Tricine, pH 7.6, 400 mM sorbitol, 5 mM $KHPO_4$,pH 7.8, 2.5 mM $MgCl_2$, 1.25 mM EDTA, 2.5 mM dithiothreitol (DTT), and 100 μM diadenosine pentaphosphate (DAPP) and were briefly exposed to low light, in order to reduce and activate the thiols on the γ-subunit of ATP synthase (Kramer and Crofts, 1989). Following the light treatment, an alternative electron acceptor, 100 μM methyl viologen (MV), was added to the LEF-simulated reactions for the rate-limiting step to depend on the light reactions rather than excess reductant (NADPH). As a final step, 1 mM of exogenous ADP was added prior to the addition of the luciferase-luciferin reagent. As shown in Figure 18 (arrow), an initial rise occurred upon the addition of luciferase reagent, presumably from endogenous ATP already present in the sample.

Following the initial rise, the rates of ATP were calculated based on the light-activated positive slopes (Figure 18) minus light-off portion (negative-slope) producing RLU (V/s). The phosphoroscope was linked to a LKB 1250 luminometer and a measuring computing system (USB-1608FS). The slopes were referenced to those from the ATP calibration curve (V/μM ATP) and dependent on the chlorophyll concentrations (μg Chl/mL). Each of the assays were repeated n≥3, immediately following confirmation of intactness using the ferricyanide assay and ATP calibration curves.

The rates were calculated based on the light-activated positive slopes minus light-off portion producing the RLU signifying V/s and referenced to the slope derived from the ATP calibration curve (V/μM ATP) and dependent on the chlorophyll concentrations (μg Chl/mL).

Photosynthetic Phenotyping

In situ chlorophyll fluorescence imaging was performed in plant growth chambers, as described in (Cruz et al., 2016a) outfitted as Dynamic Environment Photosynthesis Imager (DEPI). The large-scale screening was performed on 3-week plants Arabidopsis *ntt* plants exposed to 3 different light regimes (as described above) under a 16:8 light cycles. Processing was performed using custom software developed in the laboratory called OLIVER (https://caapp-msu.bitbucket.io/projects/oliver/index.html) to derive photosynthetic parameters, such as those mentioned above.

The photosynthetic *in vivo* spectroscopy measurements were made using wholes leaves of Arabidopsis *ntt* mutants clamped into a measuring chamber flushed with ambient air or minimal CO_2. The chamber of a nonfocusing optics spectrophotometer/chlorophyll fluorimeter constructed in-house (Sacksteder et al., 2001; Avenson et al., 2005a). The ECS decay kinetic measurements were made by perturbing the 3 minute light- exposed steady-state with a short dark period, which disturbs the system by halting proton influx and allows for equilibration of the *pmf* with the free energy of ATP synthase (Avenson et al., 2005b; Cruz et al., 2005). The fractions of $\Delta\psi$ (ECS steady-state) and ΔpH (ECS inverse) components derived from the *pmf* partitioning were measured as described previously (Cruz et al., 2001a; Takizawa et al., 2007).

Cloning of NTT1 and NTT2 into the plant transformation vector: pH2GW7.0

NTT1 (At1g80300) originally cloned into pUC19 vector (New England Biolabs) was subsequently cloned into pENTR/SD/DTOPO using a standard PCR approach according to manufacturer protocol (Invitrogen™). NTT2 (At1g15500) previously cloned into pENTR/SD/DTOPO vector (Invitrogen™) was purchased from ABRC (Scholl et al., 2000).

Using a Clonase II reaction as describe by the manufacturer protocol (Invitrogen™), cDNAs for NTT1-WT and NTT2-WT were all cloned into the plant transformation vector pH2GW7.0 (VIB;(Karimi et al., 2002). The integrity of all constructs was confirmed through sequencing performed by the RTSF at Michigan State University. Plant transformations were performed by the Arabidopsis Service Center (ASC) at Michigan State University using the floral dip Agrobacterium-mediated transformation method to complement the NTTdKD lines (Clough and Bent, 1998).

Table 4. NTT cloning primers.

Gene	Locus	Forward primer (5'->3')	Reverse primer (5'->3')
NTT1	AT1G80300	CACCATGGGAGCTGTGATTCAAACCAGAGGG	TTATAAGTTGGTGGGAGCAGATTT
NTT2	AT1G15500	CACCATGGAAGGTCTGATTCAAACCAGAGGA	CTAAATGCCAGTAGGAGTAGATTTCT

Acknowledgements

The authors would like to thank Dr. H. Ekkehard Neuhaus for providing *Atntt* double-mutant seeds. Also Dr. Nicholas Fisher, Dr. Deserah Strand and Dr. Jeffrey Cruz for helpful discussions and insight. A special thanks to Lola M. Alvarez for her assistance with laboratory maintenance and technical assistance.

APPENDIX

Table 5. Equations for fluorescence and ECS calculations

Fluorescence yield (Y_F)	= $k_F/(k_F+k_d+q_Lxk_p+k_{NPQ})$	(k=rate constants of f= fluorescence, d= heat dissipation, p= PQ pool and NPQ= non-photochemical quenching; qL= concentration of undamaged or open PSII reaction centers)
φII	= (Fm'-Fs)/Fm'	(m'= maximal fluorescence at saturating pulse with some PSII closed, s=baseline with light)
F_v/F_m	= (Fm-Fo)/Fm (optimal ≈0.8)	(m= maximal fluorescence at saturating pulse, o=baseline)
LEF	= i x A x fraction PSII x φII	(i= light intensity, A=absorptivity of the sample, and fraction of PSII=absorbed light by PSII alone, usually 0.4)
NPQ	= (Fm-Fm')/Fm'	
qI	= (Fm-Fm'')/Fm''	(m''= maximal fluorescence at saturating pulse following dark recovery)
qE	= (Fm''-Fm')/Fm' or (Fm/Fm')-(Fm/Fm'')	
qL	= ((1+NPQ) x (1/(F_v/F_m))-1))/(1/φII-1)	
ΔμH+	= $nF\Delta\Psi_{(i-o)}$ - $2.3RT\Delta pH_{(o-i)}$	(R=universal gas constant, T= absolute temperature in Kelvin, and F= Faraday's constant, subscripts "i" for inside the lumen space and "o" for outside and refer to the stroma)
ΔA_{520}(deconvoluted)	= ΔA_{520}-((ΔA_{505}-ΔA_{535})/2)	
pmf	= ΔΨ -59mV ΔpH or ΔΨ + 2.3RT/F ΔpH	
ECS_t (≈*pmf*)	= ΔA_{520}	total ECS amplitude
vH^+	= $Y_0 + Ae^{-x/\tau}$	linear fit of the initial absorbance change of the ECS decay at 520 nm
g_H+	= $1/\tau$	(τ=mean lifetime)
pmf_{LEF}	= LEF/g_H+	

REFERENCES

REFERENCES

Allen JF (2002) Photosynthesis of ATP—electrons, proton pumps, rotors, and poise. Cell 110: 273–276

Alonso JM, Stepanova AN, Leisse TJ, Kim CJ, Chen H, Shinn P, Zimmerman J, Barajas P, Cheuk R, Gadrinab C, et al (2003) Genome-wide insertional mutagenesis of *Arabidopsis thaliana*. Science 301: 653–657

Alric J (2014) Redox and ATP control of photosynthetic cyclic electron flow in Chlamydomonas reinhardtii: (II) Involvement of the PGR5–PGRL1 pathway under anaerobic conditions. Biochim Biophys Acta BBA - Bioenerg 1837: 825–834

Armisén D, Lecharny A, Aubourg S (2008) Unique genes in plants: specificities and conserved features throughout evolution. BMC Evol Biol 8: 280

Asada K (1999) The water-water cycle in chloroplasts: scavenging of active oxygens and dissipation of excess photons. Annu Rev Plant Physiol Plant Mol Biol 50: 601–639

Avenson TJ, Cruz JA, Kanazawa A, Kramer DM (2005a) Regulating the proton budget of higher plant photosynthesis. Proc Natl Acad Sci 102: 9709–9713

Avenson TJ, Kanazawa A, Cruz JA, Takizawa K, Ettinger WE, Kramer DM (2005b) Integrating the proton circuit into photosynthesis: progress and challenges. Plant Cell Environ 28: 97–109

Bailleul B, Berne N, Murik O, Petroutsos D, Prihoda J, Tanaka A, Villanova V, Bligny R, Flori S, Falconet D, et al (2015) Energetic coupling between plastids and mitochondria drives CO2 assimilation in diatoms. Nature 524: 366–369

Baker NR (2008) Chlorophyll fluorescence: a probe of photosynthesis *in vivo*. Annu Rev Plant Biol 59: 89–113

Bendall DS, Manasse RS (1995) Cyclic photophosphorylation and electron transport. Biochim Biophys Acta BBA - Bioenerg 1229: 23–38

Bolle C, Huep G, Kleinbölting N, Haberer G, Mayer K, Leister D, Weisshaar B (2013) GABI-DUPLO: a collection of double mutants to overcome genetic redundancy in *Arabidopsis thaliana*. Plant J 75: 157–171

Clough SJ, Bent AF (1998) Floral dip: a simplified method for Agrobacterium-mediated transformation of *Arabidopsis thaliana*. Plant J Cell Mol Biol 16: 735–743

Cruz JA, Avenson TJ, Kanazawa A, Takizawa K, Edwards GE, Kramer DM (2005) Plasticity in light reactions of photosynthesis for energy production and photoprotection. J Exp Bot 56: 395–406

Cruz JA, Sacksteder CA, Kanazawa A, Kramer DM (2001b) Contribution of electric field (Δψ) to steady-state transthylakoid proton motive force (*pmf*) *in vitro* and *in vivo*. Control of *pmf* parsing into Δψ and ΔpH by ionic strength. Biochemistry 40: 1226–1237

Cruz JA, Savage LJ, Zegarac R, Hall CC, Satoh-Cruz M, Davis GA, Kovac WK, Chen J, Kramer DM (2016b) Dynamic environmental photosynthetic imaging reveals emergent phenotypes. Cell Syst 2: 365–377

Eberhard S, Finazzi G, Wollman F-A (2008) The dynamics of photosynthesis. Annu Rev Genet 42: 463–515

Fiore C, Trézéguet V, Le Saux A, Roux P, Schwimmer C, Dianoux AC, Noel F, Lauquin G.-M, Brandolin G, Vignais PV (1998) The mitochondrial ADP/ATP carrier: structural, physiological and pathological aspects. Biochimie 80: 137–150

Flügge UI, Benz R (1984) Pore-forming activity in the outer membrane of the chloroplast envelope. FEBS Lett 169: 85–89

Flügge U-I, Häusler RE, Ludewig F, Gierth M (2011) The role of transporters in supplying energy to plant plastids. J Exp Bot 62: 2381–2392

Flügge UI, Heldt HW (1991) Metabolite translocators of the chloroplast envelope. Annu Rev Plant Physiol Plant Mol Biol 42: 129–144

Flügge UI, Hinz G (1986) Energy dependence of protein translocation into chloroplasts. Eur J Biochem 160: 563–570

Froehlich J (2011) Studying Arabidopsis envelope protein localization and topology using thermolysin and trypsin proteases. Methods Mol Biol Clifton NJ 774: 351–367

Hall CC, Cruz J, Wood M, Zegarac R, DeMars D, Carpenter J, Kanazawa A, Kramer D (2013) Photosynthetic measurements with the idea spec: an integrated diode emitter array spectrophotometer/fluorometer. Photosynth. Res. Food Fuel Future. Springer Berlin Heidelberg, pp 184–188

Hall DO (1972b) Nomenclature for isolated chloroplasts. Nature 235: 125–126

Hatch TP, Al-Hossainy E, Silverman JA (1982) Adenine nucleotide and lysine transport in Chlamydia psittaci. J Bacteriol 150: 662–670

Heber U (1974) Metabolite exchange between chloroplasts and cytoplasm. Annu Rev Plant Physiol 25: 393–421

Heber U, Heldt HW (1981) The chloroplast envelope: structure, function, and role in leaf metabolism. Annu Rev Plant Physiol 32: 139–168

Heber U, Santarius KA (1970) Direct and indirect transfer of ATP and ADP across the chloroplast envelope. Z Für Naturforschung Teil B Chem Biochem Biophys Biol 25: 718–728

Heineke D, Riens B, Grosse H, Hoferichter P, Peter U, Flügge U-I, Heldt HW (1991) Redox transfer across the inner chloroplast envelope membrane. Plant Physiol 95: 1131–1137

Heldt HW (1969) Adenine nucleotide translocation in spinach chloroplasts. FEBS Lett 5: 11–14

Heldt HW, Sauer F (1971) The inner membrane of the chloroplast envelope as the site of specific metabolite transport. Biochim Biophys Acta BBA - Bioenerg 234: 83–91

Hill R (1951) Oxidoreduction in chloroplasts. In FF Nord, ed, Adv. Enzymol. Relat. Areas Mol. Biol. John Wiley & Sons, Inc., pp 1–39

Jensen RG, Bassham JA (1966) Photosynthesis by isolated chloroplasts. Proc Natl Acad Sci U S A 56: 1095–1101

Joët T, Genty B, Josse E-M, Kuntz M, Cournac L, Peltier G (2002) Involvement of a plastid terminal oxidase in plastoquinone oxidation as evidenced by expression of the *Arabidopsis thaliana* enzyme in tobacco. J Biol Chem 277: 31623–31630

Joliot P, Johnson GN (2011) Regulation of cyclic and linear electron flow in higher plants. Proc Natl Acad Sci 108: 13317–13322

Kampfenkel K, Möhlmann T, Batz O, Montagu MV, Inzé D, Neuhaus HE (1995) Molecular characterization of an *Arabidopsis thaliana* cDNA encoding a novel putative adenylate translocator of higher plants. FEBS Lett 374: 351–355

Karimi M, Inzé D, Depicker A (2002) GATEWAY vectors for Agrobacterium-mediated plant transformation. Trends Plant Sci 7: 193–195

Klingenberg M (2008) The ADP and ATP transport in mitochondria and its carrier. Biochim Biophys Acta BBA - Biomembr 1778: 1978–2021

Kramer D, Avenson T, Edwards G (2004) Dynamic flexibility in the light reactions of photosynthesis governed by both electron and proton transfer reactions. Trends Plant Sci 9: 349–357

Kramer DM, Crofts AR (1989) Activation of the chloroplast ATPase measured by the electrochromic change in leaves of intact plants. Biochim Biophys Acta BBA - Bioenerg 976: 28–41

Kramer DM, Evans JR (2011) The importance of energy balance in improving photosynthetic productivity. Plant Physiol 155: 70–78

Lilley RM, Fitzgerald MP, Rienits KG, Walker DA (1975) Criteria of intactness and the photosynthetic activity of spinach chloroplast preparations. New Phytol 75: 1–10

Livingston AK, Cruz JA, Kohzuma K, Dhingra A, Kramer DM (2010) An Arabidopsis mutant with high cyclic electron flow around photosystem i (hcef) involving the NADPH dehydrogenase complex. Plant Cell Online 22: 221–233

Lundin A, Thore A (1975) Analytical information obtainable by evaluation of the time course of firefly bioluminescence in the assay of ATP. Anal Biochem 66: 47–63

Möhlmann T, Tjaden J, Schwöppe C, Winkler HH, Kampfenkel K, Neuhaus HE (1998) Occurrence of two plastidic ATP/ADP transporters in *Arabidopsis thaliana*. Molecular characterisation and comparative structural analysis of similar ATP/ADP translocators from plastids and *Rickettsia prowazekii*. Eur J Biochem FEBS 252: 353–359

Munekage Y, Hojo M, Meurer J, Endo T, Tasaka M, Shikanai T (2002) PGR5 Is involved in cyclic electron flow around photosystem I and is essential for photoprotection in Arabidopsis. Cell 110: 361–371

Neuhaus HE, Thom E, Möhlmann T, Steup M, Kampfenkel K (1997) Characterization of a novel eukaryotic ATP/ADP translocator located in the plastid envelope of *Arabidopsis thaliana* L. Plant J 11: 73–82

Neuhaus HE, Wagner R (2000) Solute pores, ion channels, and metabolite transporters in the outer and inner envelope membranes of higher plant plastids. Biochim Biophys Acta BBA - Biomembr 1465: 307–323

Neuhaus HE, Winkler HH (1999) Non-mitochondrial ATP transport. Trends Biochem Sci 24: 64–68

Nishio JN, Whitmarsh J (1991) Dissipation of the proton electrochemical potential in Intact and lysed chloroplasts: I. The electrical potential. Plant Physiol 95: 522–528

Noctor G, Foyer (2000) Homeostasis of adenylate status during photosynthesis in a fluctuating environment. J Exp Bot 51: 347–356

Nury H, Dahout-Gonzalez C, Trézéguet V, Lauquin GJM, Brandolin G, Pebay-Peyroula E (2006) Relations between structure and function of the mitochondrial ADP/ATP carrier. Annu Rev Biochem 75: 713–741

Raghavendra AS, Padmasree K (2003) Beneficial interactions of mitochondrial metabolism with photosynthetic carbon assimilation. Trends Plant Sci 8: 546–553

Reiser J, Linka N, Lemke L, Jeblick W, Neuhaus HE (2004) Molecular physiological analysis of the two plastidic ATP/ADP transporters from Arabidopsis. Plant Physiol 136: 3524–3536

Sacksteder CA, Jacoby ME, Kramer DM (2001) A portable, non-focusing optics spectrophotometer (NoFOSpec) for measurements of steady-state absorbance changes in intact plants. Photosynth Res 70: 231–240

Saier MH (2000) A functional-phylogenetic classification system for transmembrane solute transporters. Microbiol Mol Biol Rev 64: 354–411

Santarius KA, Heber U, Ullrich W, Urbach W (1964) Intracellular translocation of ATP, ADP and inorganic phosphate in leaf cells of elodea densa in relation to photosynthesis. Biochem Biophys Res Commun 15: 139–146

Scheibe R (2004) Malate valves to balance cellular energy supply. Physiol Plant 120: 21–26

Scholl RL, May ST, Ware DH (2000) Seed and molecular resources for Arabidopsis. Plant Physiol 124: 1477–1480

Schulz A, Knoetzel J, Scheller HV, Mant A (2004) Uptake of a fluorescent dye as a swift and simple indicator of organelle intactness: import-competent chloroplasts from soil-grown Arabidopsis. J Histochem Cytochem 52: 701–704

Schunemann D, Borchert S, Flugge UI, Heldt HW (1993) ADP/ATP translocator from pea root plastids (comparison with translocators from spinach chloroplasts and pea leaf mitochondria). Plant Physiol 103: 131–137

Seigneurin-Berny D, Salvi D, Joyard J, Rolland N (2008) Purification of intact chloroplasts from Arabidopsis and spinach leaves by isopycnic centrifugation. Curr Protoc Cell Biol Editor Board Juan Bonifacino Al Chapter 3: Unit 3.30

Senior AE (1988) ATP synthesis by oxidative phosphorylation. Physiol Rev 68: 177–231

Sharkey TD (1990) Feedback limitation of photosynthesis and the physiological role of ribulose bisphosphate carboxylase carbamylation. Bot Mag Tokyo 2: 87–105

Stitt M, Lilley RM, Heldt HW (1982) Adenine nucleotide levels in the cytosol, chloroplasts, and mitochondria of wheat leaf protoplasts. Plant Physiol 70: 971–977

Strand DD, Fisher N, Davis GA, Kramer DM (2016) Redox regulation of the antimycin A sensitive pathway of cyclic electron flow around photosystem I in higher plant thylakoids. Biochim Biophys Acta BBA - Bioenerg 1857: 1–6

Strand DD, Livingston AK, Satoh-Cruz M, Koepke T, Enlow HM, Fisher N, Froehlich JE, Cruz JA, Minhas D, Hixson KK, et al (2017) Defects in the expression of chloroplast

proteins leads to H2O2 accumulation and activation of cyclic electron flow around photosystem I. Front Plant Sci. doi: 10.3389/fpls.2016.02073

Takizawa K, Cruz JA, Kanazawa A, Kramer DM (2007) The thylakoid proton motive force *in vivo*. Quantitative, non-invasive probes, energetics, and regulatory consequences of light-induced *pmf*. Biochim Biophys Acta BBA - Bioenerg 1767: 1233–1244

Tjaden J, Möhlmann T, Kampfenkel K, Neuhaus GH andH. E (1998) Altered plastidic ATP/ADP-transporter activity influences potato (Solanum tuberosumL.) tuber morphology, yield and composition of tuber starch. Plant J 16: 531 –540

Tjaden J, Winkler HH, Schwöppe C, Van Der Laan M, Möhlmann T, Neuhaus HE (1999) Two nucleotide transport proteins in Chlamydia trachomatis, one for net nucleoside triphosphate uptake and the other for transport of energy. J Bacteriol 181: 1196–1202

Trentmann O, Horn M, van Scheltinga ACT, Neuhaus HE, Haferkamp I (2007) Enlightening energy parasitism by analysis of an ATP/ADP transporter from Chlamydiae. PLoS Biol 5: e231

Trentmann O, Jung B, Neuhaus HE, Haferkamp I (2008) Nonmitochondrial ATP/ADP transporters accept phosphate as third substrate. J Biol Chem 283: 36486–36493

Walker DA, Cerovic ZG, Robinson SP (1987) [15] Isolation of intact chloroplasts: General principles and criteria of integrity. Methods Enzymol 148: 145–157

Weber APM, Fischer K (2007) Making the connections – The crucial role of metabolite transporters at the interface between chloroplast and cytosol. FEBS Lett 581: 2215–2222

Winkler HH (1976) Rickettsial permeability. An ADP-ATP transport system. J Biol Chem 251: 389–396

Wood KV, de Wet JR, Dewji N, DeLuca M (1984) Synthesis of active firefly luciferase by *in vitro* translation of RNA obtained from adult lanterns. Biochem Biophys Res Commun 124: 592–596

CHAPTER 4
Concluding Remarks

Photosynthetic research has brought about a plethora of benefits to the field of science. By understanding the biochemical, structural and physiological processes that make up photosynthesis we have advanced the field of medicine, energy production, food, and the environment. Yet, a majority of the research has focused on static controlled environmental conditions without taking environmental perturbations into account. A number of more recent studies (Kramer and Evans, 2011; Suorsa et al., 2012; Tikkanen et al., 2012; Armbruster et al., 2014; Carrillo et al., 2016; Cruz et al., 2016) have confirmed more severe photosynthetic responses induced by rapidly altering CO_2 and/or light conditions, while having minimal phenotypes under constant irradiance.

For this reason, it is imperative to consider natural environmental settings in order to advance the field of photosynthesis, and science in general. This dissertation provides insight into some (of the many) mechanistic ways in which plants have evolved to cope with the dynamics of nature through modulation of *pmf* and ATP. From sensing pressures in the lumenal space (KEA3-Appendix B, Chapter 1), to modulating the activity of ATP synthase at minimal irradiances (NTRC-Chapter 2) and the balancing of chloroplasts metabolites with other pools of ATP (NTT-Chapter 3).

The collaborative work on KEA3, the K^+/H^+ antiporter, confirmed a photoprotective role by which plants dissipate excess protons upon transitioning from high-light or an extended dark-period to low light conditions. Two mutant lines of *kea3* display prolonged NPQ responses upon transitioning to lower-light intensities with associated φII responses and increased sensitivity to the *pmf*. Based on our results with MV, acting as alternative electron acceptor to PSI, we predict the thylakoid proteins KEA3 and TPK3 co-regulate photosynthetic pressures, or ATP synthase specifically, by adjusting the *pmf*. The KEA3

could function by alleviating protons from the thylakoid lumen in exchange for K+ ions, which are channeled out of the chloroplast by TPK3 (Carraretto et al., 2013; Armbruster et al., 2014). The next step for this work is to decipher the mechanism by which KEA3 senses alterations in light intensity and triggers (if any) activation of TPK3.

An emphasis is placed on the major energy-transducing enzyme in plants-ATP synthase, as it is an essential component of photosynthesis, acting as a key regulator in response to light and electron flow. Apart from using an electrochemical gradient of protons to mechanically rotate and yield ATP, this enzyme is highly dynamic in its activation, regulation and function. Previous research has shown that the γ-subunit thiols of the chloroplast ATP synthase are redox modulated for a light-activated state requiring a lower *pmf* threshold and an oxidized (off) state during the dark, to prevent wasteful hydrolysis of ATP (Ketcham et al., 1984; Hangarter et al., 1987; Junesch and Gräber, 1987). It was long been assumed that the well documented ferredoxin-thioredoxin reductase (FTR) system using stromal thioredoxins (mainly f-, m- and x-) was the mechanism of action for the rapid reduction of regulatory thiols on ATP synthase, even under minimal irradiance (Buchanan, 1980; Quick and Mills, 1986; Kramer et al., 1990).

However, our work links the chloroplast NADPH thioredoxin reductase C (NTRC) to the consequential activation behavior of ATP synthase (Chapter 2). Arabidopsis *ntrc* mutants display strong photosynthetic inefficiencies in PSII with associated increases in the stress signal NPQ and hampered conductivity of ATP synthase, specifically to low light intensities (≤100 μmol photons m^2 s^{-1}), presumably when ATP synthase is inactivated. Based on our ECS measurements to assess the re-oxidation state of ATP synthase, *Atntrc* displayed rapid kinetic responses compared to wild type. Mis-regulation was also

confirmed with the western blots of ATPC1 γ-subunit thiols confirming a partial oxidized state for the enzyme at irradiances at or below 100 μmol photons m^2 s^{-1}. We propose that NTRC co-regulates the regulatory thiols of ATP synthase with FTR at specific light intensities. Unlike the FTR, NTRC derives its reducing potential from NADPH which can provided to the stroma independent of the light reactions (Serrato et al., 2004). Our results show that NTRC is critical for maintaining photosynthesis, particularly under low and fluctuating light, and thus an important contribution to our understanding of how photosynthesis operates in the natural environment. An interesting piece to the puzzle remaining to be elucidated is the mechanism by which NTRC activates ATP synthase. The two reductase systems (FTR and NADPH) use different reducing power (Fd and NADPH, respectively); however, if NADPH is readily available (even in the dark) what prevents NTRC from activating ATP synthase remains unanswered.

Lastly, Chapter 3 explores the role of the nucleotide triphosphate transporter (NTT) as a mechanism to augment plastid levels of ATP. Based on our results of rapid ATP efflux using isolated chloroplasts (rigorously controlled for intactness), we revisit the once considered sluggish ATP/ADP+P_i transpoter (Heldt, 1969) as the mode of transport. Using a luciferase assay, we estimated rates 20-fold greater than previously suggested with spinach chloroplasts. It appears that the two NTT isoforms possess different roles, based on the dynamic differences in the photosynthetic responses of *Atntt1* and *Atntt2* under fluctuating light and low CO_2 conditions. Furthermore, gene expression studies confirmed drastic differences (log_2-fold change of 26.8 and 13.0 compared to 1.2 and 1.8, respectively) between the failed attempt of crossing single *Atntt* mutant lines to those of a double-mutant obtained (termed NTTdKD for simplicity). Even with the leaky double-mutant lines,

the photosynthetic stress response NPQ and qE displayed hysteretic behavior to fluctuating light. Additionally, ATP efflux rates were 3-fold lower in NTTdKD chloroplasts compared to wild type, confirming the role of NTT in exporting ATP at photosynthetically significant rates. These results further support the many intricate ways by which photosynthesis copes with dynamic irradiances to maintain ATP homeostasis.

APPENDIX

Permissions for use of copyrighted materials

Permission granted for reproduction of Figure 1 from Croce, R. and Amerongen, H. Van. (2014) Nature Chemical Biology, 10, 492-501. RightsLink license #4123691481624

Permission granted for reproduction of Figure I(a) from Cape, J.L., Bowman, M.K., and Kramer, D.M. (2006) Trends in Plant Science, 11, 46-55. RightsLink license #4123700803360

Permission granted for reproduction of Figure 1 from Weber J. (2007) Trends in Biochemical Sciences, 32, 53-56. RightsLink license #4123711273872

Permission granted for reproduction of Figure 1 from Flügge, U-I., Häusler, R.E., Ludewig, F., and Gierth, M. (2011) J Exp Botany, 62, 2381-2392. RightsLink license #4123721021508

Permission granted for reproduction of Supplementary Figure 1 from Dai, S., Friemann, R., Glauser, D.A., Bourquin, F., Manieri, W., Schürmann, P., and Eklund H. (2007) Nature, London, 448, 92-6. RightsLink license #4123730075446

Permission granted for reproduction of Chapter 2 from L. Ruby Carrillo, John E. Froehlich, Jeffrey A. Cruz, Linda Savage and David M. Kramer. (2016) The Plant Journal, 87, 654-663. RightsLink license #4197360981153

REFERENCES

REFERENCES

Armbruster U, Carrillo, LR, Venema K, Pavlovic L, Schmidtmann E, Kornfield A, Jahns P, Berry JA, Kramer DM, Jonikas MC (2014) Ion antiport accelerates photosynthetic acclimation in fluctuating light environments. Nat Commun 5: 5439

Buchanan BB (1980) Role of light in the regulation of chloroplast enzymes. Annu Rev Plant Physiol 31: 341–374

Carraretto L, Formentin E, Teardo E, Checchetto V, Tomizioli M, Morosinotto T, Giacometti GM, Finazzi G, Szabó I (2013) A thylakoid-located two-pore K+ channel controls photosynthetic light utilization in plants. Science 342: 114–118

Carrillo LR, Froehlich JE, Cruz JA, Savage L, Kramer DM (2016) Multi-level regulation of the chloroplast ATP synthase: The chloroplast NADPH thioredoxin reductase c (NTRC) is required for redox modulation specifically under low irradiance. Plant J 87: 654–663

Cruz JA, Savage LJ, Zegarac R, Hall CC, Satoh-Cruz M, Davis GA, Kovac WK, Chen J, Kramer DM (2016) Dynamic environmental photosynthetic imaging reveals emergent phenotypes. Cell Syst 2: 365–377

Hangarter RP, Grandoni P, Ort DR (1987) The effects of chloroplast coupling factor reduction on the energetics of activation and on the energetics and efficiency of ATP formation. J Biol Chem 262: 13513–13519

Heldt HW (1969) Adenine nucleotide translocation in spinach chloroplasts. FEBS Lett 5: 11–14

Junesch U, Gräber P (1987) Influence of the redox state and the activation of the chloroplast ATP synthase on proton-transport-coupled ATP synthesis/hydrolysis. Biochim Biophys Acta BBA - Bioenerg 893: 275–288

Ketcham SR, Davenport JW, Warncke K, McCarty RE (1984) Role of the gamma subunit of chloroplast coupling factor 1 in the light-dependent activation of photophosphorylation and ATPase activity by dithiothreitol. J Biol Chem 259: 7286–7293

Kramer DM, Evans JR (2011) The importance of energy balance in improving photosynthetic productivity. Plant Physiol 155: 70–78

Kramer DM, Wise RR, Frederick JR, Alm DM, Hesketh JD, Ort DR, Crofts AR (1990) Regulation of coupling factor in field-grown sunflower: a redox model relating coupling factor activity to the activities of other thioredoxin-dependent chloroplast enzymes. Photosynth Res 26: 213–222

Quick WP, Mills JD (1986) Thiol modulation of chloroplast CF0-CF1 in isolated barley protoplasts and its significance to regulation of carbon dioxide fixation. Biochim Biophys Acta BBA - Bioenerg 851: 166–172

Serrato AJ, Pérez-Ruiz JM, Spínola MC, Cejudo FJ (2004) A novel NADPH thioredoxin reductase, localized in the chloroplast, which deficiency causes hypersensitivity to abiotic stress in *Arabidopsis thaliana*. J Biol Chem 279: 43821–43827

Suorsa M, Järvi S, Grieco M, Nurmi M, Pietrzykowska M, Rantala M, Kangasjärvi S, Paakkarinen V, Tikkanen M, Jansson S, et al (2012) Proton gradient regulation5 is essential for proper acclimation of Arabidopsis photosystem I to naturally and artificially fluctuating light conditions. Plant Cell Online 24: 2934–2948

Tikkanen M, Grieco M, Nurmi M, Rantala M, Suorsa M, Aro E-M (2012) Regulation of the photosynthetic apparatus under fluctuating growth light. Philos Trans R Soc B Biol Sci 367: 3486–3493